Oral Session 01

Contractility and Control of Tone

OS01-1

Besides its effect on bladder contractility, caldesmon deficiency leads to a triad of morphological features: umbilical hernia, split lower part of the sternum and white liver areas

S. L. Barthel[1], M. Frohn[1], D. Metzler[1], O. Trunschke[1], S. Puetz[1], M. Koch[2], W. F. Neiss[3], M. M. Schroeter[1], G. Pfitzer[1]

[1]University of Cologne, Institute of Vegetative Physiology, Koeln, Germany

[2]University of Cologne, Institute for Dental Research and Oral Musculoskeletal Biology, Koeln, Germany

[3]University of Cologne, Institute I of Anatomy, Koeln, Germany

Background: Caldesmon (CaD) is expressed in smooth muscle (SM) and a variety of non-muscle cells. It has N-terminal myosin and C-terminal actin binding domains and additionally binds calmodulin and tropomyosin. Its physiological role is incompletely understood. Biochemical evidence indicated that CaD inhibits actomyosin MgATPase activity and, thus, presumably force, and tethers actin and myosin filaments thereby organizing the SM contractile apparatus. Therefore, targeted ablation of CaD might lead to a hyper-contractile state (hypothesis 1) or loss of force (hypothesis 2). To test for these hypotheses, we generated a CaD mouse model with targeted ablation of the *Cald1* gene. **Methods:** Ablation of CaD in smooth muscle was confirmed by western blotting. Contractile activity was measured in longitudinal triton skinned muscle strips from E18.5 fetal bladders, cross sectional area was determined from the wet weight and length of the strips, and myosin light chain phosphorylation ($pMLC_{20}$) was determined by densitometric scanning of silver stained 2D-PAGE. **Results:** Ablation of CaD resulted in perinatal lethality in homozygous KO offspring and disrupted Mendelian distribution at E18.5 (WT 19%, HET 61%, KO 19%, n=248), whereas the life span of heterozygotes (HETs) was normal. 97% of KO but only 9% of HET and none of WT exhibited an umbilical hernia. Additionally, a split lower part of the sternum and white liver segments were observed in all 27 KO but not in the HETs from 21 litters. Fetal bladder weight and body-to-bladder weight were not significantly different between groups (n= 95, 12 litters). Specific maximal Ca^{2+}-activated force (pCa 4.3) was reduced in KO by ~60% (WT: 4.6±0.3 mN/mm², n=16; KO: 1.7±0.2 mN/mm², n=11, p<0.001). This was not due to incomplete activation as force elicited by the phosphatase inhibitor, microcystin, was comparable to that induced by pCa 4.3 in both groups (n=6, p<0.001). The force-pCa relation was shifted to the left in KO (pCa_{50} WT: 6.02±0.03; KO 6.14±0.03, p<0.01) and was steeper (n_H WT: 2.7±0.2 n=16, KO: 3.4±0.3 n=10, p<0.02). Time to 50% and 80% relaxation was increased ~1.5 fold in KO (t_{80} WT: 622 ± 35s, n=10, KO: 913 ± 59s, n=8, p<0.001). As expected, the percentage of unphosphorylated MLC_{20} in relaxed bladders (WT: 48±6%, KO: 61±5%) declined in the contracted state at pCa 4.3 (WT: 19±4 %, KO: 35±4%, n=7-9). **Conclusion:** The functional effects of CaD ablation are consistent with a dual action of CaD, namely inhibition of actomyosin interaction evidenced by the increased Ca-sensitivity and slowed relaxation and tethering of actin and myosin filaments evidenced by the loss of absolute force. The morphological features are reminiscent of those of incomplete pentalogy of Cantrell. They cannot be explained at this point of our research but form a useful triad to identify KO-fetus.

OS01-2

c-Src tyrosine kinase contribution to 5-HT-mediated contraction in rat skeletal muscle arteries is Ca-dependent

O. Zavaritskaya, S. Altay, R. Schubert

Medical Faculty Mannheim, University of Heidelberg, Cardiovascular physiology, CBTM, Germany

Question: c-Src kinase, a member of the Src tyrosine kinase family, is involved in the signalling mechanism of 5-HT-induced vasoconstriction. This effect was reported to be mediated by changes in the calcium sensitivity of the contractile apparatus. Whether c-Src kinase affects also the intracellular calcium concentration, $[Ca]_i$, is unknown. Therefore, this study addressed the hypothesis that constriction of arteries is associated with a c-Src kinase-dependent alteration of the intracellular calcium concentration. **Methods:** Gracilis arteries of Wistar rats were studied using isometric myography and FURA-2 fluorimetry. **Results:** Inhibition of c-Src kinase with 10 µM PP2 in Gracilis muscle arteries resulted in a strong attenuation of serotonin-induced contractions. Incubation with 10 µM PP3, an inactive analogue of PP2, had no effect. Removal of the endothelium did not alter vessel contractile responses to 5-HT nor the influence of the inhibitor of c-Src kinase. The PP2-mediated inhibition of 5-HT-induced contraction was associated with a reduced response of $[Ca^{2+}]_i$ to 5-HT. In particular, inhibition of c-Src-kinase attenuates 5-HT-induced calcium influx as well as calcium release from intracellular stores. In contrast, the calcium sensitivity of the contractile apparatus and the filling state of the sarcoplasmic reticulum were not influenced by c-Src kinase during 5-HT-induced contractions. **Conclusion:** The results highlight that c-Src kinase activation is a powerful mechanism to produce vasoconstriction of small skeletal muscle arteries of rats. The effect of c-Src kinase is independent of the endothelium. The data suggest that the action of c-Src kinase is associated with a change in the intracellular calcium concentration and involves Ca^{2+}-entry and Ca^{2+}-release pathways.

OS01-3

Arterial stiffness and pulse wave velocity in mice lacking NO-sensitive guanylyl cyclase

S. Dünnes[1], D. Groneberg[1], V. Herold[2], P. Jakob[2], A. Friebe[1]

[1]University of Wuerzburg, Institute of Physiology, Germany

[2]University of Wuerzburg, Experimental Physics 5, Germany

Background: NO-sensitive guanylyl cyclase (NO-GC) is the most important receptor for NO. The NO signal is transmitted through an increase in cGMP to act on several effector molecules. The NO/cGMP cascade is involved in the regulation of vessel diameter ultimately contributing to set the blood pressure. Lack of NO or NO-GC leads to hypertension and is thought to alter the responsiveness of blood vessels as well as their composition. **Aims:** As arterial stiffness is an import indicator of cardiovascular risk and mortality, we aimed to determine the role of NO-GC for aortic stiffness using general KO mice (GCKO) and smooth muscle-specific KO mice (SMC-GCKO) for NO-GC. We want to correlate these findings with aortic structure to discern whether loss of the cGMP signal results in changed organization of the extracellular matrix. **Methods:** Measurement of pulse wave velocity (PWV) is frequently used to determine aortic stiffness. We used magnetic resonance tomography (17.6 Tesla) for non-invasive measurement of local aortic PWV. PWV was calculated by simultaneously measuring cross-sectional change and volume flow in a defined time. In another setup, we characterized passive aortic stiffness using a stretch stress test. Aortic rings were fixed on steel hooks in an organ bath, the ring diameter was increased incrementally and the resulting force recorded. These findings will be correlated to structural data of aorta from these strains. Therefore, we will perform histological analysis of collagen using Picrosirius-red staining and biochemical assays to determine collagen and elastin content. **Results:** In GCKO mice, the aortic diameter and wall thickness are reduced whereas pulse wave velocity and passive aortic stiffness are increased. In addition, the collagen structure of the aorta is different compared to WT animals as GCKO aorta wall is compressed and the wall thickness reduced. SMC-GCKO animals reveal an unaltered aorta with regards to PWV and structure. **Conclusion:** Deletion of NO-GC affects the physical properties of aortic tissue. This effect appears to be independent of hypertension and NO-GC in smooth muscle cells.

OS01-4

The role of alternative mRNA splicing and threonine 696/853-phosphorylation of myosin phosphatase regulatory subunit (MYPT1) in the regulation of tone of murine brain vasculature

L. T. Lubomirov, M. M. Schroeter, S. Hilsdorf, D. Filipova, S. Baransi, S. Papadopoulos, G. Pfitzer

University of Cologne, Institute of Vegetative Physiology, Germany

Question: Smooth muscle myosin phosphatase activity is inhibited by phosphorylation of its regulatory subunit (MYPT1) at T696 and T853 and is disinhibited by PKG whereby the responsiveness to PKG depends on the isoform of MYPT1 generated by alternative splicing. The isoforms differ by inclusion or exclusion of exon24 and the exon-out isoform is PKG sensitive (Dippold & Fisher 2013). Here, we investigated whether arteries from murine circle of Willis differ in the expression ratio of the alternative splice variants of MYPT1 from peripheral arteries and whether this relates to differences in regulation of tone. **Methods:** Expression of exon24-out and exon24-in alternative splice variants of MYPT1 was assessed by RT-PCR. Vascular contractility of A. communicans posterior (brain arteries=BA) and femoral artery (FA) was investigated using wire myography. Phosphorylation of MYPT1 (T696 and T853), and the regulatory light chains of myosin (MLC_{20}) at S19 were assessed by western blotting. **Results:** Expression of exon24-out MYPT1 was~ 2.5 fold higher in BA compared to femoral and tail arteries (37±5% in BA vs. 15±5% in FA, p<0.01 or 18±2% in tail arteries, p<0.05; n= 4 each). In FA, sensitivity towards thromboxane analogue U46619 was high with threshold and maximal concentrations of 0.01 and 0.1 µM respectively and a pEC_{50} value of 7.7±0.1. Inhibition of NO-release by L-NAME (100 µM) had no significant effect on the U46619 dose response curve (pEC_{50} 7.9±0.1; p=0.2; n=5). In contrast, U46619-force generation was blunted in BA, (threshold concentration 0.1 µM, pEC_{50} 6.9±0.06. p< 0.001 compared to FA) but after inhibition of NO-release the potency of U46619 was similar to that in FA (pEC_{50} 7.6±0.1; p<0.001; n=6). L-NAME increased basal tone to a significantly larger extend in BA than in FA (21±4% in BA vs. 4±3% in FA; p< 0.01; n=6-5). The larger increase in basal tone of BA was associated with increased phosphorylation of MYPT1 at T696 (~2 fold, p<0.05) and T853 (~2.5 fold, p<0.001) and MLC_{20} at S19 (~6 fold, p<0.01; n= 3 each), whereas only a small (~1.2 fold) increase in phosphorylation at MPYT1-T853 and MLC_{20}-S19, but not at MYPT1-T696 was detected in FA. Consistent with these larger effects of NO signaling in BA, 8-Br-cGMP (1 µM) relaxed submaximally activated (pCa 6.1) a-toxin permeabilized BA by 58±4% (n=4) compared to 24±4% in FA (n=3; p<0.01). **Conclusions:** Our study indicates that the higher NO/cGMP/PKG sensitivity of arteries from the circle of Willis signaling compared to large peripheral conducting arteries can at least in part be ascribed to a shift in the ratio of the splice variants of MYPT1 in favor of the PKG sensitive isoform (exon-out) and to differences in the magnitude of changes of inhibitory phosphorylation of MYPT1 at T696 and T853.Thus, MYPT1 appears to play an important role in determining differences in tone regulation between cerebrovascular and peripheral arteries.

References

Dippold RP, Fisher SA. Myosin phosphatase isoforms as determinants of smooth muscle contractile function and calcium sensitivity of force production. Microcirculation. 2014 (3):239-48.

OS01-5
Consequences of postnatal vascular smooth muscle EGF-receptor deletion on acute angiotensin II action

B. Shreier, M. Hünerberg, S. Rabe, S. Mildenberger, D. Bethmann, C. Heise, M. Gekle
Martin Luther University Halle-Saale, Julius Bernstein Institute of physiology, Halle/Saale, Germany

Epidermal growth factor receptor (EGFR) is activated by its canonical ligands and transactivated by various vasoactive substances, e.g. angiotensin II. Vascular EGFR has been proposed to be involved in vascular tissue homeostasis and remodelling. Thus, most studies focused on its role during long term vascular changes whereas the relevance for acute regulation of vascular function *in vivo* and *ex vivo* is insufficiently understood.
To investigate the postnatal role of VSMC (vascular smooth muscle cell) EGFR *in vivo* and e*x vivo*, we generated a mouse model with cell-specific and inducible deletion of VSMC-EGFR and studied the effect on basal blood pressure, acute pressure response to angiotensin II *in vivo* as well as *ex vivo*, and vessel morphometry in male mice.
In knockout animals, systolic, diastolic and mean blood pressures were reduced compared to wild-type. Furthermore, angiotensin II-induced pressure load was lower in knockout animals, as was angiotensin II-induced force development, also in the presence of the AT2-receptor inhibitor PD-123319, excluding the involvement of this receptor type. Thus, the acute vasoconstrictor response, via the AT1-receptor, to angiotensin II depends on the VSMC-EGFR.
Because the basal components of the pharmacomechanical and electromechanical coupling seem to be intact (there were no differences in force development in response to KCl, serotonin or endothelin-1 in aortae from knockout animals) and we did not detect differences in mRNA-receptor expression we investigated whether differences in functional homologous desensitization can explain the observed reduction in responsiveness to angiotensin II. For this purpose aortic rings were exposed repeatedly to 100 nM angiotensin II for 5 minutes followed by 10 minutes of complete washout to allow relaxation. Similar experiments were performed with 1 µM endothelin-1. The results obtained indicate that angiotensin II-induced homologous desensitization is accelerated in aortae from knockout animals, but not for endothelin-1. The underlying mechanism is still under evaluation, as preliminary data indicate no difference in the mRNA content of β-arrestin 1&2 as well as ATRAP in aortas from $iEGFR^{\Delta/\Delta VSMC}$ mice.

OS01-6
Aging-related progressive skeletal muscle weakness in mutant Des^{R349P} muscles: a matter of compromised cytoarchitecture

S. Diermeier[1,2], A. Buttgereit[1], C. S. Clemen[3], R. Schröder[4], O. Friedrich[1,2]
[1]Friedrich-Alexander-University Erlangen-Nürnberg (FAU), Institute of Medical Biotechnology, Germany
[2]Erlangen Graduate School in Advanced Optical Technologies (SAOT), FAU Erlangen, Germany
[3]University of Cologne, Institute of Biochemistry I, Germany
[4]University Hospitals Erlangen, Institute of Neuropathology, Germany

Background: Patients with inherited degenerative muscle diseases suffer from progression with aging. We suppose that ongoing structural derangement is in part responsible for the progressing pathology. Thus, we analyzed how the cytoarchitecture of single skeletal muscle fibres is remodeled with age. Our knock-in mouse model with a R349P mutation in the desmin gene (DES^{R349P}) corresponds to the human R350P desminopathy. A direct comparison of three age bins was conducted to obtain quantitative data on structural changes in muscles carrying the mutation. **Methods:** We examined single muscle fibers of *M. soleus (*SOL), *M. extensor digitorum longus* (EDL) and *Mm. interossei plantares* (IO) from 17-23, 35-45 and 60-80 week-old wildtype (wt) littermates of heterozygous (het) and homozygous (hom) mice with the R349P desmin mutation. *Second Harmonic Generation* microscopy was used to image the myosin architecture of single muscle fibers in 3D, and the nuclei were counterstained. Ultrastructural changes were quantified by two parameters: 'cosine angle sums' (CAS) as descriptor of myofibrillar alignment and 'vernier densities' (VD) as measure for sarcomere lattice disruptions. The number and shape (surface, volume, sphericity) of nuclei were quantified using Imaris software. **Results:** Young mice showed marked disruptions of the myofibrillar lattice only in the hom Des^{R349P} genotype. In older age bins, hom as well as het mice displayed an increased number of *'verniers'* in their muscle fibre structure. The most striking deviations from the normal architecture with the lowest CAS were found in EDL and SOL muscles from the oldest hom mice. Interestingly, slow twitch SOL fibres of the oldest het mice again reached wt-like levels of the VD and CAS, whereas the CAS of fast-twitch IO and EDL fibres from these mice were as low as in hom littermates. The number of nuclei per fibre surface was increased in SOL fibres from hom mice across all ages and to a smaller extent in EDL and IO fibres from 60-80 week-old hom mice compared to het and wt mice. SOL hom fibres showed rounder nuclei than wt fibres in every age bin. **Conclusions:** Disruptions of the single fibre cytoarchitecture were already present in the youngest hom Des^{R349P} mice and increased with age. In het mice, significant structural changes were not detectable until the oldest age bin. Therefore, progressive remodeling of the 3D myofibrillar architecture in Des^{R349P} mice may explain progressive muscle weakness during aging.

The authors acknowledge ongoing support by the German Research Foundation (DFG, FR 2993/13-1) and by the Erlangen Graduate School in Advanced Optical Technologies (SAOT) within the framework of the German excellence initiative.

OS01-7
Comparing phosphodiesterase-dependent cardiovascular and gastrointestinal smooth muscle relaxation

A. Aue, B. Lies, A. Friebe, **D. Groneberg**
University of Wuerzburg, Institute of Physiology, Germany

Background: Cyclic guanosine monophosphate (cGMP) is an important endogenous mediator for vascular relaxation and gastrointestinal motility. The balance between production and degradation is highly important for function of these systems. Degradation of cGMP is mediated by phosphodiesterases (PDE). One of the main PDEs for cGMP degradation in smooth muscle cells (SMC) is PDE5. Blockade of PDE5 with specific inhibitors is a conceivable aspect for therapy of several different diseases like heart failure, aortic stenosis, cardiac vasculopathy, impaired glucose tolerance, schizophrenia etc.PDE5-Inhibition are administered orally and enter the systemic circulation the gastrointestinal tract. Therefore, the impact of PDE5 inhibition on GI peristalsis, motility and sphincter relaxation is of interest to estimate possible side effects. **Methods**: To clarify the individual impact of cGMP on the relaxation of gastrointestinal and vascular smooth muscle, we used our mouse lines lacking NO-GC in SMC and interstitial cells of Cajal (ICC). Isometric force studies were performed to monitor the responsiveness to exogenous and endogenous NO in absence and presence of sildenafil as PDE5 inhibitor. Immunohistochemistry was employed to determine PDE5 expression. **Results and Conclusion:** PDE5 is expressed in SMC of vascular and GI system. In addition to SMC, ICC also express PDE5 in the GI tract. In the vascular and GI system, pharmacological NO-induced relaxation could be enhanced by PDE5 inhibition. Surprisingly, in the GIT endogenous NO-induced relaxation is not influenced by PDE5 inhibition, neither the strength nor the duration of relaxation was affected.In conclusion, sildenafil has no effect on endogenous GI relaxation, but in combination with other drugs targeting NO/cGMP cascade or in case of elevated NO production (e.g. inflammation), GI side-effects of PDE5 inhibition should be considered.

OS01-8
An extra kick from the giant muscle protein titin

W. A. Linke[1], J. A. Rivas-Pardo[2], E. C. Eckels[2], P. Kosuri[2], J. M. Fernandez[2]
[1]Ruhr University, Dept. of Cardiovascular Physiology, Bochum, Germany
[2]Columbia University, Biology, New York, United States

Current theories of muscle contraction propose that the power stroke of a myosin motor is the sole source of mechanical energy driving the sliding filaments of a contracting muscle. These models exclude titin, the largest protein in the human body, which determines the "passive" elasticity of muscle tissue. Here, we show that stepwise unfolding/folding of titin immunoglobulin-like (Ig) domains occurs in the elastic I-band region of intact sarcomeres at physiological sarcomere lengths and forces of 6-8 pN. We use single molecule techniques to demonstrate that unfolded titin Ig domains undergo a spontaneous stepwise folding contraction at forces below 10 pN, delivering up to 105 pN/nm of additional contractile energy, which is larger than the mechanical energy delivered by the power stroke of a myosin motor. We show that this titin "kick" is activated equally for both weak and strong Ig domains when the force on titin drops to the 4-8 pN range, as it must happen when myosin motors engage during a contraction. Using the measured values of myofibril elasticity we predict that optimal delivery of the titin "kick" occurs at sarcomere lengths near the peak of the classical length-tension relationship of muscle contraction. Strikingly, only small changes in sarcomere length are needed to activate titin folding, fully consistent with the operating range observed in living muscles. Thus, it appears that the folding of titin Ig domains is an important, but so far unrecognized contributor to the force generated by a contracting muscle.

OS01-9
C-type- not atrial- natriuretic peptide stabilizes mast cells and attenuates microvascular leakage during ischemic reperfusion

W. Chen[1], K. Völker[1], F. Werner[1], A. Rabenhorst[2], K. Hartmann[2], M. Kuhn[1]
[1]Wuerzburg University, Physiology Institute I, Germany
[2]University of Cologne, Department of Dermatology, Germany

Background: Atrial- and C-type natriuretic peptides (ANP, CNP) are released from cardiac atria and vascular endothelium, respectively. They bind to their specific cyclic GMP (cGMP)-forming guanylyl cyclase receptors A and B. cGMP-dependent protein kinase I (cGKI) was demonstrated to stabilize mast cells (MC). MC degranulation is involved in postischemic reperfusion (I/R) injury. It is unknown whether and how ANP and/or CNP modify I/R-induced MC degranulation and microvascular permeability. Here we combined intravital microscopy of mouse cremaster microcirculation with experiments on cultured MCs to address these questions. **Methods and Results:** I/R (vs sham) stimulated the degranulation of resident perivascular MC and FITC-dextran extravasation from capillaries and postcapillary venules indicating vascular leakage. Specifically in mice without connective MCs, I/R did not stimulate vascular leakage, which indicated that MCs are critically involved in ischemic inflammation. Pharmacologically local ANP superfusion during I/R significantly attenuated vascular leakage but not MC degranulation. These anti-inflammatory actions of ANP were abolished in mice with endothelial cell restricted deletion of GC-A. Notably CNP decreased both MC degranulation and vascular leakage. Then we used the transgenic mice with fluorescent GFP-expressing MCs to demonstrate that CNP local pretreatment did not change the number of the total resident MCs but reduced the number of the degranulated MCs. These CNP actions were reproduced with the cGKI-stimulator 8-Br-cGMP. The protective CNP effects

were independent of endothelial cGKI, since they were preserved in mice with endothelial cGKI deletion. Accordingly, our *in vitro* studies demonstrated that CNP, but not ANP, provoked cGMP formation in human MCs (HMC-1.1 line, Dr. Butterfield) and primary cultured murine bone marrow MCs. This was associated with phosphorylation of the cytoskeleton-associated vasoactive stimulated phosphoprotein at Ser-237. **Conclusion:** Our study demonstrates distinct cell-specific effects of NPs. CNP stabilizes resident MCs and thereby reduces postischemic vascular leakage. ANP prevents vascular leakage via endothelial actions. Our future studies will attempt to dissect the MC signaling pathways and the possible clinical implication.

OS01-10
Contribution of myogenic response to peripheral vasoconstriction during orthostatic challenge

H. Habazettl[1], A. Schwarz[1], M. Nordine[1], E. Mulder[2], H. - C. Gunga[1], O. Opatz[1]
[1]Charité Universitätsmedizin Berlin, Institute of Physiology, Germany
[2]Deutsches Zentrum für Luft- und Raumfahrt, Institut für Weltraumphysiologie, Köln, Germany

Objective: During orthostatic challenge alpha-adrenergically mediated sytemic vascular vasoconstriction contributes to maintenance of arterial pressure. We hypothesised that in the lower body myogenic vasoconstriction in response to increased arterial pressure contributes to increased vascular resistance. **Methods:** 13 healthy subjects of either sex underwent two 4 minute periods of orthostatic challenge on a short arm human centrifuge at +1 Gz and +2 Gz, each at foot level. Skin perfusion was measured by laser-Doppler at three sites along the body axis: upper arm, thigh, and pretibial skin. In addition skin perfusion was mapped by laser-Doppler imaging in a pretibial control region and an adjacent region iontophoretically treated with the alpha-receptor antagonist urapidil. **Results:** At +1 Gz, skin vascular conductance index (VCI, skin perfusion divided by mean arterial pressure) remained essentially unchanged at the upper arm, decreased by 0.06 PU/mmHg at the thigh, by 0.11 PU/mmHg in pretibial skin and remained at these levels at +2 Gz. In the control region VCI decreased from 0.77±0.06 (mean±SEM) to 0.59±0.04 and 0.60±0.04 PU/mmHg at, respectively +1 and +2 Gz. In the urapidil treated region VCI remained essentially unchanged: 1.54± 0.20, 1.70±0.25, and 1.82±0.28 PU/mmHg at, respectively, 0, +1, and +2 Gz. **Conclusion:** The increase in vasoconstriction along the body axis, which parallels the increase in local arterial pressure, indicates a marked contribution of myogenic constriction in the lower body to overall increase in vascular resistance. This notion is also supprted by maintenance of vascular resistance in urapididl treated skin despite the marked increase in local perfusion pressure. Deconditioning of this mechanism by pressure unloading in the lower body might to orthostatic dysfunction after prolonged bed rest.

Oral Session 02
Hypoxia I

OS02-1
The oxygen sensor PHD2 affects cell migration, energy metabolism and mitochondrial function in macrophages

A. Guentsch[1], A. Beneke[1], K. Farhat[1], L. Swain[1], A. Hillemann[1], S. Nagarajan[1], J. Dudek[2], A. Shah[3], D. Katschinski[1]
[1]Georg-August Universität Göttingen, Cardiovascular Physiology, Germany
[2]Georg-August Universität Göttingen, Biochemistry, Germany
[3]King´s College London, Cardiovascular Division, United Kingdom

Macrophages are commonly found in infected/inflamed and ischemic tissues including the infarcted heart. Inflamed and ischemic areas are characterized by hypoxia. Macrophages are significantly involved in ischemic tissue remodeling, which is important for reconstitution of the affected organ. For this macrophages have to enter the hypoxic tissue from the well oxygenated blood stream. Like other cells, macrophages are able to adapt rapidly to low oxygen concentrations via the hypoxia inducible factor (HIF)-pathway. We analysed the basal expression levels of the three oxygen-sensing prolyl-4-hydroxylase domain enzymes (PHDs) in bone marrow derived macrophages (BMDM) and found that PHD2 is expressed most abundantly compared to PHD1 and PHD3. To analyse the impact of PHD2 for macrophage function, we established myeloid specific conditional PHD2 knock-out mice ($Phd2^{flox/flox}$ x $LysMCre^{+/-}$) and additionally stably transduced RAW cells expressing a PHD2 shRNA construct. In PHD2-deficient BMDMs and RAW cells normoxic stabilization of HIF-1α was achieved. The corresponding induction of HIF-target genes as GLUT1, Cox4.2 and the pyruvate dehydrogenase kinase-1 (PDK1) resulted in a metabolic reprogramming, which is reminiscent of the “Warburg effect”. Metabolic alterations were associated with decreased ATP and increased lactate levels. In line with the anaerobic reprogramming, PHD2-deficient cells demonstrated a decreased oxygen consumption rate and increased glycolytic capacity. These changes were associated with a migration and phagocytosis defect.
PDK1 is the key enzyme for the metabolic switch during hypoxia. Pharmacological (DCA) and genetic (siRNA) inhibition of PDK1 reversed the metabolic phenotype of PHD2-deficient cells. Furthermore, the migration and phagocytosis defects were partly restored by PDK1 inhibition.
The identified metabolic reprogramming with the resulting functional impairment of the macrophages is important for cardiac remodelling after myocardial ischemia since the invasion of macrophages after LAD ligation was altered in $Phd2^{flox/flox}$ x $LysMCre^{+/-}$ mice. Furthermore, these mice had a significantly impaired cardiac function.
Taken together, our data indicate that PHD2 influences macrophage function by modulating the migration capacity of the cells based on changes in energy metabolism and mitochondrial function. These metabolic alterations are at least partly dependent of the induction of PDK1 and affect cardiac remodelling after myocardial infarction.

OS02-2
Hypoxia-induced myeloid cell function through hypoxia inducible factor 1 impairs the clinical course of experimental inflammatory bowel disease

V. Reichmann, S. Winning, J. Fandrey
Institute of Physiology, University of Duisburg-Essen, University Hospital Essen, Germany

Question: Inflammatory bowel disease (IBD) comprises Crohn’s disease and ulcerative colitis and affects up to 1 in 200 individuals of the Northern European region. The precise cause of IBD still remains unknown but the adaptive as well as the innate immune response play an important role. Chronically inflamed tissue sites are often hypoxic relative to healthy tissue coining the term inflammatory hypoxia. Hypoxia inducible factors (HIFs) regulate gene expression under hypoxia and have been shown to be involved in the pathogenesis of IBD. The protective role of HIF-1α in epithelial cells, T-cells and DCs during experimental colitis has already been demonstrated. Among others HIF-1 is essential for myeloid cell life span and function during inflammation. We investigated the role of myeloid HIF-1α in the pathogenesis of IBD with special regard to their function as coordinators of the immune response. **Methods:** Mice with a conditional knockout of HIF-1α in myeloid cells (LysMcre/$HIF1\alpha^{+f/+f}$) and their HIF-1α expressing siblings ($HIF\text{-}1\alpha^{+f/+f}$) were examined *in vivo* in a Dextran Sodium Sulfate (DSS) induced model of IBD. **Results:** DSS-experiments provide evidence that LysMcre/$HIF\text{-}1\alpha^{+f/+f}$ mice deficient in functional HIF-1 in myeloid cells show a milder disease with less weight loss and lower inflammatory parameters when compared to $HIF\text{-}1\alpha^{+f/+f}$ control mice. Colons of LysMcre/$HIF\text{-}1\alpha^{+f/+f}$ mice comprised lower numbers of inflammatory immune cells and a decreased expression of proinflammatory cytokines compared to those of control mice. **Conclusions:** These results indicate that HIF-1 acts as a proinflammatory regulator of myeloid cells during the course of IBD. Thus, specific inhibition of myeloid HIF-1 could provide a new therapeutic option.

OS02-3
Characterisation of the SDS-PAGE resistant protein:protein heterodimer FIH:OTUB1 – Implications for oxygen sensing?

C. Pickel[1,2], R. H. Wenger[1,2], C. Scholz[1]
[1]University of Zurich, Institute of Physiology, Switzerland
[2]Zurich Center for Integrative Human Physiology (ZIHP), Switzerland

Oxygen deprivation (hypoxia) frequently occurs in health and disease and represents a life threatening condition, if not accounted for. Metazoans have developed a regulatory system that allows them to adapt to changes in tissue and cellular oxygen levels. The asparagine hydroxylase factor inhibiting HIF (FIH), one of four known oxygen-sensing enzymes, regulates the transcriptional activity of the hypoxia-inducible factor (HIF), the master regulator of the cellular adaptation to hypoxia. But FIH has also HIF-independent functions. We recently identified ovarian tumour domain containing, ubiquitin aldehyde binding protein 1 (OTUB1) as novel FIH substrate. FIH hydroxylates this ubiquitously expressed deubiquitinase on asparagine 22 (N22), which impacts on cellular energy metabolism, possibly through a hydroxylation-dependent change of OTUB1 substrate targeting. Surprisingly, we observed an unusually strong interaction between FIH and OTUB1, resulting in a SDS-PAGE resistant protein:protein complex. A similarly strong interaction has recently been described for the prolyl hydroxylase OGFOD1 and its substrate RPS23. However, the implication of heterodimer formation is unknown. Further analysis of the FIH:OTUB1 heterodimer demonstrated that it is resistant to different disulphide bridge-reducing agents, suggesting an interaction between FIH and its substrate other than through disulphide bonds. Interestingly, mutation of the hydroxylation acceptor site N22 in OTUB1 prevented the formation of the SDS-PAGE resistant heterodimer, indicating that complex formation depends on N22 and might therefore also depend on FIH enzymatic activity. Immunoprecipitation showed that around 50% of FIH:OTUB1 interactions consist of the stable heterodimer complex. OTUB1 therefore potentially disrupts endogenous FIH homodimerisation which is known to be essential for FIH activity. Current investigations analyse the dependence of heterodimer formation on FIH enzymatic activity. Moreover, we will assess a possible OTUB1-dependent change of FIH activity by mammalian two-hybrid assays. Overall, this unusually strong interaction between OTUB1 and FIH indicates that the FIH substrate OTUB1 also affects the oxygen-sensing hydroxylase, which may have important implications for oxygen sensing and signalling.

OS02-4
Prolyl-4-hydroxylase domain enzymes 2 and 3 differentially regulate the inflammatory response in a murine model of hind limb ischemia

A. Beneke, L. Swain, D. Katschinski
University Medical Center Göttingen, Cardiovascular Physiology, Germany

Background: When cells become hypoxic they stabilize hypoxia-inducible factor (HIF), a key regulator for the transcription of genes important for adaptation to low oxygen levels. Prolyl-4-hydroxylase domain enzymes (PHD) 1-3 regulate the stability of the α-subunit of HIF by oxygen-dependent hydroxylation, thereby working as cellular oxygen-sensors. Pathologic ischemia can occur in tissues after blockage of blood vessels and commonly leads to tissue damage which triggers an innate immune response. Macrophages are extremely versatile, supporting both inflammation and wound healing processes during the course of sterile inflammation. For PHD2 a clear impact on the macrophage-mediated arteriogenic response has been demonstrated after hind limb ischemia in mice (Takeda et al., 2011) We hypothesized that PHD2 and PHD3 differentially regulate the inflammatory

response and organ recovery in a murine model of hind limb ischemia. **Methods:** Myeloid-specific PHD2 and 3 knockout mice (LysMCre^{+} x PHD2$^{fl/fl}$ or 3$^{fl/fl}$ mice, short PHD2$^{-/-}$, PHD3$^{-/-}$) were used in this study. Hind limb ischemia was induced by ligation and excision of the femoral artery. Blood flow recovery was analyzed until day 28 after surgery via laser Doppler imaging. Motor function was analyzed using a RotaRod system. Tissue-infiltrating leukocytes were analyzed via flow cytometry of hind limb muscles within 7 days after surgery. RNA from FACS-sorted macrophages isolated from the ischemic skeletal muscles were used for whole RNA sequencing. **Results and Conclusion:** Macrophages of PHD3$^{-/-}$ but not PHD2$^{-/-}$ mice showed a faster clearance from the affected skeletal muscle compared to WT litter mates with a higher expression of the anti-inflammatory M2-marker CD206, indicating a faster initiation of wound healing. Whole RNA sequencing from FACS-sorted PHD3$^{-/-}$ macrophages showed a differential regulation of inflammatory and NF-κB-related genes. However, blood flow recovery and motor function were not different between PHD3$^{-/-}$ mice and WT littermates. We are currently analyzing the extent of fibrosis 28 days after surgery. Taken together our data indicates that the function of PHD2 versus PHD3 in macrophages is non-redundant.

OS02-5
Inhibition of the nucleotide pool sanitizing enzyme MTH1 augments genotoxic effects of ionizing radiation and hypoxia on tumor cells

M. Pompsch[1], U. Brokmeier[1], H. Riffkin[1], P. Kranz[1], M. Baumann[1], K. Göpelt[1], F. Claßen[1], A. Wolf[1], U. Berglund[2], T. Helleday[2], E. Metzen[1]
[1]Universtiy of Duisburg-Essen, Institute of Physiology, Germany
[2]Karolinska Institutet, Stockholm, Sweden

MTH1 is an enzyme that removes oxidized dNTPs from the precursor nucleotide pool. 8-oxo-dGTP and 2-OH-dATP are produced due to increased reactive oxygen species (ROS) levels in tumor cells and lead to base-pairing mismatches and cell death if incorporated into DNA during replication. However, because of the usually moderate amount of ROS in non-tumor cells, MTH1 is specifically important in tumor cells and therefore an interesting target for cancer therapy. Since the influence of ionizing radiation (IR) and hypoxia on the ROS level of tumor cell is still controversial, the role of MTH1 under these conditions is also unclear. Hence, the purpose of this project was to investigate whether IR enhances the efficacy of treatment with the MTH1-inhibitor TH588 and whether hypoxic tumor cells are also affected. To assess the therapeutic potency of TH588, HCT116 colon carcinoma cells were used. In normoxia, significant TH588 effects on cell viability were detectable at 5µM. In hypoxia, however, viability was only decreased after TH588 treatment at concentrations higher than 10µM. Caspase-3-activity and PARP cleavage gave similar results. MTT assays, caspase 3 activity and PARP-cleavage revealed little or no additional effect of TH588 treatment after irradiation. In contrast, clonogenic survival as determined by colony formation assay was significantly reduced. To verify the inhibitor results, knockdown of MTH1 was performed via lentiviral transduction. Knockdown was performed in the cell lines HCT116 and SW480. The efficiency was 70-90%. MTH1 knockdown did not have a significant effect on viability, cell death or clonogenic survival. The differences between inhibitor and knockdown results may indicate that residual amounts of MTH1 were sufficient to maintain enzyme function in the knockdown experiments. Overall, the results indicate that TH588 indeed has a cytotoxic effect on hypoxic cells, even though higher concentrations are necessary as compared to normoxia. Because combination of MTH1-inhibition with irradiation decreased long term tumor cell survival, the efficacy of ionizing radiation may be augmented by adjuvant treatment with TH588.

OS02-6
Estrogen-dependent downregulation of hypoxia-inducible factor (HIF)-2α in invasive breast cancer cells

J. H. Fuady[1], K. Gutsche[1], S. Santambrogio[1], Z. Varga[2], D. Hoogewijs[3], R. H. Wenger[1]
[1]University of Zurich, Institute of Physiology, Switzerland
[2]University Hospital Zurich, Institute of Surgical Physiology, Switzerland
[3]University of Duisburg-Essen, Institute of Physiology, Germany

The involvement of estrogen (E2) and hypoxia in the tumor progression is well established. Hypoxia has been reported to activate and degrade estrogen receptor alpha (ERα) in breast cancer cells. Furthermore, E2 has been shown to regulate hypoxia-inducible factor (HIF)-1α protein, but its role in mediating HIF-2α remains largely unexplored. In this study, we found that both HIF-2α mRNA and protein were down-regulated in ER-positive but not ER-negative breast cancer cells upon treatment with E2. The analysis of 690 samples derived from 608 mixed and 82 triple-negative breast cancer patients revealed that high HIF-2α tumor levels are associated with a better prognosis in human epidermal growth factor receptor 2 (HER2)-positive patients. Consistently, triple-positive breast cancer cells displayed less pronounced downregulation of HIF-2α by E2. Inhibition of histone deacetylases (HDACs) indicates that the E2 mediated decrease in HIF-2α mRNA is due to transcriptional repression. A functional estrogen response element (ERE) was identified in the first intron of *EPAS1*, suggesting transcriptional co-repressor recruitment by ERα. Our results demonstrate a novel modulation of HIF-2α in breast cancer cells and might partially explain the association between high HIF-2α and better prognosis in triple-positive breast cancer patients.

OS02-7
Controlling the gates by nuclear import receptors: Targeting nuclear transport affects HIF-dependent hypoxia response

F. K. Kosyna, M. Nagel, W. Jelkmann, R. Depping
University of Lübeck, Institute of Physiology, Center for Structural and Cell Biology in Medicine, Germany

The transcriptional response to hypoxia is controlled by hypoxia-inducible factors (HIFs). These heterodimeric transcription factors consist of one out of three different O_2-labile α-subunits and a more constitutive HIF-1β subunit. In the presence of O_2, the HIF-α subunit is hydroxylated by specific prolyl-4-hydroxylase domain proteins (PHD1, PHD2, and PHD3) and an asparaginyl hydroxylase (factor inhibiting HIF-1, FIH-1), resulting in recognition by von Hippel-Lindau protein, ubiquitination and proteasomal degradation. HIF-dependent transcription depends on intracellular trafficking of all of the involved “players”, the HIF-α and HIF-β subunits and of the HIF-α-specific hydroxylases. Subcellular logistics of hypoxia sensing proteins require a number of nuclear transport receptors. However, nuclear import of HIF-1α mainly depends on nuclear localisation signals (NLS) and involves the classical nuclear import pathway via the importin α/β receptors. Specific inhibitors of nuclear import represent useful tools for analysing the importance of nuclear trafficking for HIF-dependent hypoxia response pathways. Strategies to develop pharmaceuticals which modulate nuclear transport events are in progress. Currently, the best-characterised available compounds for inhibiting nuclear transport prevent binding between the nuclear export receptor and its cargo proteins. Very recently, the drug Ivermectin has been identified as a specific inhibitor of nuclear import. Ivermectin specifically inhibits importin α/β-dependent import with no effects on a range of other nuclear transport pathways. Therefore, we evaluated the physiological activity of Ivermectin in the hypoxia response pathway. *In vitro* binding studies revealed that treatment with Ivermectin decreases binding activity of HIF-1α to the importin α/β-heterodimer. Moreover, HIF-1α nuclear localisation, nuclear HIF-1α protein levels, HIF-target gene expression, as well as HIF-transcriptional activity are reduced upon Ivermectin treatment. For the first time, we demonstrate the effect of specific importin α/β-inhibition on the hypoxic response on the molecular level.

OS02-8
The transcription factor WT1 regulates gonadal expression of the receptor for vascular endothelial growth factor A (KDR, VEGFR2) in a sex-specific manner

K. M. Kirschner[1], L. J. Rudigier[1], L. K. Sciesielski[2], H. Scholz[1]
[1]Charité-Universitätsmedizin Berlin, Inst. für Vegetative Physiology, Germany
[2]Humboldt Universität zu Berlin, Institut für Biologie / Experimentelle Biophysik, Germany

KDR, the receptor for Vascular Endothelial Growth Factor A (VEGFA), is an organizer of vascular development. Beside its expression on invading endothelial cells, the VEGF receptors FLT1 and KDR have been detected in Sertoli and Leydig cells of the human adult testis. In the testis, seminiferous cord formation is closely linked to vasculogenesis. Seminiferous cord formation is also highly dependent on expression of the transcription factor WT1 (Wilms tumor 1). Since the *Vegf* gene has previously been identified as a transcriptional target of WT1 we asked the question whether WT1 also regulates *Kdr* expression.
Our data indicate that the *Kdr* gene is indeed regulated and bound by WT1. In a genome wide analysis of potential WT1 transcriptional targets in mesonephros-derived M15 cells the *Kdr* gene showed significant changes in expression. *Kdr* expression in M15 cells incubated with antisense *Wt1* siRNA was significantly downregulated by [h1] 69 ± 39% compared to M15 cells treated with non-targeting siRNA. We confirmed these data by analyzing *Kdr* expression in a human cell culture system (U2OS osteosarcoma cells) with tetracyclin-repressed expression of the WT1(+KTS) or WT1(-KTS) isoform. Only the WT(-KTS) splice variant induced *Kdr* expression. Chromatin immunoprecipitation was performed to analyze binding of WT1 to the *Kdr* gene. In U2OS cells with induced expression of WT1(KTS) the *Kdr* promoter region was significantly enriched, whereas U2OS cells expressing the WT1(+KTS) isoform showed no enrichment.[h2]
To evaluate these *in vitro* data in organotypic cultures the gonads of mouse embryos (E12.5) were isolated and incubated *ex vivo* with either a specific *Wt1* antisense vivo-morpholino or a mismatch vivo-morpholino. Knockdown of WT1 with the specific antisense vivo-morpholino significantly reduced *Kdr* expression in embryonic ovaries but not in testes. Furthermore, expression of *Sox9*, a Sertoli cell specific regulator of testis development, was significantly reduced in testes treated with *Wt1* vivo-morpholino but not in ovaries. Inhibition of KDR signaling in both, testes and ovaries, significantly increased *Sox9* expression.
These data demonstrate that WT1 expression in the developing gonads is regulated in a sex-sepcific manner. It is suggested that WT1 activates KDR expression in the ovary to down-regulate expression of the testis-specific developmental regulator SOX9.

Oral Session 03

Ion Channels I: TRP & Calcium Channels

OS03-1
Conduction disorder caused by a mutation in *POPDC2*, a novel modulator of the cardiac sodium channel SCN5A

S. Rinné[1], B. Ortiz-Bonnin[1], B. Stallmeyer[2], R. F. R. Schindler[3], A. K. Kiper[1], S. Dittmann[2], C. Friedrich[2], S. Zumhagen[2], S. L. Simrick[3], W. González[4], T. Brand[3], E. Schulze-Bahr[2], N. Decher[1]

[1]Philipps-University Marburg, Institute for Physiology and Pathophysiology, Germany

[2]University Hospital Münster, Institute for Genetics of Heart Diseases, Department of Cardiovascular Medicine, Germany

[3]Imperial College, Heart Science Centre, National Heart and Lung Institute, Harefield, United Kingdom

[4]University of Talca, Center for Bioinformatics and Molecular Simulations, Chile

The genetics of cardiac conduction disorders, in particular of atrioventricular (AV) node dysfunction, are poorly understood and only a few genes are known to be involved in inherited forms of AV block. Recently, POPDC proteins were described to modulate the current density of the K_{2P} channel TREK-1 and *POPDC2* knock-out mice showed an age dependent sinoatrial bradycardia. Not only because of this strong phenotype it has been previously speculated that POPDC proteins might also modulate other ion channels. Using whole exome sequencing (WES) of twins with severe AV block in third degree, we identified a *POPDC2* mutation. The heterozygous nucleotide substitution (c.563G>A) resulted in the insertion of a premature stop codon at position 188 of POPDC2, leading to a deletion within the putative cAMP binding domain. As the mutation did not affect the TREK-1 current modulation, we used co-expression experiments to functionally screen for channels modulated by POPDC2. We found that POPDC2 modulates and co-immunoprecipitates with the cardiac sodium channel SCN5A. Molecular modelling and cAMP affinity precipitation experiments suggested that the W188* mutant still binds cAMP. POPDC2 reduces the surface expression of SCN5A, an effect which is antagonized in a cAMP-independent manner by co-expressing the channel with a mixture of POPDC2 and W188*. Consistent with the observed AV block, we found by QPCR experiments that POPDC2 is highly expressed in the human AV node. In addition, SCN5A, HCN4 and POPDC2 are co-expressed in the perinodal region of the AV node, but also within the His bundle as well as the surrounding working myocardium of the mouse heart. Patch-clamp experiments of HL-1 cells expressing the W188* mutant showed a decreased action potential frequency, with an intact modulation of the beating frequency by isoproterenol, consistent with the phenotype of the patients. Thus, POPDC2 is a previously unrecognized modulator of the cardiac sodium channel SCN5A and a novel gene for inherited forms of conduction disorders.

OS03-2
Deletion of the TRPV4 cation channel in mice does not cause marked changes of skeletal muscle structure: a comparison with dystrophic *mdx* mice

R. Dreist, M. Krautwald, **H. Brinkmeier**

University Medicine Greifswald, Institute of Pathophysiology, Karlsburg, Germany

A key requirement for the maintenance of muscle function and health is the sensitive regulation of intracellular Ca^{2+} level in skeletal muscle fibers. The dysregulation of Ca^{2+} entry via the plasma membrane and an increased intracellular calcium concentration are supposed to cause muscle weakness and fiber degeneration in Duchenne Muscular Dystrophy and its mouse model *mdx*. Among the Ca^{2+} entry pathways cation channels of the *transient receptor potential* (TRP) ion channel family have become promising candidates contributing to normal and abnormal muscular Ca^{2+} homeostasis. To elucidate the role of the TRPV4 cation channel in skeletal muscle in more detail, we analyzed development and structure of muscles from TRPV4 knock out mice. Therefore, the lower limb muscles *soleus*, *extensor digitorum longus*, and *tibialis anterior* as well as the diaphragm of 3-months old C57BL/6J wild type and TRPV4 knock out mice (n=4 each) were histologically characterized by collagen content, fiber size and fiber type composition in comparison with dystrophic muscles of *mdx* mice and its corresponding wild type C57BL/10ScSn (n=4 each). Whereas muscles of *mdx* mice showed a typical increase in fiber size variation (*soleus*: BL/10ScSn 36.6±7.5 µm vs. *mdx* 37.6±13.6 µm) and a nearly twofold higher collagen content (*soleus*: BL/10ScSn 5.15±1.59% vs. *mdx* 10.63±2.48%) characterizing the dystrophic phenotype, no significant alterations could be observed in muscles of TRPV4 knock out mice (*soleus*: 42.0±8.7 µm in fiber diameter and 5.64±1.86% collagen) or the BL/6J wild type (*soleus*: 36.0±7.3 µm in fiber size and 5.48±1.02% collagen) respectively. Also the proportions of the different fiber types were not affected in muscles lacking TRPV4. In the *soleus* for example the predominant fiber types I, IIA and IIX represent 35.0±3.9%, 47.0±15.0% and 16.7±12.7% of all fibers in BL/10ScSn and 35.5±6.3%, 44.4±19.3% and 17.8±22.2% in the BL/6J wild type. A similar composition could be observed in the *soleus* of TRPV4 knock out mice (type I, 34.7±4.3%; IIA, 37.5±14.6%; IIX, 24.9±12.5%) indicating that there is no significant difference between the two mouse strains nor introduced by TRPV4 deletion. On the contrary the *soleus* of *mdx* showed an increase of MHCI fibers (53.1±13.0%) and a decrease of MHCIIX fibers (8.4±4.8%). Our results show that the absence of functional TRPV4 cation channels has no dramatic effects on muscle development and structure and causing less pronounced changes than for example a calcium overload, which leads to a fast-to-slow switch of fiber types in dystrophic muscles of *mdx* mice.

OS03-3
Role of TRPC1 channels in pressure-mediated activation of murine pancreatic stellate cells

B. Fels, A. Schwab

University of Münster, Institute of Physiology II, Germany

Pancreatic ductual adenocarcinoma (PDAC) is a highly aggressive malignancy. It is characterized by a dense fibrotic stroma, called “desmoplasia”, primarily formed by activated pancreatic stellate cells (PSCs). Desmoplasia contributes to high pancreatic tissue pressure, which is able to directly activate PSCs. Activation of PSCs leads to an enhanced secretion of cytokines, growth factors and extracellular matrix compounds, affecting the density of the tumor microenvironment and resulting in further increase of tissue pressure. This perpetuates the recruitment of PSCs and contributes to tumor progression. In this work, we studied the effect of pressure incubation on the function of murine PSCs. We postulate that the putatively mechanosensitive canonical transient receptor potential channel 1 (TRPC1) is involved in the pressure-sensing mechanism and thereby mediates pressure-induced PSCs activation and migration.

We used primary PSCs isolated from WT and TRPC1-KO mice, pre-incubated for 24h under elevated pressure (100 mmHg). After pressurization, mRNA expressions of different mechanosensitive channels were profiled. In parallel, we monitored cell migration for 6h, using live cell imaging, and we measured calcium influx into PSCs after pressurization by means of the Mn^{2+} quench technique.

Pressurization leads to reduced mRNA expression of different mechanosensitive ion channels such as *Piezo1* (0.63; normalized expression level, compared to untreated control), *Trpm7* (0.58), *Trpv4* (0.04) and *Trpc1* (0.71). In TRPC1-KO PSCs, mRNA of most channels was repressed to a lesser extent, but did not reach the low WT expression levels. We show that TRPC1 channels play a role in mechano-sensing and migration of PSCs in response to elevated pressure. Pressurized WT PSCs migrate 65% faster than untreated cells (Δ velocity 0.15 µm/min). In contrast, pressure-incubated TRPC1-KO exhibit a lower increase in velocity of only Δ 0.1 µm/min. Migration velocity was 22% lower in TRPC1-KO than in WT after pressure pre-incubation. Additionally, pressure incubation leads to increased calcium influx into WT PSCs, which is virtually absent in TRPC1-KO cells.

We conclude that TRPC1 channels participate in the mechano-signaling and thereby influence the migratory activity of pressurized PSCs. Under control conditions, depletion of TRPC1 channels seems to be partially compensated by increased expression of other mechanosensitive ion channels like *Piezo1* or *Trpv4*. Nonetheless, knockdown of TRPC1 is sufficient to impair the pressure-induced migratory activity of PSCs, possibly by disturbing mechanically triggered calcium signaling.

OS03-4
The bovine analogue of TRPV3 conducts the NH_4^+ ion

K. Hille, G. Sponder, F. Liebe, **F. Stumpff**

Freie Universität Berlin, Institute for Veterinary Physiology, Germany

Introduction: Some 20 mol/day of ammonia are absorbed from the rumen of cattle in the form of NH_4^+, which decreases microbial protein yield, compromises protein efficiency, and leads to the pollution of the environment. The bovine representative of TRPV3 has emerged as a promising candidate gene (1), but there are no data concerning the permeability of these channels to NH_4^+. **Methods:** The bovine TRPV3 was co-expressed with green fluorescent protein (GFP) in HEK 293 cells using a bTRPV3Strep-IRES-GFP-vector (bTRPV3). The empty vector was expressed in controls (MT). Cells showing GFP fluorescence were studied using the patch clamp technique using various solutions. **Results:** The expression of bTRPV3 in plasma membrane was confirmed in Western blots of high-purity plasma membrane fractions of bTRPV3 cells, but not in MT controls. In whole cell experiments on both bTRPV3 cells (n = 21) and MT controls (n = 13) and both at -100 mV and at 100 mV, current was enhanced by superfusion with NH_4^+-Gluconate and rose significantly when divalent cations were removed from the bath. Currents for NH_4^+ and Na^+ were higher in bTRPV3, with differences reaching significance level after removal of divalent cations ($p < 0.05$ at +100 mV and $p = 0.055$ at -100 mV). Currents remained significantly higher in bTRPV3 after replacement of divalent cations in both NH_4^+ and Na^+ containing solutions. Membrane patches of bTRPV3 cells showed single channel events with 122 ± 8 pS for Na+ (n = 13) and 240 ± 4 pS NH_4^+ (n = 7). An intermediate value of 143 ± 17 pS was measured for the asymmetrical configuration with Na+ in the pipette and NH_4^+ in the bath (n = 11). **Conclusions:** In cells overexpressing bTRPV3, a conductance for Na^+ could be demonstrated with a magnitude similar to that of the human analogue. The permeability of this channel to NH_4^+ was significantly higher. TRPV3 may play an important role in the ruminal transport of ammonia and represents an interesting target gene for breeding or pharmacological modulation with the goal of reducing nitrogen wastage from livestock to the environment. **Funding:** „Akademie für Tiergesundheit“, German Academic Exchange Service (DAAD) with funds from the German Foreign Office

References

1) Rosendahl, J., Freie Universität Berlin: Berlin. 2014.

OS03-5
The photosensitization by 7-dehydrocholesterol activates TRPA1 and TRPV1 – connections to the Smith-Lemli-Opitz syndrome

C. Ciotu[1,2], A. Babes[1,2], M. Fischer[1]
[1]Institute of Physiology and Pathophysiology Friedrich-Alexander University Erlangen-Nuremberg, Germany
[2]Faculty of Biology, University of Bucharest, Department of Anatomy, Physiology and Biophysics, Romania

Question: Smith-Lemli-Opitz syndrome is a developmental disorder characterized by malformations, hypotonia, and an exaggerated erythemal response upon exposure to sunlight. The mechanism responsible for this photosensitivity is not yet fully understood. We aimed to assess the mechanism through which exposure to short wavelength light is related to the photosensitizing symptoms occurring in the Smith-Lemli-Opitz syndrome. The pathophysiology of this syndrome consists of a loss of function mutation of the enzyme reducing 7-Dehydrocholesterol (7-DHC), which can lead to a more than 1000-fold increase in 7-DHC plasma levels. **Methods:** Ratiometric calcium microfluorimetry of transfected HEK293t cells and mouse sensory neurons was used to investigate whether acute exposure or pre-exposure with 7-DHC can convey an enhanced sensitivity to light in the UVA range. **Results:** Human TRPA1-expressing HEK293t cells exposed to 360 nm and 7-DHC produced strong calcium responses in comparison to untransfected cells. Human TRPV1 caused less photosensitization under the same experimental conditions. Pre-exposure to 7-DHC for 2, 4, 6 and 15 hours lead to strong photosensitization in both TRPA1- and TRPV1-expressing cells. The light-evoked response in these cells was completely abolished by selective antagonists for TRPA1 (A967079) and, respectively, TRPV1 (BCTC). In DRG neurons, acute application of and 4-hour incubation with 7-DHC strongly potentiated light-evoked calcium transients in cultures obtained from wild type mice, effect which was markedly reduced in TRPA1 knockout mice. **Conclusions:** 7-DHC-induced photosensitization to UV light exposure is primarily mediated by TRPA1 and, to a lesser extent, by TRPV1.

OS03-6
A forward genetic screen identifies a Ca^{2+}-regulated mitochondrial metabolite carrier required for the establishment of left-right asymmetry

A. Hofherr[1], C. Seger[1], G. Walz[1], T. Watnick[2], M. Köttgen[1]
[1]Medical Center - University of Freiburg, Department of Medicine, Freiburg im Breisgau, Germany
[2]University of Maryland School of Medicine, Division of Nephrology, Baltimore, United States

TRPP2 is a cation channel that localizes to primary cilia and regulates developmental programs ranging from renal tubular morphogenesis to establishment of left-right asymmetry. Loss of TRPP2 function results in polycystic kidney disease and randomized left-right asymmetry. TRPP2-mediated Ca^{2+} signals regulate left-right asymmetry by sensing chemical or mechanical cues in cilia of vertebrate left-right organizers. But the molecular events translating TRPP2-mediated Ca^{2+} signaling into left-right asymmetry of vertebrate body plans are unknown.
Here we show that a Ca^{2+}-regulated mitochondrial metabolite carrier (MMC) constitutes an evolutionarily conserved core component of the TRPP2 signaling pathway. We conducted a large-scale forward genetic screen in *D. melanogaster* for mutants that phenocopy the TRPP2 loss of function phenotype. This screen identified a Ca^{2+}-dependent MMC as a putative downstream target of TRPP2. Ca^{2+} regulation of this MMC appears to be necessary *in vivo*, since loss of MMC in flies was rescued by expression of wild-type MMC, but not by MMC with EF-hand mutations, which abolish Ca^{2+} binding. To test the evolutionary conservation of this MMC in the TRPP2 signaling pathway we investigated its function in zebrafish. Like TRPP2, MMC is required for the determination of left-right asymmetry and acts upstream of the southpaw/nodal cascade. Rescue experiments in *Drosophila* and zebrafish suggest that MMC acts downstream of TRPP2, which is consistent with the Ca^{2+}-dependence of this mitochondrial carrier. To investigate the molecular function of MMC and TRPP2, we deleted the respective genes using TALEN technology in epithelial cells. Metabolic profiling and mass-spectrometry-based metabolomic analyses showed that TRPP2 and MMC knock-out cells display impaired mitochondrial metabolism and show concordant changes of several metabolites. Notably, the metabolic defects observed upon loss of TRPP2 or MMC do not affect ciliary motility in flies or zebrafish. We therefore propose that MMC-mediated metabolic signals are the missing link required to translate TRPP2-mediated Ca^{2+} signals in the left-right organizer into asymmetric gene expression controlling left-right asymmetry.

OS03-7
Differential control of intracellular Ca^{2+} signaling by anoctamins

I. Cabrita, R. Benedetto, P. Wanitchakool, L. Sirianant, K. Kunzelmann, R. Schreiber
University of Regensburg, Physiological Institute, Germany

Ist2, the yeast homologue of the mammalian Ca^{2+} activated Cl^- channel TMEM16A (anoctamin 1, ANO1), tethers the endoplasmic reticulum (ER) to the plasma membrane. ANO1 and ANO6 support Ca^{2+} signaling in intestine epithelial cells and osteoblasts, respectively. Sequestering of ER and Ca^{2+} signaling to plasma membrane compartments may also occur through anoctamins. We found that anoctamins either enhanced (ANO1, 5, 6, 10) or reduced (ANO4, 8, 9) localized Ca^{2+} signals triggered by activation of G-protein coupled receptors. ANO1 co-localized and interacted with IP_3 receptors, while ANO4 co-localized and interacted with SERCA, and inhibited filling of the ER Ca^{2+} store. The property of Cl^- channels of ANO1 and ANO4 is required for its Ca^{2+} signaling regulation and these proteins were found localized in distinctive lipid rafts. Attenuated Ca^{2+} signaling was found with siRNA knockdown of ANO6 and 10 and in renal epithelial cells from ANO10-/- mice. Anoctamins therefore control differential compartmentalized Ca^{2+} signaling as counter ion channels or tethering the ER to the plasma membrane.

References
Jin, X., Shah, S., Du, X., Zhang, H., & Gamper, N. (2014). Activation of Ca $^{2+}$-activated Cl –channel ANO1 by localized Ca $^{2+}$signals. *The Journal of Physiology,* n/a–n/a. http://doi.org/10.1113/jphysiol.2014.275107
Ousingsawat, J., Wanitchakool, P., Schreiber, R., Wuelling, M., Vortkamp, A., & Kunzelmann, K. (2015). Anoctamin-6 Controls Bone Mineralization by Activating the Calcium Transporter NCX1. *Journal of Biological Chemistry, 290(*10), 6270–6280. http://doi.org/10.1074/jbc.M114.602979
Schreiber, R., Faria, D., Skryabin, B. V., Wanitchakool, P., Rock, J. R., & Kunzelmann, K. (2014). Anoctamins support calcium-dependent chloride secretion by facilitating calcium signaling in adult mouse intestine. *Pflügers Archiv – European Journal of Physiology, 467(*6), 1203–1213. http://doi.org/10.1007/s00424-014-1559-2
Wolf, W., Kilic, A., Schrul, B., Lorenz, H., Schwappach, B., & Seedorf, M. (2012). Yeast Ist2 Recruits the Endoplasmic Reticulum to the Plasma Membrane and Creates a Ribosome-Free Membrane Microcompartment. *PLoS ONE, 7*(7), e39703–13. http://doi.org/10.1371/journal.pone.0039703

OS03-8
Differential accessibility to phospholipase C defines functional PI(4,5)P2 microdomains in the plasma membrane

M. G. Leitner, V. Thallmair, C. R. Halaszovich, D. Oliver
Philipps-University Marburg, Department for Neurophysiology, Germany

Cellular components of signalling pathways frequently colocalize into membrane microdomains. This subcellular organisation may be required for spatiotemporal control of the signalling machinery. Membrane phosphatidyl-(4,5)-bisphosphate ($PI(4,5)P_2$) plays a major role in a multitude of cellular processes, and thus analogous $PI(4,5)P_2$ microdomains may increase the specificity of $PI(4,5)P_2$ functions. However, the existence of distinct and functionally relevant $PI(4,5)P_2$ microdomains remains elusive.
We addressed functional $PI(4,5)P_2$ pools by using ion channels as biosensors. Reduction of $PI(4,5)P_2$ levels with the voltage-sensitive phosphatase, Ci-VSP, strongly inhibited KCNQ and Kir2.1 channels. In contrast, depletion of $PI(4,5)P_2$ by receptor-mediated activation of phospholipase C-β (PLC) selectively deactivated KCNQ channels, without affecting Kir2.1. Similarly, pharmacological and thus receptor-independent activation of PLC inhibited KCNQ channels exclusively. These results could not be explained by different $PI(4,5)P_2$ affinities of the ion channels, and thus strongly suggested the existence of distinct $PI(4,5)P_2$ domains. We further probed these microdomains by recruitment of the $PI(4,5)P_2$ 5-phosphatase Inp54 into biochemically defined membrane compartments. KCNQ channels were inhibited exclusively, when we recruited the phosphatase to lipid raft-associated compartments, but KCNQ channel activity was not affected upon phosphatase recruitment into the non-raft-associated microdomain. In contrast, Kir2.1 channels were inhibited selectively when the phosphatase was recruited into the non-raft compartment. These findings directly demonstrated two spatially distributed $PI(4,5)P_2$ compartments that probably correspond to biochemically defined lipid microdomains. Taking together, our results support the existence of at least two functionally distinct $PI(4,5)P_2$ pools in the plasma membrane. Only one of these pools may be accessible to PLC and also to KCNQ channels, whereas the other pool appears to be associated with Kir2.1 channels only.
This work was supported by a by research grants from the Deutsche Forschungsgemeinschaft to M.G.L. and D.O.

Oral Session 04
Cellular and Molecular Neuroscience I

OS04-1
FRS1l is a central determinant of AMPA-receptor biogenesis and linked to severe intellectual disability

A. Brechet[1], R. Buchert[2], J. Schwenk[1], S. Boudkkazi[1], G. Zolles[1], A. Kulik[1,3], L. Colleaux[4], R. A. Jamra[2], U. Schulte[1,3], B. Fakler[1,3]
[1]University of Freiburg, Institute for Physiology, Germany
[2]University of Erlangen, Institute of Human Genetics, Germany
[3]Center for Biological Signaling Studies (BIOSS), Freiburg, Germany
[4]INSERM UMR 1163, Paris-Descartes-Sorbonne University, Institute IMAGINE, France

AMPA-type glutamate receptors (AMPARs), key players in excitatory neuro-transmission in the brain, are macromolecular complexes whose properties and cellular functions are determined by the co-assembled constituents of their proteome. Here we identify AMPAR assemblies containing FRS1l/C9orf4 that are restricted to the endoplasmic reticulum and lack the core-subunits typical for AMPARs at the plasma membrane and the postsynaptic membrane. Bi-allelic mutations in the human FRS1l gene are associated with severe intellectual disability, cognitive impairment, speech delay and epileptic activity. Virus-directed deletion and overexpression of FRS1l in adult rats resulted in markedly reduced or increased amplitudes of the EPSCs without affecting their time course in all types of synapse or neurons investigated. Our results provide insight into AMPAR biogenesis and demonstrate its significance for synaptic transmission and higher brain function(s).

References
Schwenk J, Baehrens D, Haupt A, Bildl W, Boudkkazi S, Roeper J, Fakler B, Schulte U. *Regional diversity and developmental dynamics of the AMPA-receptor proteome in the mammalian brain.* Neuron. 2014; 84(1):41-54.
Schwenk J, Harmel N, Brechet A, Zolles G, Berkefeld H, Müller CS, Bildl W, Baehrens D, Hüber B, Kulik A, Klöcker N, Schulte U, Fakler B. *High-resolution proteomics unravel architecture and full molecular diversity of native AMPA receptor complexes.* Neuron 2012; 74(4):621-633

OS04-2
3D super-resolution mapping of synaptic proteins in brain tissue

S. Proppert[1], M. Pauli[1], M. M. Paul[1], A. - L. Sirén[2], M. Sauer[3], M. Heckmann[1]
[1]Institute of Physiology, Julius-Maximilian-University Würzburg, Department of Neurophysiology, Germany
[2]University Hospital Würzburg, Department of Experimental Neurosurgery, Germany
[3]Biocenter, Julius-Maximilian-University Würzburg, Department of Biotechnology and Biophysics, Germany

Localization microscopy (LM) more and more enters neurosciences as with its ability to map proteins with nearly molecular resolution it can nicely fill the gap between highest resolution electron microscopy (EM) and conventional fluorescence microscopy. Two key advantages of LM are its molecular specificity by using standard antibodies or toxins and the relatively fast acquisition of three-dimensional information (as compared to, e.g., EM array tomography).
3D imaging is especially interesting for the investigation of the distribution of synaptic proteins as in standard 2D-LM the measurement is prone to projection artifacts. For example, if we want to map the orientation and location of release sites relative to the cytoskeleton of the Active Zone this projection to one plane of the overall imaged volume may not give precise enough information about the underlying distribution whereas the gain in insight is significant when not only the spatial but also the axial distribution is precisely and accurately determined.
While first publications investigate synaptic proteins in neuronal cell culture [1] and brain tissue [2] we here assess the overall limitations and abilities of 3D-LM in the investigation of different specimen such as the neuromuscular junction in *Drosophila melanogaster* larvae [3] and the presynaptic cytoskeletal protein Bassoon in mouse brain. We show precise and accurate two-color-3D mapping of synaptic proteins in 1 µm tissue sections and imaging in depths of up to 20 µm. We also demonstrate that the approach is capable of imaging larger synapses in thicker slices by axially stacked image acquisition.

References

[1] Xu et al. - Actin, Spectrin, and Associated Proteins Form a Periodic Cytoskeletal Structure in Axons, Science, 25 Jan 2013, Vol 339, 452-456, DOI: *10.1126/science.1232251*
[2] Dani et al. - Superresolution imaging of chemical synapses in the brain, Neuron, 9 Dec 2010, Vol 68, 843-856, DOI: 10.1016/j.neuron.2010.11.021
[3] Ehmann et al. - Quantitative super-resolution imaging of Bruchpilot distinguishes active zone states, Nature Communications, 9 Jul 2014, Vol 5, DOI:10.1038/ncomms5650

OS04-3
Single action potentials trigger fast and clathrin-independent endocytosis at a central synapse

I. Delvendahl, S. Hallermann
Carl-Ludwig-Institute for Physiology, Leipzig, Germany

The fusion of neurotransmitter-filled vesicles during synaptic transmission is balanced by endocytotic membrane retrieval. However, the speed and mechanisms of synaptic vesicle endocytosis have remained controversial. Using time-resolved membrane capacitance measurements in intact central synapses, we show that single action potentials trigger very rapid endocytosis, retrieving fused membrane area with a time constant of 470 ms. This fast endocytosis is independent of clathrin, but mediated by dynamin and actin. In contrast, stronger stimuli evoke a slower mode of endocytosis that is clathrin-, dynamin-, and actin-dependent. Furthermore, the speed of endocytosis is highly temperature-dependent. These results demonstrate that distinct molecular modes of endocytosis with markedly different speed operate at a central synapse.

OS04-4
Dysfunction of thalamo-amygdala circuits and up-regulated TrkB/ERK-MAPK signaling leads to obsessive-compulsive-like behavior in SPRED2 KO mice

M. Ullrich[1], M. Weber[2], A. Post[2], S. Popp[3], J. Grein[1], H. Guerrero[1], N. Üçeyler[3], K. Schuh[1]
[1]University of Wuerzburg, Institute of Physiology, Germany
[2]University of Frankfurt, Germany
[3]University of Wuerzburg, Germany

Obsessive–compulsive disorder (OCD) is a common psychiatric disorder, which is marked by persistent intrusive thoughts and repetitive ritualized behaviors and affects about 2 % of the human population. Genetic mutations, dysfunction of cortico-striatal circuits and dysregulated synaptic neurotransmission have been implicated in pathogenesis of OCD. The underlying mechanisms, however, remain quite unclear to date. Here we show that the deficiency of SPRED2, a protein ubiquitously expressed in brain and a potent suppressor of Ras/ERK-MAPK cascades, causes OCD-like behavior in mice.
SPRED2 KO mice developed excessive self-grooming leading to severe facial lesions despite normal skin sensitivity. Obsessive-compulsive grooming behavior was accompanied by reduced anxiety behavior as detected by behavioral standard tests and could be significantly alleviated by treatment with the selective serotonin reuptake inhibitor fluoxetine. In addition to the prevalent involvement of cortico-striatal circuits, electrophysiological measurements revealed an altered synaptic transmission also at thalamo-amygdala synapses of SPRED2 KO mice. The detected increase in synaptic efficacy was accompanied by dysregulated expression of various pre- and postsynaptic proteins in the amygdala. The changed protein expression in SPRED2 KOs was elicited by alterations of gene transcription and triggered upstream by upregulated TrkB/ERK-MAPK signaling

the amygdala. Using the MEK inhibitor selumetenib, we suppressed TrkB/ERK-MAPK pathway activity *in vivo* and also reduced the OCD-like grooming behavior in SPRED2 KOs. We identified SPRED2 itself as a direct target of BDNF/TrkB cascades, which was phosphorylated upon BDNF-stimulated TrkB activation *in vitro*.
Together, our study unravels SPRED2 as a considerable new genetic factor, TrkB/ERK-MAPK signaling as a novel regulating pathway and thalamo-amygdala synapses as critical circuitry involved in the development of OCD.

OS04-5
Coordination of innate behaviours by GABAergic cells in lateral hypothalamus

M. Carus Cadavieco, M. Gorbati, S. van der Veldt, F. Ramm, F. Bender, A. Ponomarenko, **T. Korotkova**
Leibniz-Institut für Molekulare Pharmakologie/NeuroCure Cluster of Excellence, Behavioral Neurodynamics Group, Berlin, Germany

Questions: Lateral hypothalamus (LH) is crucial for the regulation of innate behaviors, including food intake and sleep-wake cycle. We have recently shown that LH cells regulate locomotion (Bender et al., Nature Communications, 2015) and arousal (Gutierrez Herrera et al., Nature Neuroscience, in press), yet role of LH cells in feeding behavior as well as temporal coordination of hypothalamic neuronal populations remains elusive. **Methods:** Here we used combination of high-density electrophysiological recordings and optogenetics in behaving mice. Excitatory (ChR2 or ChETA) or inhibitory (halorhodopsin, eNpHR3.0) opsins were expressed in LH of VGAT-Cre mice to ensure selective targeting of GABAergic cells. Recordings of neuronal activity and optostimulation were performed in various behavioral paradigms assessing innate behaviors, including a goal-directed behavior and a "free-will" environment where an animal could choose between compartments with food, water, enriched environment and home-cage like enclosure. **Results and conclusions:** We found that optogenetic stimulation of LH GABA cells at various frequencies as well as stimulation of projections of these neurons changed transitions between innate behaviors. Activation of LH GABA neurons increased food intake in satiated mice and decreased latency to feeding whereas optogenetic inhibition of LH GABA cells decreased feeding even despite food deprivation. Furthermore, neuronal activity of LH neurons as well as coordination between LH and its inputs were behavior- and state-dependent. To investigate neuronal mechanisms which underlie the effect of LH GABA cells on feeding, we analyzed how the activation of LH GABA neurons affects the functional LH subgroups, differentially related to feeding. We analyzed behavior-dependent activity of recorded LH cells and found 3 functional subgroups: cells which were preferentially active in the feeding zone (FZ, food-active cells), cells which were preferentially active in non-food compartment (non-FZ) and cells which activity did not show preference to a particular part of enclosure (feeding-indifferent, FI cells).We further found that optogenetic activation of LH GABA cells differentially affected these subgroups: FZ cells were activated by the LH GABA stimulation, whereas non-FZ were inhibited by it, and feeding-indifferent cells were not affected. Thus, activation of LH GABA cells amplified activity of feeding-active cells and inhibited activity of cells which were selectively active elsewhere. This reorganization of LH cells' activity upon LH GABA cells activation may underlie their actions on innate behaviors.
Funding: This work was supported by the Deutsche Forschungsgemeinschaft (DFG; Exc 257 NeuroCure, TK and AP, SPP1665, AP) and The Human Frontier Science Program (HFSP; RGY0076/2012, TK)

References

Bender F*, Gorbati M*, Carus Cadavieco M, Denisova N, Gao X, Holman C, Korotkova T*§, Ponomarenko A*§. Theta oscillations regulate the speed of locomotion via a hippocampus to lateral septum pathway. Nature Communications 6:8521 doi: 10.1038/ncomms9521 (2015).
Gutierrez Herrera C, Carus Cadavieco M, Jego S, Ponomarenko A, Korotkova T, Adamantidis A. Hypothalamic feed-forward inhibition of thalamocortical network controls arousal and consciousness. Nature Neuroscience, NN4209 (2015), in press.

OS04-6
Dendritic integration in Dentate Gyrus parvalbumin-expressing perisoma-inhibiting interneurons

C. Elgueta, M. Bartos
Albert-Ludwigs-Universität Freiburg, Physiologisches Institut I, Freiburg Im Bresigau, Germany

Parvalbumin (PV+) positive GABAergic perisoma-inhibiting interneurons (PIIs) enable cortical circuits to perform complex operations by providing precisely timed feed-forward or feedback inhibition into principal cells. In despite of their central role during neuronal network computations, little is known regarding how signals are processed in their dendritic trees. Using a combination of single cell voltage sensitive dye imaging (VSDI) and glutamate uncaging in acute slice preparations of the rat dentate gyrus, we have characterized the integrative properties of PV+ PII dendrites. First we determined speed and attenuation of back-propagating action potentials. We observe a monotonic decline in size of APs as a function of distance when traversing from the soma along both, basal and apical dendrites. In agreement with the low density of sodium conductances, blocking voltage-gated sodium channels did not changed AP attenuation. Blocking Kv3-type potassium channels with 4AP had an effect in spike width but interestingly not in action potential back-propagation. Second, a combination of VSDI and glutamate uncaging revealed strong attenuation and deceleration of locally evoked excitatory postsynaptic potentials, suggesting that PII dendrites favor precision and speed during signal integration. Moreover, irrespective of the spatial distribution of the evoked localized EPSPs, summation of excitatory signals at the soma was always sub-linear, which was in stark contrast with granule cells (GCs) that showed preferentially supralinear summation. Third, we examine how GABAA receptor-mediated inhibition modulates the EPSPs integration in PII dendrites by analyzing the effect of localized GABA uncaging using DPNI or RUBI-GABA onto the size and shape of

EPSPs evoked by glutamate microiontophoresis (miEPSPs). We observe that distal (off-path) inhibition is more effective than proximal (on-path) inhibition in reducing the amplitude of miEPSPs recorded at the soma. In contrast proximally located inhibition was generally more efficient than off-path inhibition in GCs. This differential effect depended in the size of the excitatory potential and the chloride reversal potential at the uncage locations, which was different for PIIs and GCs. In summary, our data suggest than proximal GABAA receptor-mediated inhibition is better suited to control action potential generation while distal inhibitory inputs favor the regulation of size and shape of excitatory signals.

OS04-7

Modular composition and dynamics of native $GABA_B$ receptors identified by high-resolution proteomics

J. Schwenk[1,2], E. Pérez-Garci[3], A. Schneider[1], A. Kollewe[1], W. Bildl[1], T. Fritzius[3], A. Gauthier-Kemper[4], J. Klingauf[4], M. Gassmann[3], U. Schulte[1], B. Bettler[3], B. Fakler[1,2]

[1]University of Freiburg, Institute of Physiology, Germany
[2]University of Freiburg, Center for Biological Singaling Studies (BIOSS), Germany
[3]University of Basel, Department of Biomedicine, Switzerland
[4]University of Münster, Cellular Biophysics, Germany

GABAB receptors, the most abundant inhibitory G protein–coupled receptors in the mammalian brain, display pronounced diversity in functional properties, cellular signaling and subcellular distribution. We used high-resolution functional proteomics to identify the building blocks of these receptors in the rodent brain. Our analyses revealed that native GABAB receptors are macromolecular complexes with defined architecture, but marked diversity in subunit composition: the receptor core is assembled from GABAB1a/b, GABAB2, four KCTD proteins and a distinct set of G-protein subunits, whereas the receptor's periphery is mostly formed by transmembrane proteins of different classes. In particular, the periphery-forming constituents include signaling effectors, such as Cav2 and HCN channels, and the proteins AJAP1 and amyloid-bA4, both of which tightly associate with the sushi domains of GABAB1a. Our results unravel the molecular diversity of GABAB receptors and their postnatal assembly dynamics and provide a roadmap for studying the cellular signaling of this inhibitory neurotransmitter receptor.

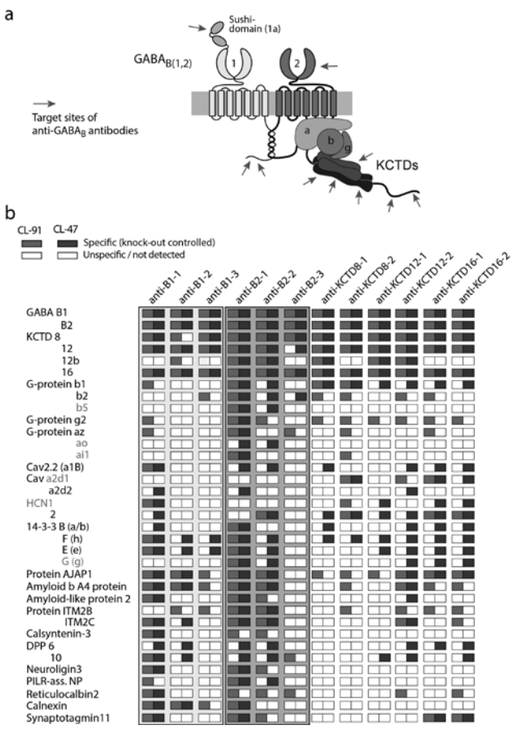

Figure 1: ME-AP proteomics identify the protein constituents of native GABAB receptors.

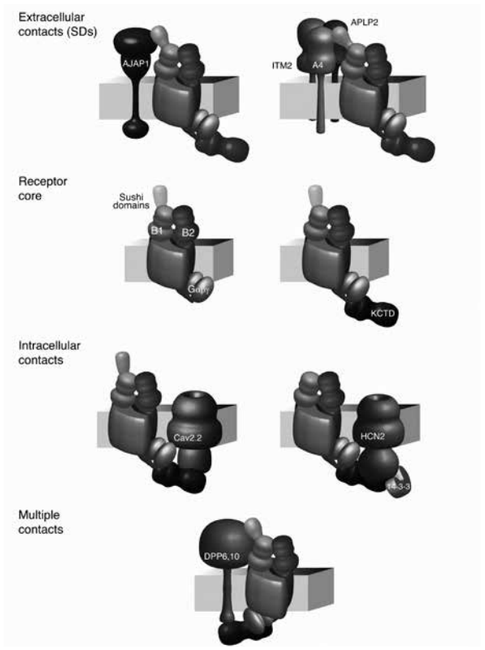

Figure 2: Nano-architecture and modular assembly of native GABAB receptors derived from proteomic and biochemical analyses, as well as from properties reported in literature.

OS04-8

Molecular architecture of parallel fibre-to-Purkinje cell active zones elucidated by *d*STORM

M. M. Paul[1], S. Proppert[1], M. Pauli[1], A. - L. Sirén[2], M. Sauer[3], M. Heckmann[1]

[1]Julius-Maximilians-University, Institute of Physiology, Department of Neurophysiology, Würzburg, Germany
[2]University Hospital of Würzburg, Department of Neurosurgery, Germany
[3]Julius-Maximilians-University, Department of Biotechnology and Biophysics, Würzburg, Germany

Presynaptic active zones (AZs) are elaborated subneuronal compartments specialized for vesicle fusion and neurotransmitter release. They show complex protein-protein interactions within a range of a few hundred nanometers which require the use of high-resolution imaging techniques to analyze their molecular architecture. Here, we used 2D and 3D *direct* stochastic optical reconstruction microscopy (*d*STORM, Heilemann et al., 2008; van de Linde et al., 2011) to investigate the molecular arrangement of parallel fibre-to-Purkinje cell AZs in the cerebellum of male 3-4 weeks old C57BL/6 mice. Presynaptic parallel fibre boutons typically harbour one single AZ with a small number of docked vesicles (Xu-Friedman et al., 2001) in a coupling distance of less than 30 nm to voltage-gated calcium channels (Schmidt et al., 2013). In this study, we used parasagittal cryoslices of 1 µm thickness which allowed us to clearly identify single AZs in side view using an N-terminal antibody against the scaffolding protein Bassoon (Bsn). Bsn clusters show a stereotypic form of a rectangular badge-like perforated structure with a length of 520 ± 90 nm. We imaged presynaptic PQ-type calcium channels relative to Bsn and found 3.5 ± 1.9 clusters per AZ. With an antibody against the N-terminal, vesicle-binding region of the AZ-protein RIM (Rab3-interacting molecule) we identified 4.6 ± 1.6 RIM-clusters per AZ. Correlation between localization numbers of Bsn and RIM was relatively high ($r = 0.5$ with $p < 0.001$) and lower between Bsn and calcium channels ($r = 0.28$ with $p < 0.05$). These data illustrate the contribution of superresolution imaging techniques to a better understanding of the molecular architecture of chemical synapses in the mammalian brain.

References

Heilemann M, van de Linde S, Schüttpelz M, Kasper R, Seefeldt B, Mukherjee A, Tinnefeld P, Sauer M. (2008) Subdiffractionresolution fluorescence imaging with conventional fluorescent probes. Angew Chem Int Ed Engl 47:6172-6.

Schmidt H, Brachtendorf S, Arendt O, Hallermann S, Ishiyama S, Bornschein G, Gall D, Schiffmann SN, Heckmann M, Eilers J (2013) Nanodomain coupling at an excitatory cortical synapse. Curr Biol. 23:244-9.

van de Linde S, Löschberger A, Klein T, Heidbreder M, Wolter S, Heilemann M, Sauer M (2011) Direct stochastic optical reconstruction microscopy with standard fluorescent probes. Nat. Protocols 6: 991-1009.

Xu-Friedman MA, Harris KM, Regehr WG (2001) Three-dimensional comparison of ultrastructural characteristics at depressing and facilitating synapses onto cerebellar Purkinje cells. J Neurosci. 21:6666-72.

Oral Session 05

Renal Physiology

OS05-1

Vascular endothelial growth factor receptor inhibition upregulates renal epithelial sodium channel

A. Koenen, J. Lampe, R. Rettig, O. Grisk

University of Greifswald, Institute of Physiology, Karlsburg, Germany

Question: Vascular endothelial growth factor receptor (VEGFR) inhibitors, such as sunitinib, are widely used in tumor therapy. Their clinical use is often limited by rapidly developing arterial hypertension. In a previous study, we found that fractional sodium excretion was significantly reduced in sunitinib-treated rats without alterations in fractional lithium excretion suggesting increased sodium reabsorption in the distal nephron and/or collecting ducts (CD). Therefore, we tested the hypothesis that sunitinib increases epithelial sodium channel (ENaC) expression in the renal cortex and medulla. In addition, we investigated if sunitinib alters subcellular ENaC localization in the rat renal CD. **Methods:** Three-month-old, male Wistar rats were sham-treated or treated with sunitinib [15 mg/(kg*d), n = 7 per group], for four days. Renal cortical and medullary ENaC expression was determined by quantitative real-time PCR and Western blot analyses. Immunofluorescence staining of α-, β- and γ-ENaC subunits was performed in renal transverse cryosections and analyzed by confocal laser scanning microscopy. **Results:** Sunitinib had no significant effects on cortical and medullary ENaC subunit mRNA abundances but significantly increased α-ENaC protein abundance by 57% in the renal medulla. Mean cortical and medullary β- and γ-ENaC subunit protein abundances were also higher in sunitinib-treated rats than in controls, but these differences did not reach statistical significance. Subcellular localization studies with confocal laser microscopy revealed that sunitinib increased the α-ENaC subunit within the apical plasma membrane of principal cells in the cortical and medullary CD. The subcellular localization of the β- and γ-ENaC subunits was similar in sunitinib-treated and sham-treated animals. **Conclusions:** Our data show that sunitinib elevates renal medullary α-ENaC protein abundance in the plasma membrane and increases the fraction of α-ENaC subunits localized within the apical plasma membrane of cortical and medullary CD principal cells, which may raise ENaC activity and renal Na^+ reabsorption. Based on these findings, we suggest that enhanced renal ENaC activity contributes to the pathogenesis of VEGFR inhibitor-induced arterial hypertension.

OS05-2
Inflammation triggers FGF23 expression in kidneys of chronic kidney disease mouse models

D. Egli-Spichtig[1], P. H. Imenez Silva[1], B. Glaudemans[1], N. Gehring[1], C. Bettoni[1], D. Schönenberger[1], M. Rajski[1], D. Hoogewijs[1], F. Knauf[2], I. Frey-Wagner[3], G. Rogler[3], M. Föller[4], F. Lang[5], R. H. Wenger[1], I. Frew[1], C. A. Wagner[1]
[1]Universität Zürich, Institute of Physiology, Switzerland
[2]Universitätsklinikum Erlangen, Nephrologie und Hypertensiologie, Germany
[3]University Hospital Zurich, Clinic for Gastroenterology and Hepatology, Zürich, Switzerland
[4]Martin-Luther-Universität Halle-Wittenberg, Ernährungsphysiologie, Halle/S., Germany
[5]Universität Tübingen, Institute of Physiology, Germany

Question: Fibroblast growth factor 23 (FGF23) regulates phosphate homeostasis and is directly linked to all-cause mortality in chronic kidney disease (CKD). Here, we examined whether inflammation triggers excessive FGF23 expression in chronic kidney disease. **Methods:** We investigated two models of chronic kidney disease, the polycystic kidney disease conditional KO mouse model (*Pkd1* mice) and as well as the oxalate induced nephropathy mouse model (0,63% oxalate in calcium-free diet). Moreover, we examined the *Il10* KO mouse, a model of inflammatory bowel disease. If indicated, animals were treated with anti-TNFα antibody or control IgG for 1 or 2 days. Protein and RNA were isolated from various organs for qPCR and Western Blot. Mouse osteocytes were isolated from long bones and used for primary cell cultures. **Results:** In CKD mouse models, plasma FGF23 and renal *Fgf23* mRNA increased, however, *Fgf23* mRNA expression in bone was unchanged. Kidneys from CKD mice were affected by inflammation showing increased renal *Tnfα* and *Tgfβ* mRNA expression. *Runx2* mRNA levels – an osteogenic marker – was increased in kidneys as well. In *Pkd1* mice there was increased phosphorylation of the NfκB subunit p65 in the kidney and the TNFα/NfκB signaling increased *Nurr1* expression, an orphan nuclear receptor involved in the regulation of *Fgf23* expression in bones. Nuclear NURR1 overlapped with FGF23 protein expression in the kidneys of Pkd1 mice. The inflammatory cytokine TNFα stimulated *Fgf23* expression in primary mouse osteocytes and was paralleled by *Nurr1* expression. Antibody-mediated neutralization of TNFα led to reduced renal *Tnfα* mRNA expression in *Pkd1* animals and concomitantly decreased plasma FGF23 levels in both *Pkd1* and wild type mice. Oxalate fed mice treated with TNFα antibody showed lower plasma FGF23 as well. To further test the role of inflammation in triggering FGF23 expression, we used also *Il10* KO mice which showed highly elevated colonic *TNFα* mRNA levels and high plasma FGF23 while they have normal renal function. **Conclusions:** In *Pkd1* and oxalate nephropathy mice, ectopic renal *Fgf23* expression is triggered by the inflammatory cytokine TNFα. In *Pkd1* this may involve a NfκB-Nurr1 dependent pathway and TNFα blockade normalizes expression of FGF23 expression regulators in kidney along with decreased plasma FGF23 levels. Elevated FGF23 plasma levels of *Il10* KO mice indicate that systemic inflammation, independent from renal function, may stimulate FGF23 expression.

OS05-3
Inhibition of endogenous proteases prevents epithelial sodium channel (ENaC) activation by aldosterone in $mCCD_{cl1}$ mouse renal cortical collecting duct cells

M. Bertog, M. K. Mansley, C. Korbmacher
Friedrich-Alexander-Universität Erlangen-Nürnberg (FAU), Institut für Zelluläre und Molekulare Physiologie, Germany

Question: The epithelial sodium channel (ENaC) is critically involved in sodium absorption across tight epithelia such as the aldosterone-sensitive distal nephron (ASDN). Appropriate regulation of renal ENaC activity is important for maintaining total body sodium balance and the long term control of arterial blood pressure. ENaC is a heteromeric channel composed of three subunits (α, β, γ). Its main hormonal regulator is aldosterone. Proteolytic cleavage by the Golgi-associated convertase furin at putative furin sites (two in α-, one in γ ENaC) is thought to be important for ENaC maturation in the biosynthetic pathway before the channel reaches the plasma membrane. The pivotal final step in proteolytic ENaC activation probably takes place at the plasma membrane where γ ENaC is cleaved by membrane-bound proteases and/or extracellular proteases in a region distal to the furin cleavage site. The aim of this study was to investigate whether proteolytic channel activation is required for ENaC stimulation by aldosterone. **Methods:** A highly differentiated murine principal cell line ($mCCD_{cl1}$) derived from a microdissected cortical collecting duct was used and cells were grown on permeable supports. ENaC-mediated sodium transport was assessed by recording the amiloride-sensitive equivalent short circuit current (I_{SCAmi}) in Ussing chambers. Cells were exposed to protease inhibitors and/or aldosterone (3 nM) for up to 6h. As protease inhibitors we used an intracellularly acting convertase inhibitor (furin inhibitor-1) and extracellularly acting protease inhibitors (aprotinin or nafamostat). **Results:** In untreated control cells apical application of chymotrypsin showed no stimulatory effect on I_{SCAmi}. Apical exposure to aprotinin (30 µg/ml) / nafamostat (1 µM) or to furin inhibitor-1 (40 µM) strongly reduced baseline I_{SCAmi}. A combination of aprotinin / nafamostat and furin inhibitor-1 essentially abolished I_{SCAmi}. Subsequent apical application of chymotrypsin stimulated *I*SC-Ami back to baseline levels. Exposure of the $mCCD_{cl1}$ cells to aldosterone for 2.5 h stimulated I_{SCAmi} about 2.5-fold. Subsequent application of chymotrypsin had no additional stimulatory effect. Pre-treatment of the cells with aprotinin / nafamostat or with furin inhibitor-1 partially reduced the stimulatory effect of aldosterone on I_{SCAmi}. Furin inhibitor-1 in combination with aprotinin / nafamostat essentially prevented ENaC stimulation by aldosterone. Importantly, subsequent chymotrypsin rapidly and completely rescued the stimulatory effect of aldosterone in all groups treated with protease inhibitors. **Conclusion:** Stimulation of ENaC activity by aldosterone requires proteolytic channel activation by endogenous proteases. These probably include intracellular convertases and also membrane-bound proteases. Tubular proteases regulating ENaC activity are potential therapeutic targets.

OS05-4
Natriuretic peptides exert marked renoprotective effects via guanylyl cyclase-A dependent suppression of TRPC6 in podocytes

J. Staffel[1], D. Valletta[1], A. Federlein[1], M. Kuhn[2], F. Schweda[1]
[1]University of Regensburg, Institute of Physiology, Germany
[2]University of Würzburg, Institute of Physiology, Germany

The cardiac natriuretic peptides (NPs) ANP and BNP play a crucial role in the regulation of fluid homeostasis and the arterial blood pressure. Both peptides signal via the activation of their common receptor guanylyl cyclase-A (GC-A). In the kidney, GC-A is expressed in the entire nephron with highest expression levels in the glomerular podocytes. These highly differentiated cells cover the glomerular capillaries with their foot processes and build a slit diaphragm to exclude macromolecules like albumin from filtration. In order to investigate the yet unknown functional role of GC-A in podocytes, a podocyte specific GC-A knockout mice (Podo GC-A KO) was used.
Under control conditions no differences in renal function were detected between Podo GC-A KO and control mice (Podo GC-A CTR). In contrast, treatment of Podo GC-A KO mice with the mineralocorticoid DOCA and a high salt diet resulted in massive albuminuria (5400-fold vs. baseline), and marked glomerular damage including podocyte foot process effacement, mesangial expansion and glomerulosclerosis, while only mild renal damage was observed in Podo GC-A CTR. Staining of 4-HNE, indicating oxidative stress, was clearly enhanced in glomeruli of Podo GC-A KO mice. Immunohistochemical analysis revealed a reduced expression of the podocyte slit diaphragm proteins podocin, synaptopodin and nephrin in Podo GC-A KO but not in CTR. Conversely, the transient receptor potential canonical channel TRPC6, which is known to play a critical role in glomerular diseases, was upregulated in podocytes of Podo GC-A KO but not CTR and an enhanced ATP dependent Ca^{2+} influx in podocytes of freshly isolated glomeruli could be measured only in DOCA treated Podo GC-A KO mice. This Ca^{2+} influx was prevented by the TRPC blocker SKF96365, suggesting a functional role of TRPC6. In fact, concomitant treatment of Podo GC-A KO mice with SKF96365 reduced the albuminuria to 16% of vehicle treated Podo GC-A KO mice, accompanied by a marked amelioration of podocyte damage and renal histology.
In conclusion, the deletion of the natriuretic peptide receptor GC-A in podocytes leads to marked glomerular damage accompanied by massive albuminuria, ROS formation, and an upregulation of TRPC6 channel expression and activity under DOCA treatment. Concomitant application of the TRPC blocker SKF 96365 attenuates albuminuria and glomerular damage in vivo, suggesting that the marked protective effects of NPs on podocytes are mediated by a suppression of TRPC6 expression and activity.

OS05-5
Distribution, interaction and function of claudins in the thick ascending limb of Henle's loop

S. Milatz[1], N. Himmerkus[1], V. C. Wulfmeyer[1], H. Drewell[2], K. Mutig[2], T. Breiderhoff[3], M. Fromm[3], J. Hou[4], M. Bleich[1], D. Günzel[3]
[1]Christian-Albrechts-Universität zu Kiel, Physiologisches Institut, Germany
[2]Charité - Universitätsmedizin Berlin, Institut für Vegetative Anatomie, Germany
[3]Charité - Universitätsmedizin Berlin, Institut für Klinische Physiologie, Germany
[4]Washington University Medical School, St. Louis, Department of Internal Medicine - Renal Division, United States

Question: Paracellular epithelial transport is determined by the composition of the tight junction (TJ). Claudins seal the paracellular cleft or form size-, charge- and water-specific pores. To achieve this, different claudin proteins interact within the same plasma membrane (*cis*-interaction) and across neighboring plasma membranes (*trans*-interaction) and by this form a complex TJ strand meshwork. Claudins consist of four transmembrane segments, a small intracellular loop and two extracellular loops. The thick ascending limb of Henle's loop (TAL) drives paracellular Na^+, Ca^{2+} and Mg^{2+} reabsorption via the TJ. The question to which extent single claudins contribute to TAL ion selectivity has been addressed in various studies using overexpression cell models or deficiency in mice. However, a direct correlation between the expression of a certain claudin and transport function of the TAL tubule is difficult. **Methods:** In order to correlate claudin expression and ion permeability, single segments were obtained from cortex or medulla. Microperfusion and electrophysiological measurements were carried out. Subsequently, claudin expression of the respective TAL segment was analyzed by immunostaining and confocal laser-scanning microscopy. Moreover, to gain insight into the molecular composition of TAL TJ strands, claudin *cis*- and *trans*-interaction were examined after overexpression in TJ-free HEK 293 cells using live cell imaging and Förster/fluorescence resonance energy transfer (FRET). To reveal determinants of interaction properties, a set of TAL claudin protein chimeras was created and analyzed. **Results:** TAL of cortical or medullary origin differed in their paracellular permeability properties and their equipment with claudins. A correlation between predominance of specific claudins within the TJ and ion selectivity was observed. Most of the TAL claudins were co-expressed within the TJ. However, some of them failed to interact with each other in *cis*- or in *trans*-configuration. Analyses of claudin chimeras suggested an involvement of the extracellular loops of TAL claudins in interaction properties. **Conclusion:** We reveal a specific claudin expression pattern in the TAL which can be explained by the particular interaction capabilities of different claudins. On that basis, we suggest the existence of at least two spatially distinct types of paracellular pores with different preferences for Na^+, Ca^{2+} and Mg^{2+} in the TAL.

Supported by DFG FOR 721/2; National Institutes of Health Grant R01DK084059

OS05-6
The Atp6ap2/(Pro)-renin receptor is involved in Receptor Mediated Endocytosis by the Renal Proximal Tubule

M. Figueiredo[1], G. Sihn[2], D. Müller[2], G. Nguyen[3], M. Bader[2], M. Bader[2], C. A. Wagner[1]
[1]Universität Zürich, Physiologisches Institut, Switzerland
[2]Max-Delbrück-Center for Molecular Medicine, Berlin, Germany
[3]College de France, Paris, France

Atp6ap2 may be an accessory subunit of the V-type H^+ ATPase which regulates organellar, cellular, and systemic acid-base homeostasis. Here we examine whether the knock-down of Atp6ap2 affects renal V-ATPase function in the proximal tubule. There, V-ATPases are important for receptor-mediated endocytosis of low molecular weight proteins from urine via the megalin/cubilin receptors. In order to elucidate the role of Atp6ap2 in this function we used an inducible shRNA Atp6ap2 knockdown rat model (Kd) and a doxycycline-inducible kidney specific Atp6ap2 knockout mouse model (Flox(P)RRPax8+). Both Atp6ap2 knockdown animal lines had normal kidney function but showed higher proteinuria with elevated albumin, vitamin D binding protein, and cathepsin. To further examine proximal tubular endocytosis, we injected animals with markers for fluid phase endocytosis (FITC- dextran, 10 kDa) and for receptor mediated endocytosis (human transferrin) and obtained kidneys after 10 and 40 minutes. Immunofluorescence of kidney slices from both animal groups did not show a difference in FITC-dextran accumulation or localization. In contrast, evaluation of receptor mediated endocytosis of human transferrin, showed in immunofluorescence stainings no differences between the animal groups at 10 min. but after 40 min. Kd rats and Flox(P)RRPax8+ mice accumulated more transferrin in vesicles in comparison with control group. Furthermore, expression of several proteins involved in receptor-mediated endocytosis was altered. In the rat model, there is significant downregulation of ATP6V0a4 (V-ATPase subunit a4) and upregulation of CLC-5 in the Kd animals. In the mouse model, Flox(P)RRPax8+ animals also show a downregulation of ATP6V0a4 together with downregulation of CLC-5. Expression of megalin and cubilin is not affected in both animal models. Hence, our data suggests a possible role for ATP6ap2 for proximal tubule function in the kidney with a mild defect in receptor-mediated endocytosis in mice and rats.

OS05-7
The tubular renin system contributes to high circulating prorenin levels and the development of albuminuria in diabetes mellitus

A. Federlein, D. Valletta, J. Staffel, F. Schweda
University of Regensburg, Institute of Physiology, Germany

The renin angiotensin system plays a pivotal role in the maintenance of salt, volume and blood pressure homeostasis of the body. Moreover it is critically involved in cardiovascular – and kidney diseases, such as the diabetic nephropathy. In addition to juxtaglomerular (JG) cells, renin is expressed in renal tubules under pathological conditions such as in diabetes mellitus. In these patients the plasma level of proteolytical active renin remains largely unaltered, whereas the plasma prorenin concentration is markedly elevated, which is associated with a more rapid progression of diabetic nephropathy. The functional relevance, as well as the source of this circulating prorenin is currently unclear. To address this question we generated mice with a specific deletion of the renin gene in all renal tubular segments (tubule-renin KO).
Under control conditions the tubular renin expression is very low. Although the renin expression in the tubule-renin KO mice is further reduced (20% of WT), there is no difference in plasma renin and prorenin concentrations, blood pressure and salt and water excretion between both genotypes. Diabetes mellitus was induced by low dose streptozotocin resulting in an increase in fasting blood glucose (5-fold of control) and an elevation of diuresis (10-fold of control) in tubule-renin KO and WT mice. Renin immunostaining in JG-cells remained unaltered even 12 weeks after induction of diabetes, whereas additional marked renin expression was observed in the tubular system especially in connecting tubules and collecting ducts (CDs). While in diabetic WT 62% of CDs showed renin staining only 21% of CDs of diabetic KO mice were renin-positive. In line with the augmented upregulation of tubular renin expression in WT, significant urinary renin excretion occurred in WT but not in KO. Similar to previous results in diabetic patients, plasma prorenin levels were significantly elevated in diabetic WT mice (baseline: 119.7 $\pm$ 9.9 ng/ml; 12 weeks after induction of diabetes: 272.8 $\pm$ 34.5 ng/ml; n=9, $p < 0.001$), while the plasma concentration of active renin (PRC) was slightly reduced (baseline: 59.9 $\pm$ 4 ng/ml; diabetes: 38.2 $\pm$ 3.8 ng/ml; n=9, $p < 0.001$). This pattern was completely changed in KO mice, since plasma prorenin levels remained steady in diabetes (baseline: 105.7 $\pm$ 6 ng/ml; diabetes: 144.2 $\pm$ 25.3 ng/ml; n=9, n.s.) while PRC was slightly elevated (baseline: 53.5 $\pm$ 4.6 ng/ml; diabetes: 87.9 $\pm$ 14.5 ng/ml; n=9, $p < 0.05$). Diabetes mellitus was accompanied by enhanced albumin excretion in both genotypes. However, albuminuria was significantly lower in diabetic tubule-renin KO mice compared with WT mice (WT: 124.2 $\pm$ 4.9 µg/mg creatinine vs. KO: 97.8 $\pm$ 4.4 µg/mg creatinine; $p < 0.01$).
Taken together, the data indicate that the tubular renin system contributes to high circulating prorenin levels and aggravates albuminuria in diabetic mice.

OS05-8
Unfolding paradigm: A spring-like multi-layered protein scaffold to maintain the interpodocyte slit of glomerular podocytes

F Grahammer[1], C Schell[1], O Kretz L Völker[2], D Kerjaschki[3], A Fornoni[4], J Miner[5], T Benzing[2] , A. Frangakis[6],TB Huber[1]
[1]Renal Division University of Freiburg, Germany
[2] Department of Nephrology, University of Cologne, Germany
[3]Department of Pathology, University of Vienna, Austria, [4]Department of Medicine, Miller School of Medicine – University of Miami, USA
[5]Division of Biology and Biomedical Sciences, Washington University, St.Louis, USA
[6]Institute of Biophysics, Goethe University, Frankfurt, Germany

Question: The slit diaphragm is a multiprotein complex and constitutes the final component of the glomerular filtration barrier. Despite intense research for more than one decade its molecular ultrastructure and function of individual components have remained mostly elusive. **Methods:** We established a complimentary set of conditional and constitutive *Neph1, Neph2, Neph3* and *Nphs1* knock-out mice. To compare SDs across the animal kingdom, chicken and mice kidneys were used. *Detailed analysis was performed with functional assays, WB, light microscopy, IF, STORM-Microscopy, TEM, Immuno-EM, SEM, Helium-Ion-Microscopy, as well as Cryo-Electrontomography combined with 3D reconstruction.* **Results:** As expected NEPHRIN and NEPH1 are essential to build a proper slit diaphragm. Yet in both types of constitutive knock-out animals rudimentary SDs based on the remaining Super-IgG molecule could be detected. Interestingly, Neph2 and Neph3 constitutive KO mice, while being postulated to be expressed in podocytes, did not show any obvious phenotype over a 2 year observational period. Within the native cryopreserved SD ultrastructural analysis revealed that in contrast to previous reports the SD is a multi-layered cell-cell contact that does not overlap in the midline, but rather forms individual junctions. Components arch from cell membrane to cell membrane in a spring-like fashion. Immuno-EM localized NEPH1 to the basal and narrower aspects of this junction, while NEPHRIN molecules form the top layer facing Bowman's space. Despite NEPHRIN's fundamental role in mammals, birds live healthily without NEPHRIN and present with narrower and leakier NEPH1 based slit diaphragms. **Conclusion:** This unique comparative approach revealed fundamentally new insights into the composition of the slit diaphragm. While NEPHRIN is essential for the formation of the slit diaphragm in mammals, it is dispensable in birds. NEPH1 seems to form the basal aspects of this junction in mammals and is the main component in birds. These structural findings, in combination with the flexibility inherent to the repetitive immunoglobulin (Ig)-folds of NEPHRIN and NEPH1, indicate that the SD represents a highly flexible cell-cell contact that forms an adjustable barrier based on a molecular spring-like mechanism. Our data provide a new understanding of the glomerular filtration barrier, and might explain why the renal filter does not clog.

Oral Session 06
Vascular Signaling, Angiogenesis & Platelets

OS06-1
Uridine triphosphate thio analogues as $P2Y_{12}$ receptor antagonists and inhibitors of platelet aggregation

M. Aslam[1,2], C. Hamm[2], R. Schulz[1], D. Gündüz[2]
[1]Justus Liebig University, Institute of Physiology, Giessen, Germany
[2]Justus Liebig University, Cardiology and Angiology, Giessen, Germany

Background and Aims: Platelets express two ADP receptors namely P2Y1 and P2Y12 that regulate ADP and other agonists-induced platelet aggregation. P2Y1 receptor activation causes platelet shape change while P2Y12 receptor activation induces platelet aggregation. The aim of the present study was to characterise the effects of uridine triphosphate (UTP) and its thio-(S)-analogues (2S-UTP, 4S-UTP, and 4S isobutyl UTP) on ADP-induced platelet aggregation. **Methods:** The experiments were performed on platelet rich plasma freshly isolated from blood donated by healthy human volunteers. **Results:** UTP inhibited $P2Y_{12}$ receptors and antagonised ADP-induced platelet aggregation in a conc.-dependent manner with an IC50 value of ~150 mM. A 5-fold increase in the platelet inhibitory activity was observed by adding a thio (-S) group at position 2 (2S-UTP) of the nucleotide ring with an IC_{50} value of 30 mM against ADP (10 mM). Interestingly, a 500-fold increase in anti-platelet aggregation activity was observed when a (-S) was introduced at position 4 of the nucleotide ring (4S-UTP) with an IC_{50} value of 0.36 mM. However, introducing a isobutyl group at the 4S- position reduced its activity by 50-fold with IC50 of 15 mM. Likewise, all the nucleotides tested were also able to antagonise collagen (2 m/ml)- and adrenaline (10 mM)-induced platelet aggregation. However, UTP and its (–S) analogues had no effect on ADP- and MRS2365 ($P2Y_1$ receptor agonist)-induced platelet shape change suggesting their inactivity at $P2Y_1$ receptors. **Conclusion:** The novel data demonstrate for the first time that thio (-S) analogues of UTP, particular 4S-UTP, are potent P2Y12 receptor antagonists and can be useful candidates for therapeutic intervention.

OS06-2
von Willebrand factor mediated platelet string formation and leukocyte extravasation in the microcirculation *in vivo*

S. Tahir[1,2], A. H. Wagner[1], S. Dietzel[2], U. Pohl[2], M. Hecker[1]
[1]University of Heidelberg, Cardiovascular Physiology, Germany
[2]Ludwig-Maximilians-University of Munich, Walter Brendel Centre of Experimental Medicine, Germany

Introduction: von Willebrand factor (vWF) is stored in endothelial cell vesicles called Weibel-Palade bodies (WPB). CD40 ligation on endothelial cells leads to the release and deposition of so-called ultra large von Willebrand factor (ULVWF) multimers on their surface. It is thought that circulating platelets rapidly adhere to these ULVWF multimers (forming

"platelet strings") and turn P-selectin positive, thereby enhancing recruitment of circulating monocytes and eventually, their diapedesis into the vessel wall. ULVWF multimers are specifically cleaved by the zinc metalloproteinase ADAMTS13. It is not yet known whether the interaction between the cell surface molecules, CD154 on platelets and CD40 on endothelial cells, plays a role in microvessels *in vivo* and whether the shear stress dependency of ULVWF formation observed *in vitro* plays any major role in the formation of platelet strings specifically in arterioles. **Methods:** Two-photon microscopy was used to study platelet string formation in the cremaster microcirculation of wild type and ADAMTS13 knockout mice. Platelets were labelled *ex vivo* with carboxy fluorescein diacetate (CFDA), injected into the circulation and observed for their interaction with CD31 positive endothelium and/or CD45 labelled leukocytes before and after sCD154 stimulation both in cremaster arterioles and veins. **Results:** sCD154 stimulation enhanced the formation of platelet strings in small veins (mean diameter 60 µm) and in arterioles (mean diameter 53 µm), and the effect was increased by about 2-fold in mice lacking ADAMTS13. Regardless of having higher shear rates (mean shear rate of 366 s^{-1} in arterioles vs. 238 s^{-1} in veins), arterioles exhibited less platelet strings in comparison to veins. This was also true when arterial and venous vessels were studied at comparable shear rates. The number of perivascular leukocytes were very low in arterioles as compared to veins in which the leukocyte extravasation was significantly enhanced under sCD154 stimulation. **Conclusion:** *In vivo* platelet string formation under sCD154 stimulation occurs mainly in veins. The absence of ADAMTS13 enhances the effect which may become important in disease states characterized by low plasma levels of ADAMTS13, as observed e.g. in patients after myocardial infarction. sCD154 also enhances leukocyte extravasation but primarily in veins.

OS06-3
Notch signaling and VEGF determine a balanced VE-cadherin dynamics during angiogenesis via endothelial shape change

J. Cao[1], M. Ehling[2], R. Adams[2], H. - J. Schnittler[1]
[1]University of Münster, Institute of Anatomy and Vascular Biology, Muenster, Germany
[2]Department of Tissue Morphogenesis, Max Planck Institute for Molecular Biomedicine, Münster, Germany

VEGF induces angiogenesis and formation of tip cells that migrate into the tissue and retain connection to the lumen-forming stalk cells via highly dynamic intercellular junctions. VEGF activity is counter-balanced by the Dll4 that binds to Notch receptor and down regulates the VEGF receptor. The activation of Notch induces the releases of a cytoplasmic NICD fragment that modulates gene expression and leads to a stable, non-angiogenic endothelial cell phenotype with relative stable cell junctions, a process that strongly involve VE-cadherin. However, the mechanism how VE-cadherin dynamics is balanced in angiogenesis is largely unknown. Here, we showed in HUVEC cultures that both VEGF-application and inhibition of Notch signaling by DAPT or shRNA-Dll4 decreased local VE-cadherin concentration at cell junctions while the total VE-cadherin expression per cell remained constant. Both VEGF and DAPT reduced the local junction-localized VE-cadherin due to increased cell size and cell elongation, parameters that increased the cell border length at which a given amount of VE-cadherin was distributed. Data were confirmed in mouse retina model *in vivo* as the endothelium of the angiogenic front in DAPT-treated retina displayed increased angiogenic sprouting with increased cell size and reduced VE-cadherin expression at the junctions. As a consequence of diminished local VE-cadherin concentration, we found increased formation of Arp2/3 complex controlled and actin driven formation of junction associated intermittent lamellipodia (JAIL), a structure that drives VE-cadherin dynamics and entire cell motility but still maintains the endothelial integrity by forming new VE-cadherin adhesion clusters. In addition, dynamic JAIL formation and cell migration was upregulated upon VEGF. Lamellipodia at tip cells and JAIL between the junctions were observed in sprouting HUVEC in 3D *in vitro* angiogenesis model. Inhibition of the Arp2/3 complex blocked endothelial tube formation. In conclusion, VEGF treatment or loss of Notch signaling decreases junction-localized VE-cadherin expression mostly due to increased cell border length that, in turn, accelerate VE-cadherin dynamics and cell motility by increasing the size and the sequence of JAIL formation.

OS06-4
Deletion of the AMPKα1 subunit in endothelial cells impairs angiogenesis and endothelial migration

B. Fißlthaler, R. Abdel Malik, H. Stingl, N. Zippel, I. Fleming
University Frankfurt, Institute for Vascular Signalling, Germany

The activation of the AMP-activated protein kinase (AMPK) by pharmacological activators accelerates vascular repair after ischemia. Given that endothelial cells express both catalytic AMPKα subunits this study focussed on determining the relative contribution of the α1 and α2 subunits for angiogenesis and vascular repair.
Mice lacking the AMPKa in endothelial cells ($AMPK\alpha^{\Delta EC}$) were generated breeding floxed AMPKα mice with VE-cadherin Cre mice. Vascular repair was studied after femoral artery ligation. Isolated lung endothelial cells were used to study proliferation, migration and protein expression.
In $AMPK\alpha1^{DEC}$ mice ischemia-induced revascularisation after femoral artery ligation was attenuated compared to the wild-type littermates. Endothelial sprouting was significantly impaired in aortic ring assays from the $AMPK\alpha1^{\Delta EC}$ mice. In cultured endothelial cells deletion of the AMPKα1 decreased proliferation and migration. As migration is linked to focal adhesion sites (FA) paxillin, as a maker for FAs, was used in immunofluorescence studies. In the $AMPK\alpha1^{\Delta EC}$ the size of paxillin positive FAs was significantly increased. Also the paxillin protein expression was increased in $AMPK\alpha1^{\Delta EC}$ cell lysates. None of these effects were detected in $AMPK\alpha2^{\Delta EC}$ mice or cells. Proteomic comparison of wild-type and $AMPK\alpha1^{\Delta EC}$ endothelial cells revealed a decreased in the expression of mitochondrial proteins as well as a significant attenuation of 14-3-3 protein expression. 14-3-3 proteins are known integrators of FAs and involved in cell migration and the overexpression of 14-3-3γ rescued the impaired migration in the $AMPK\alpha1^{\Delta EC}$ cells.
Endothelial cell specific deletion of the AMPKα1 but not the AMPKα2 subunit impairs vascular repair, angiogenesis and migration by a mechanism partially attributed to a change in the function of the FAs which is possibly mediated by down-regulation of 14-3-3 protein expression.

OS06-5
Augmentation of phosphate-induced osteo-/chondrogenic transformation of vascular smooth muscle cells and vascular calcification by homoarginine

J. Voelkl[1], I. Alesutan[1], M. Feger[1], R. Tuffaha[1], T. Castor[1], K. Musculus[1], S. S. Buehling[1], C. L. Heine[2], M. Kuro-O[3], B. Pieske[4], K. Schmidt[2], A. Tomaschitz[5], W. Maerz[6,7], S. Pilz[8], A. Meinitzer[6], F. Lang[1]
[1]University of Tübingen, Department of Physiology, Tuebingen, Germany
[2]Medical University of Graz, Department of Pharmacology and Toxicology, Austria
[3]Jichi Medical University, Center for Molecular Medicine, Tochigi, Japan
[4]Charité-Universitaetsmedizin Berlin, Campus Virchow-Klinikum, Department of Cardiology, Germany
[5]University of Graz, Department of Cardiology, Austria
[6]Medical University of Graz, Clinical Institute of Medical and Chemical Laboratory Diagnostics, Austria
[7]University of Heidelberg, Medical Clinic V (Nephrology, Hypertensiology, Rheumatology, Endocinology, Diabetology), Medical Faculty Mannheim and Synlab Academy, Synlab Services GmbH, Mannheim and Augsburg, Germany
[8]Medical University of Graz, Division of Endocrinology and Metabolism, Department of Internal Medicine, Austria

Question: Low circulating homoarginine concentrations are associated with mortality, heart failure and disease progression in chronic kidney disease (CKD) patients. The high cardiovascular mortality of CKD patients is associated with vascular calcification. Vascular calcification is fostered by increased extracellular phosphate levels and involves osteo-/chondrogenic phenotypical transformation of vascular smooth muscle cells (VSMCs). The present study therefore investigated the effects of homoarginine on phosphate-induced osteo-/chondrogenic transformation of VSMCs and vascular calcification. **Methods:** Experiments were performed in klotho-hypomorphic (*kl/kl*) and corresponding wild-type mice, in primary human aortic smooth muscle cells (HAoSMCs) and by measuring nitric oxide synthase (NOS) enzyme activity. **Results:** Plasma homoarginine levels were significantly lower in hyperphosphatemic *kl/kl* mice than in wild-type mice and in both genotypes increased by lifelong treatment with homoarginine. Surprisingly, the excessive vascular calcification of *kl/kl* mice was further enhanced by treatment with homoarginine. This effect was associated with augmented *Msx2, Cbfa1, Alpl* and *Pai1* mRNA expression in aortic tissue of homoarginine-treated *kl/kl* mice. Plasma calcium and phosphate, arginine, FGF23 and aldosterone concentrations were not modified by homoarginine treatment. Similarly, in HAoSMCs, the phosphate-induced calcium deposition, alkaline phosphatase activity and *MSX2, CBFA1, ALPL* and *PAI1* mRNA expression were increased by addition of homoarginine. Homoarginine treatment in HAoSMCs alone triggered up-regulation of osteogenic signaling in a dose-dependent manner. Homoarginine reduced citrulline formation from arginine by all three NOS isoforms. Nitric oxide (NO) formation from NOS was reduced by using homoarginine as a substrate instead of arginine. The NO synthase inhibitor L-NAME mimicked the effects of homoarginine on osteoinductive signaling in HAoSMCs. The homoarginine-induced osteoinductive signaling was abrogated by additional treatment with the NO donors DETA-NONOate and PAPA-NONOate. Furthermore, homoarginine treatment significantly reduced aconitase activity, superoxide dismutase (SOD) activity and total antioxidant capacity in HAoSMCs. Addition of the SOD mimetics TEMPOL and TIRON ameliorated the osteo-/chondrogenic signaling in HAoSMCs induced by homoarginine. **Conclusions:** Homoarginine augments the phosphate-induced osteo-/chondrogenic transformation of VSMCs and promotes vascular calcification. The osteoinductive effects of homoarginine involve impaired NO formation from homoarginine.

OS06-6
RhoA ambivalently controls prominent myofibroblast characteristics by involving distinct signaling routes

A. Jatho[1], S. Hartmann[2], N. Kittana[2], F. Mügge[2], C. Würtz[1], M. Tiburcy[2], W. H. Zimmermann[2], D. Katschinski[1], S. Lutz[2]
[1]University Medicine Göttingen, Cardiovascular Physiology, Germany
[2]University Medicine Göttingen, Pharmacology, Germany

Introduction: The role of RhoA in cardiac fibroblasts (CF) is still poorly understood. During cardiac remodeling CF undergo a transition towards a myofibroblast phenotype thereby showing an increased proliferation and migration rate. Both processes involve the remodeling of the cytoskeleton. Since RhoA is known to be a major regulator of the cytoskeleton, we analyzed its role in CF and its effect on myofibroblast characteristics in 2D and 3D models. **Results:** Downregulation of RhoA in neonatal rat CF by about 80% was accompanied by a disorganization of higher order actin structures including stress fibers, geodesic domes and focal adhesion sites. Functionally, the knockdown of RhoA increased the adhesion velocity on plastic and collagen surfaces. On a molecular level, the expression of actin cytoskeleton-associated proteins investigated were found unchanged besides a decrease in the myofibroblast marker α-sm-actin. Interestingly, in RhoA-depleted neonatal rat CF the fraction of acetylated tubulin, which is involved in intracellular vesicle-dependent transport processes, was found elevated. This data led to the investigation of serum response factor (SRF) activity and secretory processes with focus on profibrotic factors like CTGF, TGFβ and collagens. It was found that SRF activity as well as the expression of the investigated profibrotic factors is regulated in a complex manner by RhoA signaling in CF. In assays accessing three different types of migration, we demonstrate that RhoA/ROCK/Dia1

are important for 2D migration and the repression of RhoA and Dia1 signaling accelerates 3D migration. Additionally it was found that proliferation of myofibroblasts rely on RhoA and tubulin acetylation. Finally, we show that a downregulation of RhoA in NRCF impacts the viscoelastic and contractile properties of engineered tissues. While engineered connective tissues containing RhoA knockdown cells show a delayed failure point, engineered heart muscle complemented with the same cells display a reduction in contractile force by 50%. **Conclusion:** Dependend on the environmental conditions RhoA positively or negatively influences myofibroblast characteristics by differential signaling cascades. Reduction of RhoA leads to an increase in viscoelasticity and a decrease in contractile force in engineered cardiac tissue.

OS06-7
p38MAPKα is protective in the early phase of cardiac remodeling in response to pressure overload

K. Bottermann[1], L. M. Leitner[1], M. Pfeffer[1], J. Nemmer[1], R. Denen[2], K. Köhrer[2], J. Stegbauer[3], A. Gödecke[1]
[1]Heinrich-Heine University Düsseldorf, Cardiovascular Physiology, Germany
[2]Heinrich-Heine University Düsseldorf, BMFZ, Germany
[3]Heinrich-Heine University Düsseldorf, Nephrology, Germany

Question: At present it is known, that p38MAPK plays an important role in afterload induced cardiac remodelling. Nevertheless, it is still unclear, if this role is rather protective or detrimental as several *in vivo* studies draw an ambiguous image. **Methods:** A tamoxifen inducible, cardiomyocyte specific p38MAPKα KO mouse model was created by crossing p38 flox/flox mice with alpha-MHC cre-deleter mice. As pressure overload model mice received Angiotensin II (AngII) (1,5mg/kg/d) via osmotic mini pumps. Echocardiography was performed at baseline and after 12, 24 and 48 hours. Hearts were excised at the same time points and analyzed histologically and for gene expression levels. In addition, granulocyte depletion was performed using anti-Ly6G-antibody and hearts were analyzed after 48 hours of Angiotensin II - treatment.
Results: While cardiac parameters were comparable between KO and control mice under basal conditions (EF: Ctrl: 58±2%, KO: 59±11%, EDV: Ctrl: 80±13µl, KO: 90±27µl, ESV: Ctrl: 34±6µl, KO: 40±20µl) 48 hours of AngII-treatment led to a heart failure phenotype with severe cardiac dilation and reduced pump function (EF: Ctrl.: 49±12%, KO: 29±8%, EDV: Ctrl: 80±11µl, KO: 110 ±15µl, ESV: Ctrl.:39±10µl, KO: 78±16µl). Timeline analysis after 12 and 24 hours revealed that both, control and KO mice showed a reduction in pump function after 12 hours (EF: Ctrl: 42±12%, KO: 33±6%) from which control mice could recover after 24 hours (EF: Ctrl: 47±4%) while KO mice showed a further reduction in pump function (EF: KO: 24±5%) and a cardiac dilation (EDV: 129±19µl, ESV: 99±20µl).The histological analysis of these hearts showed an accumulation of lipids and an infiltration with neutrophil granulocytes in KO hearts after 48 hours. Interestingly, lipids seemed to accumulate already after 12 hours in both control and KO hearts. While this was transient in control hearts, KO hearts stored these lipids in big lipid droplets, a mechanism which seemed to be promoted by granulocyte infiltration as a co-localization of granulocytes and lipid droplets after 24 hours indicated. To further analyze the role of granulocyte infiltration in this context, mice were depleted from neutrophil granulocytes and hearts analyzed after 48 hours of AngII-treatment. KO mice which were depleted from granulocytes showed a preserved cardiac function (EF: KO, isotype ctrl.: 22±3%, KO, α-Ly6G-AB: 53±14%) and no lipid accumulation.
Conclusion: Our data point to a protective role of p38MAPKα especially during the early phase of cardiac remodelling in response to pressure overload, which seems to be promoted by an anti-inflammatory role of p38MAPKα.

OS06-8
Involvement of vascular aldosterone synthase in phosphate-induced osteo-/chondrogenic signaling and calcification of vascular smooth muscle cells

I. Alesutan[1], J. Voelkl[1], M. Feger[1], T. Castor[1], S. Mia[1], M. Sacherer[2], R. Viereck[1], O. Borst[1,3], C. Leibrock[1], M. Gawaz[3], M. Kuro-O[4], S. Pilz[5], A. Tomaschitz[2], B. Pieske[6], C. A. Wagner[7], F. Lang[1]
[1]University of Tübingen, Department of Physiology, Tuebingen, Germany
[2]Medical University of Graz and Ludwig Boltzmann Institute for Translational Heart Failure Research, Div. of Cardiology, Austria
[3]University of Tuebingen, Department of Cardiology and Cardiovascular Medicine, Germany
[4]Jichi Medical University, Center for Molecular Medicine, Yakushiji, Japan
[5]Medical University of Graz, Department of Internal Medicine, Division of Endocrinology and Metabolism, Austria
[6]Charité-Universitaets Medizin Berlin, Campus Virchow-Klinikum, Department of Cardiology, Germany
[7]University of Zurich, and the National Center for Excellence in Research NCCR Kidney, Institute of Physiology, Switzerland

Question: Vascular calcification resulting from hyperphosphatemia is a determinant of mortality of chronic kidney disease (CKD) patients. Aldosterone fosters and mineralocorticoid receptor (MR) antagonist spironolactone suppresses osteoinductive transformation and calcification of vascular smooth muscle cells (VSMCs). Further studies were performed to investigate a possible role of local aldosterone synthase (CYP11B2) expression in phosphate-induced osteoinductive transformation of VSMCs. **Methods:** Experiments were performed in primary human aortic smooth muscle cells (HAoSMCs), primary mouse aortic smooth muscle cells isolated from aldosterone synthase-deficient and corresponding wild-type mice (MAoSMCs), klotho-hypomorphic mice (*kl/kl*) and right coronary artery tissue of patients with reduced and maintained renal function. **Results:** Silencing and pharmacological inhibition (spironolactone, eplerenone) of MR ameliorated phosphate-induced osteo-/chondrogenic transformation and calcification of HAoSMCs even in the absence of exogenous aldosterone. High phosphate up-regulated CYP11B2 expression and MR-dependent transcriptional activity in HAoSMCs. Silencing (HAoSMCs) and deficiency (MAoSMCs) of CYP11B2 ameliorated phosphate-induced osteo-/chondrogenic transformation and calcification of VSMCs. Addition of exogenous aldosterone blunted the effects of CYP11B2 silencing and deficiency. Elevated phosphate levels induced nuclear export of APEX1, a transcriptional repressor of *CYP11B2*. Silencing of APEX1 upregulated *CYP11B2* expression and osteo-/chondrogenic signaling in HAoSMCs, an effect not modified by phosphate but suppressed by spironolactone. APEX1 overexpression suppressed phosphate-induced osteo-/chondrogenic signaling and calcification in HAoSMCs. In aortic tissue of hyperphosphatemic *kl/kl* mice, *Cyp11b2* expression was higher than in wild-type mice. Following dietary rescue of *kl/kl* mice, vascular osteo-/chondrogenic transformation was ameliorated by spironolactone, but not adrenalectomy. In adrenalectomized *kl/kl* mice, spironolactone was still able to ameliorate aortic osteoinductive reprogramming. *CYP11B2* mRNA expression was up-regulated in right coronary artery tissue of patients with reduced renal function as compared to patients with maintained renal function and correlated with the expression of osteogenic transcription factor *CBFA1*. **Conclusions:** Expression of CYP11B2 is up-regulated by phosphate-induced nuclear export of APEX1 in VSMCs and is required for osteoinductive effects of phosphate. Local aldosterone formation may promote osteogenic transformation of VSMCs and vascular calcification during hyperphosphatemia independent of circulating aldosterone levels

Oral Session 07

Cardiomypathies & Cardiac Regeneration

OS07-1
Mosaic mitochondrial respiratory chain deficiency causes cardiac arrhythmia during ageing

R. J. Wiesner[1,2], O. Baris[1], J. Neuhaus[1], S. Ederer[1], J. - C. von Kleist-Retzow[3], G. Zsurka[4], V. Peeva[4], W. S. Kunz[4], T. Hickethier[5], A. Bunck[5], J. W. Schrickel[6], F. Stöckigt[6]
[1]University of Cologne, Center of Vegetative Physiology, Germany
[2]University of Cologne, CECAD - Cluster of Excellence, Köln, Germany
[3]University Hospital Köln, Department of Pediatrics, Germany
[4]University Bonn, Department of Epileptology and Life and Brain Center, Germany
[5]University Hospital Köln, Department of Radiology, Germany, Germany
[6]University Hospital Bonn, Department of Medicine II – Cardiology, Germany

Question: During normal ageing, the human heart becomes a mosaic of many normal and few randomly distributed cardiomyocytes, which have accumulated high levels of mutated mtDNA and suffer from severe mitochondrial dysfunction. However, it was unclear whether these few cells could be responsible for the cardiac dysfunction generally observed during ageing. **Methods:** To approach this question, we have generated mice expressing a dominant-negative variant of the mitochondrial helicase TWINKLE in the myocardium (K320E-Twinkle^{Myo}). **Results:** At 18 months, mutant heart homogenates had 60-fold increased levels of deleted mtDNA species and displayed a mosaic pattern, with 1 out of 200 cardiomyocytes (0.56% ± 0.39) showing low cytochrome c oxidase activity (COX$^-$ cells), which were never found in control hearts. The deleted molecules were highly abundant in COX$^-$ cells, accounting for > 60%, but only few were found in COX-positive cardiomyocytes from K320E-Twinkle^{Myo} mice. Analysis of long-term ECG recordings of freely moving mice revealed an elevated rate of spontaneous ventricular premature contractions, which was further aggravated by swimming stress and accompanied by an increase in spontaneous AV-blocks. Strikingly, no enhanced occurrence of arrhythmia was observed in 12 month-old mutant mice, which had 3-fold lower proportion of COX$^-$ cardiomyocytes (0.17% ± 0.12). A generalized mitochondrial dysfunction induced by the genetic intervention was excluded, as mtDNA copy number, abundance and activity of respiratory chain complexes were unchanged compared to controls. Also, heart pump function, determined by cardiac MR imaging, was normal, and no signs of compensatory cardiac hypertrophy or fibrosis were observed. Finally, no preferential accumulation of COX$^-$ cardiomyocytes was found in the conduction system. **Conclusion:** In conclusion, we have unambiguously demonstrated that very few, randomly distributed COX$^-$ cardiomyocytes are sufficient to promote cardiac arrhythmias. Thus, we propose that the disposition to arrhythmias typically found in the ageing human heart is due to the accumulation of mtDNA deletions and the subsequent mosaic respiratory chain deficiency.

OS07-2
Functional imbalance among individual cardiomyocytes caused by cell-to-cell variation in mutant mRNA expression. Random burst-like transcription as a possible trigger for Hypertrophic Cardiomyopathy

T. Kraft[1], J. Montag[1], M. Makul[1], P. Ernstberger[1], S. Tripathi[1], S. Dunda[1], A. Perrot[2], A. Francino[3], F. Navarro-Lopéz[3], **B. Brenner**[1]
[1]Hannover Medical School, Molecular and Cell Physiology, Germany
[2]Charité-Universitätsmedizin Berlin, Experimental & Cinical Research Center (ECRC), Germany
[3]Hospital Clinic, Cardiology, Barcelona, Spain

Background: Familial hypertrophic cardiomyopathy (HCM) has been related to many different mutations in at least 20 different sarcomeric and some non-sarcomeric proteins. While development of the HCM phenotype is thought to be triggered by the respective mutation, a common mechanism has not yet been identified. **Hypothesis:** We hypothesized that (i) functional imbalance among individual cardiomyocytes, similar to functional imbalance seen in our previous work among *M. soleus* fibers of patients with different β-myosin heavy chain (β-MyHC) missense mutations, is due to cell-to-cell variation in the expression of mutated myosin, and that (ii) this functional imbalance triggers development of the HCM-phenotype. **Methods:** We tested this hypothesis by recording force-pCa relations of individual cardiomyocytes of two HCM-patients with β-MyHC mutations R723G and A200V. In addition, we quantified expression of mutant β-MyHC mRNA in individual cardiomyocytes using quantitative single cell RT-PCR with allele specific restriction digest. Cardiomyocytes were isolated by laser capture microdissection. **Results:** For both mutations, cardiomyocytes showed a large cell-to-cell variation in Ca^{++}-sensitivity with some cells being essentially indistinguishable from controls as if they did not express mutant β-MyHC, while other cells had highly reduced Ca^{++}-sensitivity suggesting substantial levels of mutant MyHC. Quantification of the fraction of mutant β-MyHC mRNA in individual cardiomyocytes of both patients showed a wide spectrum from cardiomyocytes expressing essentially pure mutant β-MyHC-mRNA to cells with essentially pure wildtype β-MyHC-mRNA.This behavior could be modelled on the basis of random, independent, burst-like transcription of the mutant and wildtype alleles using known turnover rates of the β-MyHC-protein and β-MyHC-mRNA. **Conclusions:** Our data and modelling suggest that random, independent, burst-like transcription of mutant and wildtype alleles causes large cell-to-cell variation in mutant mRNA and related cell-to-cell functional variation. Over time this most likely induces structural distortions, i.e., cellular and myofibrillar disarray which may trigger altered cell signaling leading to interstitial fibrosis, a second hallmark of the HCM phenotype. Such a mechanism may well act for other mutations in other proteins as well.

OS07-3
The troponin I mutation ΔK184 blunts the effects of PKA-mediated phosphorylation on contraction and relaxation kinetics but not on Ca^{2+}-sensitivity

D. Möhner, F. Elhamine, R. Stehle, G. Pfitzer
Institute of Vegetative Physiology, University of Cologne, Germany

Protein kinase A (PKA) phosphorylation of troponin I (cTnI), myosin binding protein-C (MyBP-C) and titin constitutes an important pathway of ß-adrenergic regulation of the inotropic and lusitropic response of the heart. Their specific modulatory effects in presence of familial hypertrophic cardiomyopathy (FHC)-related mutations are highly debated. We studied the PKA-mediated effects on the kinetics of myofibrillar activation and relaxation and the Ca^{2+}-sensitivity in skinned cardiac fibres and subcellular myofibrillar bundles of wild-type and transgenic mice carrying the FHC-linked mutation $cTnI^{\Delta K184}$. Transgenic mice displayed a higher Ca^{2+}-sensitivity, a lower cooperativity and an overall slower relaxation kinetic compared to wild-type. We treated the mice with propranolol prior to the isolation of myofibrils and the following PKA treatment to reduce the otherwise high levels of cTnI and MyBP-C phosphorylation. PKA treatment reduced the Ca^{2+}-sensitivity in wild-type and transgenic mice to a similar extent by 0.2 pCa-units. PKA decreased the resting force in transgenic but not in wild-type mice. Maximal tension was unaffected. Following PKA treatment, the contraction kinetic was accelerated in wild-type but not in transgenic myofibrils. In wild-type, PKA phosphorylation accelerated the early slow phase of relaxation predominantly reflecting the duration of crossbridge-detachment under loaded conditions. This effect was absent in transgenic myofibrils. The faster phase of relaxation was not affected.
In conclusion, treatment with PKA accelerated the activation as well as the relaxation kinetic in wild-type myofibrils whereas those effects were blunted in presence of the FHC-linked mutation $cTnI^{\Delta K184}$. However, the Ca^{2+}-desensitizing effect of PKA was not abolished in transgenic mice suggesting that the phosphorylation propensity is not altered in presence of the mutation.

OS07-4
Contractile function of myofibrils within human embryonic stem cell-derived cardiomyocytes with known cardiac myosin isoform composition using a novel micromechanical approach

B. Iorga[1], M. Wendland[1], K. Schwanke[2,3], S. Greten[1], N. Weber[1], U. Martin[2,3], R. Zweigerdt[2,3], B. Brenner[1], T. Kraft[1]
[1]Hannover Medical School, Institute of Molecular and Cell Physiology, Germany
[2]Leibniz Research Laboratories for Biotechnology and Artificial Organs (LEBAO), Department of Cardiothoracic, Transplantation and Vascular Surgery (HTTG), Hannover, Germany
[3]Hannover Medical School, REBIRTH-Center for Regenerative Medicine, Germany

Background and aim: Human induced pluripotent or embryonic stem cells-derived cardiomyocytes (hESCCMs) are used for e.g., cellular disease models, tissue engineering, and drug testing. Using typical differentiation protocols, hESCCMs express significant levels of the fast atrial α-myosin heavy chain (αMyHC), while in human ventricular myocardium most cardiomyocytes only express the slow βMyHC isoform. In this study we aimed to understand how the myosin-driven contractile function of individual hESCCMs is influenced by the expression of cardiac myosin heavy chain isoforms using an approach to directly measure the axial component of contractile force developed by myofibrils within single hESCCMs. **Methods:** To obtain hESCCMs with exclusive βMyHCcontaining sarcomeres (βMyHCCMs), hESCCMs were differentiated and propagated as “cardiac bodies” in suspension culture and then plated for long-term cultivation on a more rigid substrate, e.g., laminin-coated glass coverslips. To switch the hESCCMs towards pure expression of αMyHC (αMyHCCMs), some plated hESCCMs were treated for one week with triiodothyronine (T3). First, hESCCMs were chemically *d*emembranated (*d*hESCCMs) to be able to study the contractile function of the myofibrils within the cardiomyocytes independent of the intracellular Ca^{2+}transients. Then, *d*hESCCMs were mounted in a nN-sensitive micromechanical setup, allowing rapid switching of free Ca^{2+}-ion concentration, i.e., switching between Ca^{2+}activation and relaxation. Finally, maximum developed isometric force (F_{ACT}) per crosssectional area of myofibrils within *d*hESCCMs and two key parameters of cross-bridge cycling kinetics were determined: the rate constant of force redevelopment (k_{TR}) and the rate constant of the isometric phase of force relaxation (k_{LIN}). **Results:** F_{ACT} (~42 kPa) generated by *d*hESCCMs was independent of MyHC isoform. Yet, k_{TR} and k_{LIN} were significantly faster for *d*-α-MyHCCMs vs. *d*-β-MyHCCMs: k_{TR} was 2.44±0.30 s^{-1} and 0.67±0.10 s^{-1}, k_{LIN} was 1.47±0.38 s^{-1} and 0.30±0.09 s^{-1} for *d*-αMyHCCMs and *d*-βMyHCCMs, respectively. The kinetic values of *d*-βMyHCCMs were very similar to those of myofibrils isolated from ventricular cardiomyocytes of human donor hearts (k_{TR} = 0.64±0.09 s^{-1}, k_{LIN} = 0.24±0.08 s^{-1}). Importantly, similar maximum isometric force (F_{ACT}) but faster k_{LIN} of *d*αMyHCCMs yields much higher tension cost (=ATPase/Force) of *d*αMyHCCMs compared to the energetically more economical *d*βMyHCCMs, like in adult ventricular myocardium. **Conclusions:** We conclude that well-defined cardiac disease models, generation of artificial heart tissue, or drug testing with hESCCMs require assessment of contractile function of individual CMs in conjunction with characterization of MyHC isoform expression at the single cell level.

OS07-5
Modulation of Ca^{2+}-regulatory function by three novel mutations in TNNI3 associated with severe infant restrictive cardiomyopathy

D. Cimiotti[1], A. Kostareva[2], N. Smolina[2], M. Majchrzak[1], D. Möhner[3], A. Wies[3], H. Milting[4], R. Stehle[3], G. Pfitzer[3], A. Mügge[5], K. Jaquet[1]
[1]St. Josef Hospital, Clinic of the Ruhr-University Bochum, Molecular Cardiology, Germany
[2]Karolinska Institute, Department of Women’s and Children’s Health, Stockholm, Sweden
[3]University of Cologne, Institute of Vegetative Physiology, Köln, Germany
[4]Heart and Diabetes Center NRW, Bad Oeynhausen, Germany
[5]St. Josef Hospital, Clinic of the Ruhr-University Bochum, Med II - Kardiologie, Germany

Restrictive cardiomyopathy (RCM) – a rare heart muscle disease defined by impaired relaxation and increased myocardial stiffness – is often caused by mutations in the gene encoding for cardiac troponin I (cTnI). The phenotype of these mutations is probably determined by altered Ca^{2+}-regulation of contraction. Inter-filament protein interactions are pivotal for the function of the sarcomere and the Ca^{2+}-dependent regulation of contraction. Therefore this work focused on interactions between proteins of the thin filament including the N-terminal fragment of myosin binding protein C (MyBP-C C0-C2). Three RCM causing mutations within cTnI (D127Y, R170G and R170W) were recently identified in infant patients who died within few months after diagnosis. D127 is located near the inhibitory region within the IT arm of cTnI and R170 in the C-terminal domain, that modulates the function of the inhibitory region and binds to actin in a Ca^{2+}-dependent manner.
All three mutations resulted in altered interactions of thin filament proteins. In cosedimentation assays, binding of cTnI to reconstituted thin filaments was significantly decreased for R170W compared to wildtype, probably due to a disturbed interaction of R170W with actin, as measured via surface plasmon resonance spectroscopy. In contrast, D127Y and R170G showed a stronger binding to actin compared to wildtype. Additionally, the affinity towards tropomyosin was highly increased for all three cTnI-mutants. While D127Y did not affect actin-myosin S1 ATPase activity, R170G and R170W caused a strong Ca^{2+}-desensitization of actin-myosin S1 ATPase, a very new finding for RCM causing mutants. In presence of MyBP-C C0-C2, however, actin-myosin S1 ATPase activity of R170G/W was restored to wildtype levels. Interestingly, all three mutants showed a significant Ca^{2+}-sensitization of force generation of skinned cardiac fibres from guinea pigs, which is in good agreement with the RCM phenotype.
The fact that MyBP-C abolished the Ca^{2+}-desensitizing effect of R170G/W demonstrates a direct impact of protein

interactions beyond the thin filament for the pathogenesis of cTnI mutants. Moreover, other protein interactions within the sarcomere could as well be altered by these mutations, resulting in an overall Ca^{2+}-sensitized phenotype. Thus, early childhood RCM could conceivably be defined rather by altered protein interactions and resulting structural perturbances within the sarcomere, than solely by cTnI-induced changes in Ca^{2+}-sensitivity.
Our findings underline the relevance of protein interactions within the sarcomere for RCM development and deepen our understanding of the function of the cardiac contractile machinery.

OS07-6
Long-term inhibition of AP-1 by JDP2 overexpression provokes cardiac dysfunction

G. Euler[1], J. Heger[1], A. Würfel[1], C. Hill[1], R. Gáspár[2], J. Pálóczi[2], B. Meyering[1], Z. Varga[2], M. Sárközy[2], P. Bencsik[2], T. Csont[2], A. Aronheim[3], P. Ferdinandy[4,5], R. Schulz[1]
[1]JLU Gießen, Physiologisches Institut, Germany
[2]University of Szeged, Department of Biochemistry, Hungary
[3]Technion-Israel Institute of Technology, Department of Molecular Genetics, Haifa, Israel
[4]Pharmahungary Group, Szeged, Hungary
[5]Semmelweis University, Department of Pharmacology and Pharmacotherapy, Budapest, Hungary

Aims: JDP2 (Jun dimerization protein 2), an inhibitor of the transcription factor AP-1, has been identified as a prognostic marker for patients to develop heart failure after myocardial infarction. However, if JDP2 is involved in the process of heart failure development remained unclear. Studies on isolated cardiomyocytes of JDP2-overexpressing mice revealed anti-hypertrophic and anti-apoptotic effects of JDP2, but simultaneously a reduced contractile function of JDP2-overexpressing cells was observed. Therefore, we now performed in vivo studies on JDP2-overexpressing mice, to clarify the impact of JDP2 on the cardiac phenotype. **Methods and Results:** Cardio-specific JDP2 overexpression was prevented by doxycycline-feeding of transgenic mice for 4 weeks. Then, JDP2 was overexpressed for 5 or 11 weeks in adult mice. In JDP2-mice blood pressure was reduced compared to wild type mice. Ejection fraction was impaired and left ventricular dilatation developed. Heart weight/body weight and ANP-mRNA expression was increased. At the same time massive cardiac fibrosis and enhanced expression of collagen- and fibronectin-mRNA could be detected. As an additional sign of elevated extracellular matrix remodeling matrix metalloproteinase 2 activity increased in JDP2-mice. Thus, inhibition of AP-1 by JDP2 overexpression is deleterious to heart function in vivo. **Conclusions:** Long-term inhibition of AP-1 in transgenic adult JDP2-mice provokes cardiac dysfunction that is accompanied by hypertrophy and fibrosis. Thus, AP-1 is an essential factor for preserved cardiac function. Therefore, induction of the AP-1 inhibitor JDP2, as it is found after myocardial infarction, is a maladaptive response that contributes to heart failure development.

OS07-7
Epicardium-derived cells as source of pro-inflammatory and pro-fibrotic cytokines after myocardial infarction

J. Hesse, S. Leberling, D. Friebe, T. Schmidt, B. Steckel, Z. Ding, J. Schrader
Heinrich-Heine-Universität Düsseldorf, Institut für Molekulare Kardiologie, Germany

Epicardium-derived cells (EPDC) play a fundamental role in heart development and can be reactivated in the adult heart in response to myocardial infarction. They are considered as endogenous cell source with the potential to mediate cardiac regeneration. EPDC highly express CD73, a widely used marker enzyme of mesenchymal cells. CD73 catalyses the formation of adenosine, an important paracrine factor. The functional role of CD73 on EPDC, however, is unknown. In the present study we explored the extracellular purine metabolism and adenosine-mediated signalling of EPDC in culture, purified from the infarcted rat heart.
We found that EPDC rapidly generated adenosine from ATP and, surprisingly, also from NAD (HPLC analysis). Quantitative RT-PCR showed that EPDC highly expressed the adenosine receptors A_{2A} and A_{2B}. Activation of A_{2B} with BAY 60-6583 induced the secretion of major pro-inflammatory cytokines such as IL-1β, CCL5/RANTES and IL-6 (Bio-Plex analysis). EPDC also showed strong secretion of CCL2/MCP-1, although it was not further increased after A_{2B} activation. Analyses of IL-1β and IL-6 secretion in the presence of caspase-1 inhibitors strongly suggested the involvement of inflammasome activation. This was supported by the observation that EPDC abundantly expressed the pro-fibrotic matricellular protein tenascin-C (qRT-PCR, immunofluorescence), a known endogenous activator of Toll-like receptor 4 providing pro-IL-1β for the inflammasome. Further analyses showed that A_{2B} activation induced the vesicular release of ATP and NAD from intracellular stores (HPLC), creating an autocrine mechanism for the sustained adenosine-dependent pro-inflammatory cytokine release. Similar data were acquired in human atrial EPDC isolated from atria obtained during cardiac surgery.
Our data are the first to demonstrate that EPDC avidly degrade ATP and NAD to adenosine, which induces secretion of pro-inflammatory cytokines, acting via A_{2B} in an autocrine manner. Together with the expression of the pro-fibrotic protein tenascin-C, our data suggest that an inflammasome-dependent cytokine secretion by EPDC is involved in ventricular and atrial remodelling.

OS07-8
Generation of highly pure physiologically and pharmacologically functional Sinus-Nodal-Bodies from Pluripotent Stem Cells

J. J. Jung[1], C. Rimmbach[1], B. Husse[2], J. Stieber[3], P. Vasudevan[1], A. Dendorfer[4], R. David[1]
[1]Universitätsmedizin Rostock, Klinik für Herzchirurgie, Germany;
[2]Universitätsklinik Innsbruck, Klinik für Innere Medizin III, Austria;
[3]Universität Erlangen, Lehrstuhl für Pharmakologie und Toxikologie, Germany;
[4]Ludwig-Maximillian-Universität München, Walter-Brendel-Zentrum, Germany

Aim: The "sick sinus syndrome" comprises pathological, symptomatic sinus bradycardia, sinoatrial block, sinus arrest as well as the tachycardia-bradycardia syndrome. Therapeutic possibilities rely on electrical pacemakers. However, the latter lack hormone responsiveness and bear hazards such as infections and battery shortage. This may be overcome via "biological pacemakers" derived from pluripotent stem cells (PSCs). **Methods:** Our group has previously shown that "forward programming" of pluripotent stem cells towards specific cardiomyocyte (CM) subtypes is feasible using cardiovascular transcription factors such as MesP1 (leading to early/intermediate CM) and Nkx2.5 (ventricular CM). In order to generate pacemaker cells we used the T-box transcription factor Tbx3, as it is required for normal size and function of the sinoatrial node (SAN). Tbx3 is a transcriptional repressor acting to suppress the atrial myocyte phenotype and therefore specifying SAN versus atrial cells. **Results:** Here we first demonstrate directed differentiation of PSCs which leads to CM aggregates consistent of over 80% physiologically and pharmacologically functional pacemaker cells. These induced sinoatrial bodies ("iSABs") exhibited highly increased beating frequencies (300-400 bpm) for the first time close to mouse hearts. Additionally performed Ca^{2+} measurements showed Calcium gradients typical for pacemaker cells. Our iSABs were able to robustly pace myocardium *ex vivo*. We are now assaying the cells in a preclinical situation using transgenic mice with an inducible sick sinus syndrome. **Conclusions:** Overall, we provide the first example of highly pure functional cardiac pacemaker tissue derived from pluripotent stem cells, a crucial step towards future cell therapy and drug-testing *in vitro*.

Oral Session 08
Hypoxia II

OS08-1
Characterization of renal erythropoietin producing cells *in vivo*

K. A. Nolan[1], F. Imeri[1], S. Pfundstein[1], S. Santambrogio[1], I. Abreu-Rodríguez[1], P. Spielmann[1], E. Hummler[2], C. C. Scholz[1], D. Hoogewijs[3], R. H. Wenger[1,4]
[1]University of Zürich, Institute of Physiology and Zurich Center for Integrative Human Physiology, Switzerland
[2]University of Lausanne, Transgenic Animal Facility (TAF), Switzerland
[3]University of Duisburg Essen, Institute of Physiology, Germany
[4]National Centre of Competence in Research "Kidney.CH", Switzerland, Zürich, Switzerland

Question: The healthy adult kidney is an important sensor of molecular oxygen (O_2) and the PHD/VHL/HIF pathway is essential for the physiological response to reduced O_2 supply. In order to unravel the mechanisms involved in hypoxia-induced erythropoietin expression, a greater understanding of the nature of renal erythropoietin (Epo) producing (REP) cells is required. **Methods:** We developed a novel transgenic mouse model (Epo-Cre^{ERT2}) with inducible Cre recombinase expression under the control of a 220 kb DNA fragment containing the mouse *Epo* gene locus which, when crossed with the Rosa26-$^{fl}Stop^{fl}$-tdTomato reporter, allows us to permanently tag REP cells in response to an Epo inducing stimulus. We investigated localization of REP cells within the renal cortex in normoxia, following 8% FiO_2 hypoxia (physiological stimulus) as well as following 0.1% CO inspiration (profound tissue hypoxia) and followed the fate of these cells over time. Furthermore we have used RNAScope technology to localise Epo mRNA. **Results and Conclusion:** Our results demonstrate that REP cells are localised in the interstitium of the juxtamedullary cortex and that only few cells are needed to maintain Epo production under physiological conditions. Increased demand for Epo is met (at least partly) by an increase in the number of REP cells *in vivo*. Furthermore, our data indicate REP cell proliferation following an Epo inducing stimulus.

OS08-2
Organ specificity of in vivo erythropoietin expression by PDGF-receptor ß bearing cells

K. Gerl[1], B. Kurt[1], R. Adams[2], A. Kurtz[1]
[1]University of Regensburg, Institute of Physiology, Germany
[2]Max Planck Institute for Molecular Biomedicine, Department of Tissue Morphogenesis, Münster, Germany

Renal fibroblast/pericyte like interstitial cells expressing the PDGF-receptor beta (PDGFRß) have been identified as the physiological erythropoietin (EPO) producing cells. EPO expression there is triggered by the hypoxia signaling pathway mediated by the transcription factor HIF-2. Since

the expression of PDGF-receptor beta is a characteristic of fibroblast/pericyte like cells in almost all organs, the question arises, what renders renal cells so special to be able to produce EPO. In this study we therefore aimed to distinguish, whether this special feature arises from the selective capability of renal cells to transcribe the EPO gene or from the special organ architecture of the kidney that makes interstitial cells more sensitive to activate the hypoxia signaling pathway.

For this aim we therefore directly activated the hypoxia signaling pathway by inducible cell specific deletion of the von Hippel-Lindau (Vhl) protein in PDGFR-ß expressing cells of adult mice, which leads to constitutive activity of hypoxia-induced transcription factors. This maneuver led to an increase of HIF-transcription factors in all organs and to an increase of plasma erythropoietin concentration from 250pg/ml to 200ng/ml which was prevented by codeletion of Vhl together with HIF-2. Organ profiling revealed strong increases of EPO mRNA in kidneys and adrenal glands, but not in other organs, suggesting that the capability of PDGFRß-expressing cells to produce erythropoietin is restricted to cells of (ad) renal lineage. Profiling of gene coexpression together with EPO in the kidney and adrenal glands revealed upregulation of COX-2, ADM and RGS4. Upregulation of those genes was also found in liver, lung and heart.

In conclusion, it appears as if among all PDGFRß expressing cells, the capability to express EPO in a regulated fashion, is restricted to cells of the developmental (ad)renal lineage. Since these do not display a more general unique expression profile of HIF-2 triggered genes, we speculate that the capability to express the EPO gene is triggered by developmental regulator genes, as it is also known for the expression of renin.

OS08-3
Anti-oxidative role of cytoglobin in podocytes: potential association with chronic kidney disease?

E. Randi[1,2], M. Tsachaki[3], M. Lindenmeyer[1], C. Cohen[1], O. Devuyst[1,2], A. Odermatt[3], R. H. Wenger[1,2], D. Hoogewijs[1,4]
[1]University of Zürich, Institute of physiology, Zurich, Switzerland
[2]Zurich Center for Integrative Human Physiology (ZIHP), Switzerland
[3]University of Basel, Department of Pharmaceutical Sciences, Switzerland
[4]University of Duisburg-Essen, Institute of Physiology, Germany

Cytoglobin (CYGB) is a recently discovered member of the mammalian globin family, in addition to hemoglobin and myoglobin. Despite extensive research efforts, its physiological role remains unknown, but possible functions include reactive oxygen species (ROS) detoxification and signaling. Accumulating evidence suggests that ROS play a crucial role in podocyte detachment and/or apoptosis during diabetic nephropathy. To assess the putative anti-oxidative function of CYGB in podocytes, we are using the human podocyte cell line AB8/13, which expresses high endogenous CYGB levels. We generated stable CYGB knockdown and overexpressing cell models and we are currently studying CYGB-dependent gene expression, cell viability and oxidative stress response.

CYGB deficient cells showed an increase in cell death and up-regulation of genes involved in apoptosis and redox balance. These effects were even more pronounced upon treatment with either antimycin A, H_2O_2 or high glucose. A ROS sensing dye (H_2-DCF-DA) and redox-sensitive GFP probes were used to demonstrate that CYGB knock-down cells are more sensitive to oxidative stress compared to CYGB overexpressing podocytes. Interestingly, gene array expression analysis of biopsies from CKD patients showed a pronounced CYGB induction in diabetic nephropathy, validated by RT-qPCR in independent nephropathy samples. Moreover, genome-wide association studies (GWAS) revealed that CYGB is potentially implicated in chronic kidney disease (CKD).

In conclusion, data of our study demonstrate for the first time that CYGB (i) is expressed in a human podocyte cell line, (ii) protects podocytes from oxidative stress and cell death, and (iii) may be involved in CKD, particularly in diabetic nephropathy. In parallel to validating our findings in an independent podocyte model, we will study CYGB-dependent transcriptome changes and differentiation processes to gain further functional insight in the molecular mechanism of CYGB in podocytes.

OS08-4
Role of the hypoxia-inducible factor pathway in cardiovascular system development in zebrafish

C. Gerri, R. Marín-Juez, A. Rossi, D. Y. R. Stainier
Max Planck Institute for Heart and Lung Research, Developmental Genetics, Bad Nauheim, Germany

Targeted inactivation of key players of the hypoxia-inducible factor (HIF) pathway results in abnormal cardiovascular (CV) development and embryonic lethality in mouse [1][2]. The zebrafish model provides advantages to elucidate the role of the HIF family in CV formation: transparency of embryos allows *in vivo* blood vessel imaging that combined with hypoxia tolerance enables studies not feasible in mouse [3][4]. Here, we generated mutations using the TALEN technology [5] targeting key members of the HIF pathway: hif1ab, hif2ab and phd2b. Neither differences in gross morphology nor abnormalities in CV formation were evident in mutant compared to wild-type (wt) embryos. qPCR analysis on hif1ab, hif2ab and phd2b mutants detected a decrease in transcript levels compared to wt siblings indicating an enhanced mRNA degradation rate. Moreover, we found that other genes of the HIF family were upregulated in the mutants. The HIF pathway appears to be a complex network and the absence of phenotypes could be explained by genetic compensation mediated by other HIF family members. In view of these results, we set out to generate double mutants for hif1-/- (hif1aa-/-/hif1ab-/-), hif2-/- (hif2aa-/-/hif2ab-/-) and phd2-/- (phd2a-/-/phd2b-/-). hif1-/- embryos show brain vasculature defects, which are exacerbated after hypoxia induction. In addition, half the mutants show disconnections

in the trunk blood vessels only when stressed in hypoxia. Microarray results comparing the transcriptomes of wt and hif1-/- embryos in normoxia and hypoxia are under extensive analysis. Recent evidence suggests that contact of macrophages with blood vessels coordinates the fusion of emerging vascular sprouts [6][7]. Moreover, it has been shown that HIF1α plays an important role in macrophage maturation [8]. Our results support these observations suggesting a possible implication of macrophages in the stabilization of the vascular network. mfap4 (macrophage marker) WISH showed that macrophages are usually located both outside (circulating) and inside the hematopoietic stem cell (HSC) niche in wt embryos, and upon hypoxia treatment mfap4+ cells increase their exit from the HSC niche. hif1-/- embryos displayed a reduced number of macrophages with most of the mfap4+ cells remaining within the HSC niche. Strikingly, after hypoxic insult, macrophages in hif1 mutants do not change their location. Overall these results suggest that macrophages in hif1 mutants are not undergoing proper maturation, limiting the number of circulating macrophages. Wheter this defect is involved in the stabilization of the vasculature in stress conditions is a question we are investigating. However, other hypotheses are currently being tested. In addition, hif2-/- and phd2-/- are under screening and will be analyzed in the near future. Altogether, these mutants will help us elucidate the role of the HIF pathway during vascular development.

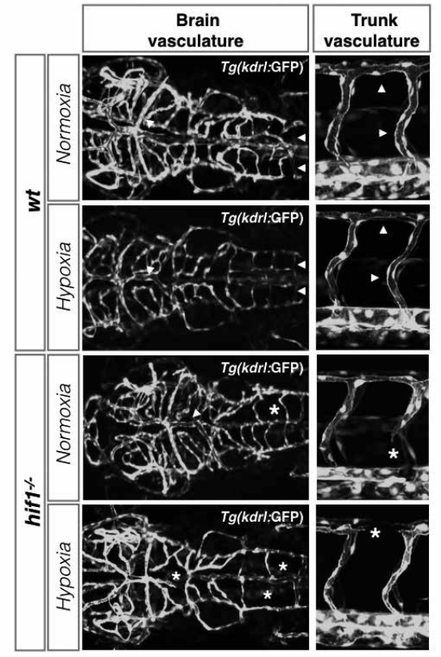

hif1-/- phenotype:
hif1-/- embryos show brain vasculature defects, more severe when treated in hypoxia; interestingly hif1-/- embryos also show disconnections in the trunk vasculature but only when stressed in hypoxia.

mfap4 WISH:
hif1-/- embryos show significantly fewer macrophages, which show an inability to migrate outside the HSC niche compared to wt controls.

References
[1] CW Pugh and PJ Ratcliffe, Nat. Med., 2003, 9, 677-684.
[2] SL Dunwoodie, Dev. Cell., 2009, 17, 755-773.
[3] Gore AV, Cold Spring Harb Perspect Med, 2012, 2(5):a006684.
[4] PA Padilla, Proc Natl Acad Sci USA, 2001, 98(13), 7331-5.
[5] JK Joung, Nat. Rev. Mol. Cell. Biol., 2013, 14, 49-55.
[6] A Fantin, Blood, 2010, 116(5), 829-40.
[7] C. Baer, Exp Cell Res, 2013, 319(11), 1626-34.
[8] T. Oda, Am J Physiol Cell Physiol, 2006, 291(1), C104-13.

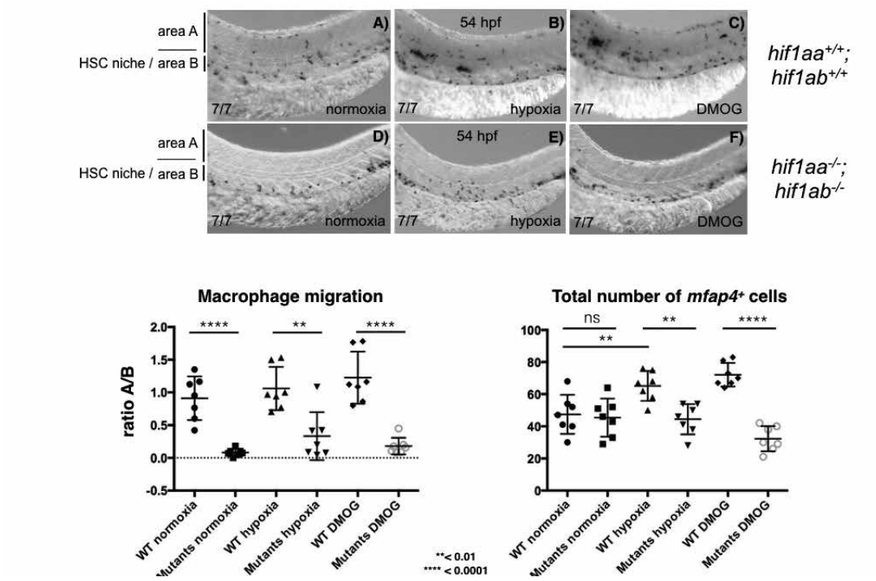

OS08-5
Hydrogen peroxide derived from the NADPH oxidase Nox4 is required for endothelial cells differentiation

F. Moll, S. Harenkamp, R. P. Brandes, K. Schröder
Goethe-Universität, Institut für kardiovaskuläre Physiologie, Frankfurt am Main, Germany

The NADPH oxidase Nox4 is a constitutive source of hydrogen peroxide. Compared to other cells of the cardiovascular system, endothelial cells express high levels of Nox4. Nox4 maintains endothelial cell quiescence and prevents inflammation. We hypothesize that Nox4 contributes to differentiation of endothelial cells and that loss of Nox4 promotes de-differentiation.
As a system of defined differentiation, induced pluripotent stem cells (iPSCs) derived from mouse embroyonic fibroblasts (MEFs) were used. Differentiation of iPSCs into endothelial cells was induced by VEGF and BMP4. Endothelial marker expression was demonstrated by staining with isolectin B4 and for VEGFR2 and CD31 at the surface of the cells as well as by analyzing VEGFR2 mRNA level.
Nox4 deficiency results in genomic instability, which is a prerequisite for de-differentiation. Accordingly in the course of de-differentiation the number of colonies formed from Nox4 deficient MEFs was higher than from MEFs of wildtype littermates, while the size of the iPSC colonies was smaller in the absence of Nox4. Therefore it appears that Nox4 deficiency promotes the formation of iPSC colonies but not the proliferation of colony cells. In the course of differentiation Nox4 expression in wildtype cells increased and Nox4-deficient cells were less endothelial like than wildtype cells when differentiated for 6 days. Additionally tube formation of wildtype iPSCs derived endothelial cells was much higher than that of Nox4 deficient cells 25 days after induction of differentiation. Together out data provide evidence that Nox4 deficiency promotes de-differentiation of MEFs into iPSCs. In contrast Nox4 promotes differentiation of endothelial cells out of iPSCs. We conclude that Nox4 maintains cellular differentiation state and supports the process of endothelial differentiation.

OS08-6
Dexamethasone promotes pulmonary vascular remodeling by activation of the NOX-HIF-1alpha axis

D. Kracun[1], A. Petry[1,2], I. Kanchev[1], K. Chalupsky[1], A. Görlach[1]
[1]German Heart Center Munich at the Technical University Munich, Experimental and Molecular Pediatric Cardiology, Germany
[2]German Center for Cardiovascular Research (DZHK), partner site Munich Heart Alliance, Germany

The synthetic glucocorticoid dexamethasone (DEX) is widely used as a potent anti-inflammatory and immunosuppressive drug with only minimal mineralocorticoid effects. Besides its beneficial effects, the chronic use of glucocorticoids can cause various side effects including cardiovascular complications such as hypertension, atherosclerosis and heart failure. However, the effects of DEX on the pulmonary vasculature are less well understood.
In this study we found that treatment of pulmonary vascular cells with low dose DEX induced a proliferative response which was accompanied by increased levels of reactive oxygen species (ROS) derived from NADPH oxidases. In fact, DEX treatment of vascular cells or murine pulmonary arteries enhanced the levels of the NADPH oxidase subunits NOX2, NOX4 and p22phox, and subsequently resulted in increased levels and activation of the transcription factor HIF-1alpha. Depletion of NADPH oxidase subunits prevented HIF-1alpha upregulation and vascular proliferation.
Chronic application of low dose DEX for 8 weeks induced not only left ventricular hypertrophy and increased left ventricular pressure, but also enhanced right ventricular mass and pressure. Moreover, the number of small muscularized pulmonary vessels was enhanced in DEX-treated mice concomitant with enhanced levels of NADPH oxidases and HIF-1alpha. Importantly, mice deficient in a functional NADPH oxidase or HIF-1alpha expression in smooth muscle or endothelial cells were protected against DEX-induced pulmonary vascular remodeling.
These data indicate that low dose DEX treatment can affect pulmonary vascular proliferation and remodeling via induction of the NOX-HIF-1alpha pathway.

OS08-7
The pharmacological Gq inhibitor FR900359 induces airway relaxation without systemic side effects

M. Matthey[1], R. Schröder[2], R. Roberts[3], M. Kuschak[4], I. Hall[5], H. Meurs[6], C. Müller[4], G. König[7], E. Kostenis[2], B. K. Fleischmann[1], **D. Wenzel**[1]
[1]University of Bonn, Institute of Physiology I, Germany
[2]University of Bonn, Molecular-, Cellular-, and Pharmacobiology Section, Institute of Pharmaceutical Biology, Germany
[3]University Hospital of Nottingham, Pharmacology Research Group, United Kingdom
[4]University of Bonn, Institute of Pharmaceutical Chemistry I, Germany
[5]University Hospital of Nottingham, Division of Respiratory Medicine, United Kingdom
[6]University of Groningen, Department of Molecular Pharmacology, Germany
[7]University of Bonn, Institute of Pharmaceutical Biology, Germany

Question: G proteins are key mediators of airway constriction under physiological and pathophysiological conditions. Because of the lack of pharmacological inhibitors that directly and specifically affect Gq proteins the investigation of Gq protein function as well as its therapeutic modulation in airway disease has been only feasible so far using GPCR (ant)agonists and/or genetic models. Recently, our group could demonstrate that the depsipeptide FR900359 is a very specific pharmacological Gq inhibitor. Thus, in the current study we tested the effect of this peptide on airway tone in health and obstructive lung disease. **Methods:** To prove Gq specificity of FR900359 in airway smooth muscle cells (ASMCs) dynamic mass redistribution (DMR) and bioimpedance measurements were exerted. The effect of the peptide on airway tone in different species was determined by isometric force measurements or precision cut lung slices (PCLS) *ex vivo*. After local intrapulmonary application of FR900359 *in vivo*, airway resistance, cardiovascular parameters as well as tissue and plasma levels of the peptide were determined. **Results:** The peptide FR900359 specifically inhibited Gq-dependent responses in DMR and bioimpedance measurements or Ca^{2+} imaging experiments of human and mouse ASMCs. In isometric force measurements FR900359 induced a dose-dependent bronchorelaxation in tissues from mouse, pig and human. High concentrations of the pharmacological Gq inhibitor could inhibit airway constriction by Gq dependent agonists completely. Also in PCLS FR900359 was able to reverse Gq-dependent constriction of intrapulmonary airways. When FR900359 was directly applied to the lung of animals *in vivo*, high local concentrations of the peptide were obtained that prevented the increase of airway resistance by Gq-dependent agonists without inducing cardiovascular side effects. This strong airway relaxing effect was also found in the ovalbumin-induced asthma model. **Conclusion:** Our data demonstrate that the pharmacological Gq inhibitor FR900359 is a powerful bronchorelaxant in health and disease without inducing systemic side effects.

OS08-8
Contribution of the gasotransmitter hydrogen sulfide to hypoxic inhibition of pulmonary transepithelial sodium absorption

N. Krause[1], H. Kutsche[1], F. Santangelo[1], J. Pott[1], L. Münch[1], K. Olson[2], M. Althaus[1]
[1]Justus-Liebig University, Institute for Animal Physiology, Giessen, Germany
[2]Indiana University School of Medicine-South Bend, Department of Physiology, United States

Question: In lung epithelial cells, hypoxia decreases the expression and activity of sodium transporting molecules, thereby reducing the rate of transepithelial sodium absorption. The mechanisms underlying the sensing of hypoxia and subsequent coupling to sodium transporting molecules remain unclear. Hydrogen sulfide (H_2S) has recently been recognized as a cellular signaling molecule whose intracellular concentrations critically depend on oxygen levels. Therefore it was questioned whether endogenously produced H_2S contributes to hypoxic inhibition of sodium transport. **Methods:** Expression of the H_2S-generating enzymes cystathionine-γ-lyase (CSE), cystathionine-β-synthase (CBS) and 3-mercaptopyruvate sulfurtransferase (3-MST) was analyzed in H441 lung epithelial cells by reverse transcriptase PCR and immunoblotting. H_2S production was measured with an amperometric H_2S-sensitive electrode. Transepithelial sodium absorption was electrophysiologically measured across cultured H441 monolayers in Ussing chambers. **Results:** All H_2S-generating enzymes were present in human H441 lung epithelial cells. In addition, H_2S-production was detected in H441 lysates and H_2S-production inversely correlated with oxygen concentrations. In Ussing chamber experiments, exogenous application of H_2S by the sulfur salt Na_2S inhibited amiloride-sensitive sodium transport by cultured H441 monolayers. Furthermore, acute hypoxia which was established by decreasing oxygen concentrations from 10 % to 0.1 % for 30 min also decreased amiloride-sensitive sodium transport by these cells. Pre-treatment with the CSE-inhibitor D/L-propargylglycine (PAG) decreased hypoxic inhibition of sodium transport, whereas inhibition of CBS (with aminooxy-acetic acid; AOAA) or 3-MST (with aspartate) had no effect. Inhibition of all H_2S-generating enzymes with a combination of AOAA, PAG and aspartate abrogated the hypoxic inhibition of sodium transport. By contrast, increasing the concentrations of L-cysteine, pyridoxalphosphate and α-ketoglutarate, precursors of H_2S production, did not enhance the effect of hypoxia. **Conclusion:** These data indicate that H441 lung epithelial cells endogenously produce H_2S during hypoxia and this might contribute to hypoxic inhibition of transepithelial sodium absorption.

Oral Session 09
Cellular and Molecular Neuroscience II

OS09-1
A skilled forelimb motor task to investigate how noradrenaline shapes cortical motor control

J. Schiemann, J. Dacre, J. Ammer, I. Duguid
University of Edinburgh, Centre for Integrative Physiology, United Kingdom

Cortical processing is under potent neuromodulatory control. One such neuromodulator, noradrenaline, has been shown to facilitate concerted attention and flexible switching of goal-directed actions under different behavioural states. We recently demonstrated how noradrenaline shapes the activity of primary motor cortex (M1) output neurons during self-paced locomotion in mice [Schiemann et al., 2015]. Using whole-cell patch clamp recordings in awake, behaving mice, we found that during locomotion noradrenaline mediates an increase in excitatory drive to a subpopulation of layer 5B pyramidal neurons that elevates firing rates and selectively enhances the signal-to-noise ratio for information transmission. Blocking noradrenergic input to primary motor cortex significantly impaired motor coordination during walking / running on a cylindrical runged treadmill.
But how noradrenaline shapes the cellular and circuit activity in M1 during dexterous, learned motor movements remains largely unknown. To address this, we have developed a novel behavioural paradigm to train head-restrained mice to execute a goal-directed lever push task. Upon presentation of an auditory cue, mice push a lever forward (5 mm) with their left forelimb to receive a water reward. Within 7–10 days of training (one 30 min session per day) mice consistently learn

the new motor skill and perform > 100 successful actions per 30 min. Learning curves were characterised by quantitative parameters such as a significant increase in cued responses (tone efficiency: day 1: 44±6 %, day 10: 93±5 %, p=0.0025) and a marked decrease in reaction time (day 1: 3.9±0.3 s, day 10: 1.3±0.1 s, p=0.0003). Forelimb movement trajectories were mapped using high-speed digital imaging and multi-point kinematic analysis.

To investigate the involvement of forelimb M1 ($M1_{FL}$) for task execution and the specific role of noradrenaline during skilled motor behaviour, we employ a multi-level strategy combining quantitative behaviour, selective pharmacology, intersectional viral strategies and *in vivo* optogenetics. First, blocking $M1_{FL}$ output either by pharmacological $GABA_A$ receptor activation or by optogenetic activation of channelrhodopsin (ChR2)-expressing inhibitory interneurons interferes with behavioural performance. Second, to assess how noradrenaline controls M1 output, we selectively express archaerhodopsin (ArchT) in $M1_{FL}$-projecting locus coeruleus noradrenaline neurons allowing us to optogenetically silence noradrenergic neurotransmission in $M1_{FL}$ during task execution.

This quantitative behavioural paradigm will facilitate the combination of high-resolution *in vivo* electrophysiology or 2-photon imaging with virus-based optogenetic interrogation of neural circuits involved in skilled movement control.

References

Schiemann et al., Cell Reports, 2015, 11(8):1319-30

OS09-2
Delta oscillations organize prefrontal network activity during wakefulness

J. - F. Sauer, J. M. Biskamp, M. Bartos

Albert-Ludwigs-Universität Freiburg, Insitute of Physiology I, Germany

The medial prefrontal cortex (mPFC) integrates inputs from various brain areas and is a key structure for cognitive processes such as decision making and working memory. A potential mechanism alllowing mPFC to integrate signals is the emergence synchronous theta oscillations (6-12 Hz), which have been proposed to underlie long-range synchronization of neuronal network activity (1). These oscillations entrain prefrontal spiking activity (2) as well as local gamma oscillations (3), an alleged correlate of conscious information processing (4). Theta-coupled gamma activity might be important to bind features encoded by distinct neurons into a coherent perception (through synchronous spiking within a given gamma cycle) as well as to keep different perceptual items separate (by nesting several gamma cycles within one theta wave). However, a fundamental caveat of organizing prefrontal network activity by theta oscillations is that this activity pattern strongly depends on motion: Power and amplitude of hippocampal theta oscillations substantially drop when the animals rest (5). While it is clear from everyday experience that information processing also takes place in the absence of movement, the neural mechanisms that might underlie network computations when theta oscillations are unavailable remain elusive. Here, we investigated prefrontal neural dynamics in freely moving mice during immobility. Using local field potential recording we find that immobile phases are dominated by delta (1-4 Hz) oscillations while theta activities occur predominantly during movement. Awake immobility-related delta oscillations entrain prefrontal gamma as well as single-unit activity. Using *in vivo* tracing and optophysiological methods we furthermore show that awake delta oscillations are driven by input from the olfactory bulb. Jointly, our data suggest that awake delta activities complement the role of theta and take part in the organization of prefrontal activity patterns.

References

(1) Sigurdsson T, Stark KL, Karayiorgou M, Gogos JA, Gordon JA (2010) Impaired hippocampal- prefrontal synchrony in a genetic mouse model of schizophrenia. Nature 464:763-969.

(2) Jones MW, Wilson MA (2005) Theta rhythms coordinate hippocampal-prefrontal interactions in a spatial memory task. Plos Biol e402.

(3) Voloh B, Valiante TA, Everling S, Womelsdorf T (2015) Theta-gamma coordination between anterior cingulate and prefrontal cortex indexes correct attention shifts. PNAS 112:8457-8462.

(4) Crick F, Koch C (2003) A framework for consciousness. Nat Neurosci 6:119-126.

(5) McFarland WL, Teitelbaum H, Hedges EK (1975) Relationship between hippocampal theta activity and running speed in the rat. J Comp Physiol Psychol 88:324-328.

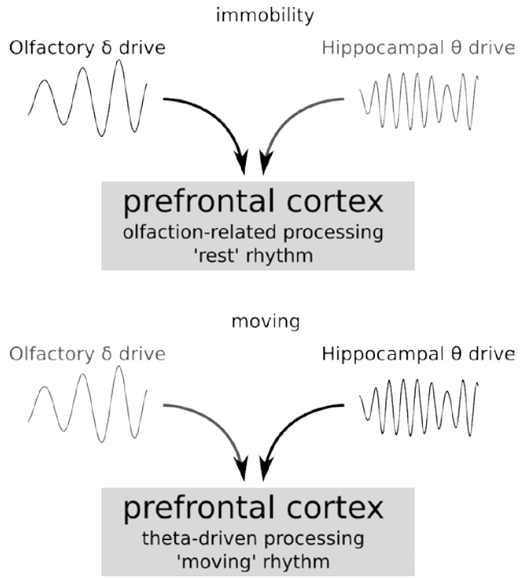

Awake prefrontal delta:
Delta and theta oscillations occur during distinct behavioral states of movement and immobility. We propose that the both rhythmic activity patterns participate in the organization of prefrontal network activity in a behavior-dependent manner.

OS09-3
Adenosine-mediated modulation of olfactory bulb network activity and odour information processing

N. Rotermund, T. Fregin, M. Buchta, D. Hirnet, **C. Lohr**

University of Hamburg, Division of Neurophysiology, Germany

In the olfactory bulb, ATP is released as a co-transmitter together with glutamate from axon terminals of sensory neurons. The mitral cells, the principal neurons in the olfactory bulb, receive this input and convey the information after intense processing via local circuits to higher brain centres such as the piriform (olfactory) cortex. Accordingly, mitral cells receive synaptic input from, and give synaptic input into most if not all types of neurons in the olfactory bulb. Brief and rapid application of ATP excites the neuronal network of the olfactory bulb measured as spontaneous synaptic currents in voltage-clamped mitral cells. Sustained application of ATP, in contrast, results in a reduced network activity and in hyperpolarisation and hence inhibition of mitral cells. This hyperpolarisation can be mimicked by adenosine, suggesting that ATP degradation to adenosine accounts for the inhibition of mitral cells (Fig. 1A). A_1 receptor-deficient mice lack the inhibitory effect of adenosine (Fig. 1B), and adenosine fails to hyperpolarize mitral cells in the presence of the A_1 antagonist DPCPX, indicating that the adenosine-dependent inhibition is mediated by A_1 receptors. Similar to the slow application of ATP, adenosine significantly reduced the frequency of synaptic events, indicating that the inhibition of mitral cells reduces the activity of the entire network. The direct synaptic input from sensory neurons to mitral cells, in contrast, was not affected by adenosine. The unchanged sensory input in conjunction with the reduced background network activity results in an increased signal-to-noise ratio upon stimulation of sensory neurons in the presence of adenosine. This renders adenosine as a good candidate to modulate odour information processing in the olfactory bulb.

Supported by the DFG (LO779/6-1)

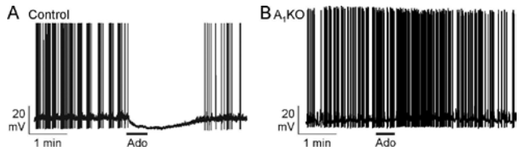

Fig. 1:
Adenosine hyperpolarizes mitral cells in wild type (Control), but not in A1 receptor knock out mice (A1KO).

OS09-4
Spinal Tumor Necrosis Factor-α generates spinal hyperexcitability by recruiting spinal Interleukin-6 trans-signaling

C. König[1], E. Morch[1], A. Eitner[1], C. Möller[1], B. Turnquist[2], H. -G. Schaible[1], A. Ebersberger[1]

[1]Jena University Hospital, Institute of Physiology I/Neurophysiology, Germany

[2]Bethel University, Department of Math & Computer Science, St. Paul, MN, United States

Proinflammatory cytokines such as Tumor Necrosis Factor-α (TNF-α) and Interleukin-6 (IL-6) have been linked to the pathogenesis of many diseases e.g. of the joints such as rheumatoid arthritis. But they are also mediators of inflammatory pain by directly acting on the nociceptive system on peripheral and central sites contributing to states of hyperalgesia. The inflammation-associated release of these cytokines within the spinal cord can lead to spinal hyperexcitability. So far it is largely unknown whether or how these cytokines influence each other.

We performed *in vivo* extracellular recordings of mechanonociceptive deep dorsal horn neurons in normal rats. This integrative approach allowed us to monitor responses from single neurons to repetitive mechanical stimulation at innocuous and noxious stimulus intensities for several hours, and to apply compounds to an area in which the neurons are recorded. Using immunohistochemical approaches we localized TNF-α acting sites and IL-6 in sections of the lumbar spinal cord of rats. ELISA analyses on supernatants of the spinal cord and of microglia cell line experiments were used to explore interactions of TNF-α and IL-6.

We revealed an upstream function of TNF-α to initiate an IL-6 trans-signaling process which generates spinal hyperexcitability. Spinal application of TNF-α increased spinal neuronal responses during mechanical stimulation of knee and ankle joints but also increased the release of spinal IL-6. Sources of spinal IL-6 in healthy rats are most likely neurons. IL-6 alone was not capable to increase responses of spinal nociceptive neurons but requested its soluble IL-6R (sIL-6R) to allow IL-6 trans-signaling. Interestingly, soluble gp130, an inhibitor of IL-6/sIL-6R complexes, almost attenuated the TNF-α dependent increase of spinal neuronal activity. Also the use of minocycline in the presence of TNF-α at the spinal cord prevented the increase of spinal neuronal responses but this was rescued by concomitant application of sIL-6R. However, TNF-α but not IL-6 induced an increased minocycline-sensitive release of sIL-6R from microglia cells. Finally, minocycline was ineffective in reducing the effect of IL-6/sIL-6R.

These findings indicate a regulatory function of TNF-α on neurons and microglial cells leading to IL-6 trans-signaling which furthers development of spinal hyperexcitability. Specifically, TNF-α furthers the release of IL-6 from neurons and recruits microglial cells to liberate sIL-6R. Then soluble complexes of IL-6 and sIL-6R can interact with ubiquitously expressed membrane-anchored gp130 in neurons to initiate the generation of spinal hyperexcitability.

OS09-5
TRPA1-mediated pain in human subjects

M. Schwarz, M. Fischer
University of Erlangen-Nürnberg, Institute of Physiology and Pathophysiology, Germany

TRP channels play a key role in sensing environmental and endogenous stimuli. TRPA1 is expressed in primary afferent neurons and senses a multiplicity of exogenous and endogenous chemicals. Agonists can be separated in non-electrophilic and electrophilic agents. Previously established human pain models targeting TRPA1 rely on the electrophilic agonists cinnamon aldehyde and mustard oil. We established a human pain model with the injection of the non-covalent agonist carvacrol, which is found e.g. in thyme and oregano. Pain ratings were regularly reported on a numerical analog scale and skin perfusion was detected with a Laser Doppler-based measurement. Carvacrol also activates TRPV3 with an EC_{50} of 0.5 mM, which is slightly above what has been reported for TRPA1. In favour of TRPA1, mouse neurons lacking the channel knocking show a largely reduced responsiveness to carvacrol. To validate TRPA1 as the target for carvacrol in humans, a TRPA1 antagonist was coinjected. No difference was found in the carvacrol-induced hyperaemia. However, the reported pain intensity was substantially lower in the presence of a TPRA1 antagonist. As reference for painful stimulation and fractional receptor inhibition, a TRPV1 antagonist was tested against capsaicin in human subjects. In conclusion, TRPA1 activation could be validated by pharmacological channel inhibition in human subjects.

OS09-6
Achaete-scute homolog 1 determines the differentiation fate of neuroblastoma cells

M. Kasim, V. Heß, H. Scholz, P. Persson, M. Fähling
Charité - Universitätsmedizin Berlin, Institut für Vegetative Physiologie, Germany

The basic helix-loop-helix transcription factor achaete-scute homolog 1 (hASH1/Mash1), encoded by the *ASCL1* gene, plays an important role in neurogenesis and is dysregulated in neuroblastoma primary tumors. Recently, using a neuroblastoma cell line, we showed that hASH1 is rapidly down-regulated in hypoxia through promoter-independent post-transcriptional mechanisms. Down-regulation of hASH1 has also been observed during neuron differentiation although the mechanism behind this has not been fully investigated. To more clearly define the role of hASH1 during differentiation, we analyzed two neuroblastoma cell lines, Kelly and SH-SY5Y, expressing different levels of hASH1 for retinoic acid induced differentiation. We show that although both cell lines respond to retinoic acid, cells expressing higher levels of hASH1 are refractory to differentiation as assessed by morphological changes and neurite extension. Preconditioning these neuroblastoma cells to a brief period of hypoxia, which decreases hASH1 levels, rescues the differentiation defect. Over-expression and siRNA mediated knock-down of hASH1 further revealed that hASH1 levels inversely regulate expression of a retinoic acid response element (RARE) containing luciferase plasmid; thus, implicating hASH1 in directly interfering with the binding of proteins to the RARE that are necessary to activate transcription. These findings indicate that ASCL1 levels are critical in determining the differentiation fate and also highlight the therapeutic potential of targeting ASCL1 for the treatment of neuroblastomas resistant to differentiation therapy.

OS09-7
Food intake and energy turnover – time of day makes a difference

G. Gohla, N. Herzog, S. Janka, T. Baumann, J. C. Martens, A. Kistenmacher, E. K. Wardzinski, K. M. Oltmanns
University of Lübeck, Section of Psychoneurobiology, Germany

Question: The question if the time of day plays a relevant role in terms of diet-induced energy turnover has been extensively discussed since the number of obese individuals has reached an epidemic dimension worldwide. Previous studies were contradictive and mostly suffered from deficits in the standardization of their examination conditions due to a survey approach. Because it is known that glucose tolerance underlies diurnal rhythmicity, we hypothesized that diet-induced thermogenesis (DIT) and glucose metabolism significantly differ depending on the time of day if examined under strictly controlled laboratory conditions. **Methods:** Under blinded conditions with Maltodextrin, 16 normal-weight men underwent a 2 day in-laboratory randomized crossover study to examine the impact of time-dependent food intake in this context. Volunteers consumed a predetermined high caloric (70 % of individual daily kilocalorie requirement) breakfast and low caloric dinner (10 %) in one condition and reverse calorie contents of breakfast and dinner in the other one. Lunch was equal in both conditions. Total daily calorie and macronutrient content was identical in both conditions (100 % of individual daily kilocalorie requirement) and corresponded to subjects' personal basal metabolic rate by Harris–Benedict equation. DIT was measured by indirect calorimetry and key parameters of systemic glucose metabolism as well as hypothalamic-pituitary-adrenal (HPA) axis activity, which may exert some influence metabolic turnover, were determined. **Results:** Comparing both conditions, identical calorie consumption clearly led to higher DIT in the morning than in the evening ($p < 0.001$ for all values). DIT increased after high caloric breakfast by 1.7 times and after low caloric breakfast by 6.5 times compared with isocaloric dinner-meals. Surprisingly, the DIT fell below pre-prandial levels 1.5 h after low caloric dinner. As expected, food-induced increase of blood glucose, insulin, and C-peptide levels was lower after breakfast than after dinner. **Conclusions:** Our data demonstrate that diet-induced energy turnover is clearly higher in the morning than in the evening, which is in line with a number of known factors regulating energy expenditure such as stress hormones and glucose metabolism. Extensive breakfasting should therefore be preferred over large dinner meals to prevent obesity or to lose weight within the scope of a diet.

OS09-8
Light-induced pain in porphyrias and photodynamic therapy involves TRPA1 and TRPV1

A. Babes[1,2], C. Neacsu[2], L. Moparthi[3], T. Kichko[2], S. Sauer[2], B. Namer[2], M. Filipovic[4], P. Zygmunt[3], P. Reeh[2], M. Fischer[2]
[1]University of Bucharest, Department of Anatomy, Physiology and Biophysics, Romania
[2]University of Erlangen-Nuremberg, Institute of Physiology and Experimental Pathophysiology, Germany
[3]Lund University, Department of Biochemistry and Structural Biology, Center for Molecular Protein Science, Sweden
[4]University of Erlangen-Nuremberg, Department of Chemistry and Pharmacy, Germany

Question: Photosensitization, an exaggerated sensitivity to normally innocuous light, occurs genetically in rare diseases such as porphyrias, unintentionally by contact with plants that contain photosensitizers, and intentionally in photodynamic therapy when cellular toxicity is induced in order to ablate superficial neoplasms like actinic keratosis. A common feature of these conditions is the experience of pain from bright light, the mechanism of which is still poorly understood. Our aim was to elucidate the signaling pathways involved in light-evoked pain in porphyrias and photodynamic therapy. **Methods:** We used Fura-2 calcium microfluorimetry and patch clamp to monitor light-induced activation of recombinant and native TRPA1 and TRPV1. Fluorescent indicators were used to detect generation of reactive oxygen species. Single-channel recordings were performed on TRPA1 channels purified and reconstituted in planar lipid bilayers. Light-evoked calcitonin gene-related peptide (CGRP) release was measured in mouse skin and trachea preparations. **Results:** In the absence of photosensitization, exposure of cells to blue and near ultraviolet light constitutively activated TRPA1 and, to a lesser extent, TRPV1 channels in heterologous expression systems and cultured mouse sensory neurons. However, pretreatment with aminolevulinic acid, as used in photodynamic therapy, or with protoporphyrin IX dramatically increased the light sensitivity of both TRPA1 and TRPV1 via generation of reactive oxygen species. The enhanced photosensitivity in the presence of aminolevulinic acid or protoporphyrin IX was strongly diminished in dorsal root ganglion neurons from TRPA1- and TRPV1-null mutant mice. Artificial lipid bilayers equipped with purified human TRPA1 showed substantial single-channel activity only in the presence of protoporphyrin IX and 405 nm blue light. Finally, photosensitization by aminolevulinic acid or protoporphyrin IX was also demonstrated in freshly isolated tissue (trachea and skin) and led to TRP channel-dependent release of proinflammatory neuropeptides upon illumination. **Conclusion:** With antagonists for the TRP channels in clinical development, this might pave the way to not only alleviate pain during photodynamic therapy but also to realize disease modification in porphyria patients.

Oral Session 10
Ion Channels II: ENac/Acid- & Other

OS10-1
Functional ENaC inhibition induces endocytosis of the channel

L. Niedzielski, F. Fischer, M. Maase, K. Kusche-Vihrog
Institute of Physiology II, Münster, Germany

The mechanical stiffness of endothelial cells strongly depends on the membrane abundance of the amiloride-sensitive epithelial Na^+ channel (ENaC) which in turn is important for the function of the vascular endothelium in that stiff cells release less nitric oxide than soft cells. The ENaC-dependent changes of endothelial rigidity can be related to interaction of ENaC with the cortical acto/myosin complex located beneath the plasma membrane. Interestingly, in endothelial cells amiloride, a specific inhibitor of ENaC function (i.e. Na^+ influx), was shown to dramatically decreases ENaC surface abundance and softens the endothelial cell cortex. ENaC membrane abundance depends on the rate of retrieval from the apical membrane. In epithelial cells the C-terminal domain of the channel, located in the cell, contains proline-rich motifs (PPxY), referred to as PY-motifs, which were shown to interact with the E3 ubiquitin-protein ligase NEDD4-2. This ubiquitination is a signal for internalization and Clathrin-mediated endocytosis (CME).

To study the underlying mechanism of the amiloride-induced disappearance of ENaC in endothelial cells, stiffness of the endothelial cortex was monitored by using nanoindentation measurements with the Atomic Force Microscope (AFM). For time course experiments amiloride (1 µM) or its analog benzamil (0.1 µM) were acutely applied. In addition, to resolve the underlying mechanisms, the amiloride/benzamil-dependent cortical softening was monitored with (i) jasplakinolide (0.5 µM), a stabilization agent of actin (ii) pitstop (30 µM), an inhibitor of CME and (iii) endothelial cells transfected with siNEDD4-2. To verify the existence of NEDD4-2 in an endothelial cell line (EAhy.926) and primary cultured endothelial cells (human umbilical vein endothelial cells, HUVEC) Western Blots were performed.

Analysis of the time course experiments revealed that amiloride/benzamil lead to an immediate significant decrease in cortical stiffness within the first 2 minutes from 0.99±0.19 pN/nm to 0.81±0.14 pN/nm (-18%, n= 7) and 0.97±0.22 pN/nm to 0.87±0.09 pN/nm (-10%, n= 6), respectively. Both jasplakinolide and pitstop prevented the amiloride/benzamil-induced endothelial softening. For EAhy.926 and HUVEC NEDD4-2 has been detected on the protein level.

We conclude that inhibition of Na^+ influx via ENaC induces a rapid rearrangement (depolymerization) of the cortical actin web, leading to softening of the cell cortex followed by clathrin-mediated ENaC internalization via NEDD4-2.

A new mechanism is postulated whereby changes of the Na^+ permeability induce a rapid feedback regulation of ENaC in endothelial cells.

OS10-2
Cono-RFamide from *Conus textile* targets Acid-Sensing Ion Channel 3 (ASIC3)

C. Reimers[1], H. Kalbacher[2], Y. Tian[1], S. Stevanović[3], S. Kauferstein[4], D. Mebs[4], S. Gründer[1]
[1]RWTH Aachen University, Institute of Physiology, Germany
[2]University of Tübingen, Interfaculty Institute of Biochemistry, Germany
[3]University of Tübingen, Department of Immunology, Institute for Cell Biology, Germany
[4]University of Frankfurt, Institute of Legal Medicine, Germany

Acid-sensing ion channels (ASICs) are proton-gated sodium channels belonging to the DEG/ENaC superfamily. They are expressed throughout the nervous system and involved in numerous physiological conditions. Several studies showed that especially ASIC3 is expressed in nociceptors and involved in the pain pathway. Individuals being stung by a cone snail report this to be immensely painful. Each cone snail species produces a complex venom containing a wide range of specifically acting toxins and non-toxic peptides. These provide us with a large amount of potential pharmacological tools. The goal of this work was to identify and characterize cone snail venom components to target ASICs. The screening of several cone snail venoms on their effects on ASICs expressed in *Xenopus* oocytes resulted in the identification of a small peptide from the *Conus textile* venom to specifically affect ASIC3. This peptide belonged to the family of Cono-RFamides and hence to the group of non-toxic venom components. It potentiated the proton-evoked ASIC3 current and strongly enhanced the desensitization time. These effects were similar to the ones being described previously for other RFamides (e.g. FMRFa) on ASICs. However, the EC_{50} of 2.9 ± 0.35 µM of the newly identified peptide proved it to be much more potent. Surprisingly, this peptide did not affect the FMRFa-activated sodium channel (FaNaC), a molluscan member of the DEG/ENaC family. As *Conus textile* is a molluscivorous snail these results underline a potential role of the cono-RFamide rather in the defense mechanism of the cone snail instead of predation.
Furthermore, the peptide elicited the effects described above also on ASIC3-like currents in mouse dorsal root ganglia (mDRG) neurons, recorded using the whole-cell patch-clamp technique. Additionally, we were able to show that the cono-RFamide is capable of altering mDRG neuron excitability in response to acidic and electric stimuli. These results suggest that an individual's susceptibility to pain might be changed by this peptide, depending on the corresponding conditions.
In the present study we showed that ASICs are a target of cono-RFamides. This provides us with a potent tool to further characterize the biochemical features and the physiological role of ASIC3. Moreover, these results help us to better understand the role of non-toxic cone snail venom components.

OS10-3
The degenerin region of the human bile acid sensitive ion channel is involved in channel inhibition by calcium and activation by bile acids

A. Ilyaskin[1], A. Diakov[1], H. Sticht[2], C. Korbmacher[1], **S. Haerteis[1]**
[1]Friedrich-Alexander-Universität Erlangen-Nürnberg (FAU), Institut für Zelluläre und Molekulare Physiologie, Germany
[2]Friedrich-Alexander-Universität Erlangen-Nürnberg (FAU), Institut für Biochemie, Germany

Question: Recently, it has been shown that the human bile acid sensitive ion channel (hBASIC), a member of the ENaC/degenerin ion channel family, can be activated by bile acids and removal of extracellular divalent cations (Lefèvre et al., *Pflügers Archiv*, 466:253-63, 2014). The aim of this study was to investigate in more detail the biophysical mechanism/s by which calcium removal and bile acids activate hBASIC. **Methods**. hBASIC was heterologously expressed in *Xenopus laevis* oocytes. Channel activity was investigated using the two-electrode voltage-clamp method and the outside-out configuration of the patch-clamp technique. Tauro-conjugated deoxycholic acid (t-DCA, 500 µM) was used to activate hBASIC. Homology modelling of hBASIC (based on the crystal structures of the acid-sensing ion channel 1 in desensitized and open state) together with a molecular docking approach and site-directed mutagenesis were used to identify putative calcium and bile acid binding site/s. **Results:** Our results show that t-DCA and calcium removal activate hBASIC in a synergistic manner mainly by increasing the channel activity (NPo). Both maneuvers, slightly but significantly, increase single-channel current amplitude which suggests an interaction of calcium and t-DCA with the pore region of the channel. Importantly, mutating an aspartate residue in the degenerin region of hBASIC to alanine (D444A) significantly reduces channel stimulation by calcium removal and enhances t-DCA stimulation in the presence of calcium. Molecular docking analysis predicts that t-DCA binds to the degenerin region in the open conformation of the channel. This suggests that calcium and t-DCA may have overlapping binding sites in the degenerin region of the channel. **Summary:** Our data demonstrate that the degenerin region of hBASIC is involved in channel inhibition by calcium and activation by bile acids. We conclude that calcium binding to aspartate (D444) stabilizes the closed state of the channel, whereas bile acids may function as intersubunit spacers stabilizing the open state of hBASIC.

OS10-4
The interplay between ion channels of the Degenerin / Epithelial Sodium Channel family and the lipid bilayer

A. Schmidt[1], R. Alsop[2], M. Rheinstadter[2], S. Gründer[1], D. Wiemuth[1]
[1]Uniklinik Aachen, Institute of Physiology, Germany
[2]McMaster University, Department of Physics & Astronomy, Hamilton, Canada

The Degenerin / Epithelial Sodium Channel (DEG / ENaC) family of ion channels in mammals comprises ENaC, Acid-Sensing Ion Channels (ASICs) and the Bile Acid Sensitive Ion Channel (BASIC). We previously demonstrated membrane mediated gating of BASIC by bile acids. This sensitivity to membrane alterations could be a common feature among DEG/ENaC channels and might be a principle underlying the regulation of ASICs by a variety of agents.
We expressed ASIC-1a, -2a and -3, α-β-γ-ENaC and the unrelated purinergic receptor P2X2 heterologously in Xenopus laevis oocytes and electrophysiologically tested the effects of agents that are known to affect membrane properties. In parallel we characterized the structural changes these agents induce in synthetic multilamellar phospholipid membranes made of DMPC (1,2-dimyristoyl-sn-glycero-3-phosphocholine) using X-ray diffraction. The membrane modifying agents used were ursodeoxycholic acid, sarkosyl, chlorpromazine and Triton X-100.
All ion channels were affected by the agents, however ASIC3 and P2X2 showed the most pronounced sensitivity to changes in their membrane environment. The diffraction experiments displayed marked effects of the substances on the membrane curvature. ASIC1a and ASIC3 were affected in a similar manner. Ursodeoxycholic acid as well as sarkosyl enhanced ASIC1a and ASIC3 proton-evoked currents and induced negative membrane curvature. In contrast, ATP-evoked P2X2 currents were inhibited by UDCA but enhanced by sarkosyl. Chlorpormazine inhibited proton-evoked currents of ASIC1a and ASIC3 as well as ATP-evoked P2X2 currents. In addition chlorpromazine induced positive membrane curvature. Triton X-100 displayed neither a clear effect on ion channel activity, nor on membrane curvature. Currently we correlate structural and functional data by the use of ion channel homology models in different conformational states.
As expected, changes in membrane properties induced by membrane active agents affected different ion channels. The interplay between membrane and ion channels cannot easily be generalized and strongly depends on the ion channel subtype studied as well as on the introduced membrane changes. Taken together, our results show that membrane properties should not be neglected when studying DEG/ENaC channel.

OS10-5
The phosphorylation site T613 in the β-subunit of rat epithelial Na^+ channel (ENaC) modulates channel inhibition by Nedd4-2

B. Krueger, C. Korbmacher, R. Rauh
Friedrich-Alexander-Universität (FAU) Erlangen-Nürnberg, Institut für Zelluläre und Molekulare Physiologie, Germany

Question: In sodium absorbing epithelia the rate of sodium transport critically depends on the apical expression of the heterotrimeric epithelial sodium channel (ENaC). Retrieval of rat ENaC from the plasma membrane is thought to be enhanced by phosphorylation of its β- and γ-subunits at residues βT613 and γT623, which directly precede PY binding motifs for the ubiquitin ligase Nedd4-2.[1,2,3] In this study we investigate the underlying mechanism by which these sites affect ENaC retrieval. **Methods:** Rat ENaC was expressed in *Xenopus laevis* oocytes and functional expression was measured as amiloride-sensitive whole-cell currents (ΔI_{ami}) with the two-electrode voltage-clamp technique. Intracellular and biotinylated cell surface fractions of βENaC were detected by Western blot. Phosphorylation of βT613 was detected with a phospho-specific antibody. **Results:** Preventing phosphorylation of βT613 and γT623 by mutating these residues to alanine (βT613A, γT623A) increased ΔI_{ami} in ENaC expressing oocytes, as shown before.[3] At the cell surface of αβγENaC expressing oocytes, two bands of βENaC were found with a predominant band running at ~120 kDa and an additional band at ~105 kDa. In the intracellular fraction only the ~105 kDa band was present. Phosphorylation of βT613 could be detected at the cell surface at ~120 kDa and in the intracellular fraction at ~105 kDa. To inhibit glycosylation of ENaC, αβγENaC expressing oocytes were treated with the ER mannosidase I inhibitor kifunensine. This treatment had no effect on ΔI_{ami} but the ~120 kDa band disappeared and βENaC was detectable only at ~105 kDa. This suggests that the ~120 kDa band is the mature glycosylated form of βENaC. Co-expression of Nedd4-2 with mutant channels in which subunits with inactivated PY-motifs (α_L, β_L, γ_L) were combined with intact βENaC ($\alpha_L\beta\gamma_L$) or γENaC ($\alpha_L\beta_L\gamma$) showed increasing inhibition of ΔI_{ami} with increasing amounts of Nedd4-2. However, when the intact PY-motif in βENaC was combined with the βT613A mutation ($\alpha_L\beta_{T613A}\gamma_L$), higher amounts of Nedd4-2 were needed to inhibit ΔI_{ami}. This was not the case when the intact PY-motif in γENaC was combined with the γT623A mutation ($\alpha_L\beta_L\gamma_{T623A}$). The inhibitory effect of Nedd4-2 on ΔI_{ami} was accompanied by a reduction of βENaC at the cell surface. **Conclusion:** Our results suggest that phosphorylation of βT613, but not of γT623, favours binding of Nedd4-2 to ENaC and enhances channel retrieval from the plasma membrane. Thus, phosphorylation and dephosphorlyation of βT613 may be a regulatory mechanism to modulate the affinity of Nedd4-2 to ENaC.

References

1. Shi et al., J Biol Chem 2002, 277:13539
2. Michlig et al., J Biol Chem 2005, 280:38264
3. Yang et al., J Biol Chem 2006, 281:9859

OS10-6
Connexin 30 inhibits human epithelial sodium channel (ENaC) expressed in *Xenopus laevis* oocytes by reducing channel surface expression

A. Ilyaskin, C. Korbmacher, **A. Diakov**
Friedrich-Alexander-Universität Erlangen-Nürnberg (FAU), Institut für Zelluläre und Molekulare Physiologie, Germany

Question: Recently, it has been reported that mice lacking connexin 30 (Cx30) develop salt-sensitive hypertension (Sipos A. *et al.*, JASN, 20:1724-32, 2009) and demonstrate increased epithelial sodium channel (ENaC) activity in the distal nephron (Mironova E. *et al.*, J Biol Chem, 286:1054-60, 2011). However, the molecular mechanisms of Cx30-mediated ENaC inhibition are not yet fully understood. In this study co-expression experiments were used to investigate the mechanisms responsible for ENaC inhibition by Cx30. **Methods**: Human ENaC and human Cx30 were heterologously expressed in *Xenopus laevis* oocytes and whole-cell currents were measured using the two-electrode voltage-clamp technique. ENaC and Cx30 mediated whole-cell currents were determined by measuring amiloride-sensitive currents (ΔI_{ami}) and currents elicited by extracellular removal of divalent cations (Ca^{2+}, Mg^{2+}), respectively. ENaC surface expression was estimated using an extracellularly FLAG-tagged βENaC subunit and a chemiluminescence assay. Open probability of ENaC was assessed in the outside-out configuration of the patch-clamp technique. Site-directed mutagenesis was employed to identify channel regions relevant for the functional interaction of ENaC and Cx30. **Results:** Our results show that co-expression of Cx30 with ENaC in *Xenopus laevis* oocytes significantly reduced amiloride-sensitive currents. The inhibitory effect of Cx30 on ENaC was associated with a reduction of channel surface expression without a significant decrease in channel open probability. Each of the three ENaC subunits (αβγ) contains a PY-motif within its cytosolic C-terminus. The PY-motifs are thought to be critically involved in Nedd4-2-dependent channel retrieval from the cell surface. Simultaneous truncation of the C-termini of all three ENaC subunits abolished the Cx30-mediated channel inhibition. Importantly, truncation of γENaC C-terminus alone was sufficient to prevent ENaC downregulation by Cx30. **Conclusion:** ENaC inhibition by Cx30 is mainly caused by a reduction of ENaC expression at the cell surface. The inhibitory effect of Cx30 may depend on the presence of an intact PY-motif in the C-terminus of γENaC. These findings suggest that Cx30 stimulates a retrieval machinery involving a critical region in the C-terminus of γENaC.

OS10-7
The rapid membrane insertion of the endothelial sodium channel is induced by shear stress and stiffens the cell cortex

Z. C. Cosgun, M. Wilhelmi, K. Kusche-Vihrog
Institut für Physiologie II, Münster, Germany

The endothelial sodium channel (EnNaC) determines endothelial nanomechanics in that an increased membrane abundance of EnNaC stiffens the endothelial cell cortex. This may lead to an increase in vascular tone and blood pressure. EnNaC expression and membrane abundance are mainly regulated by aldosterone via the mineralocorticoid receptor (MR). Endothelial cells are constantly exposed to wall shear stress by blood flow, whereas disturbed blood flow causes and maintains atherosclerotic processes. It is hypothesized that EnNaC serves as a flow sensor. Thus we tested whether physiological unidirectional laminar shear stress (LSS) and non-laminar shear stress (NLSS) influence EnNaC membrane abundance and endothelial stiffness.
Therefore, we established an *in vitro* model for smaller arteries: A defined magnitude of LSS (8 dyn/cm²) was applied by a shear stress pump (ibidi Pump System) on human umbilical vein endothelial cells (HUVEC) seeded on μ-and y-Slides with branching regions in the presence of 1nM aldosterone to simulate blood flow under defined conditions. After applying shear stress (chronic 48h and acute 15min) HUVEC were fixed. EnNaC membrane abundance was quantified by using a specific anti-αEnNaC primary antibody and a Quantum Dot-conjugated secondary antibody. The cortical stiffness was monitored by using nanoindentation measurements via atomic force microscopy (AFM) in LSS and NLSS regions of the slides.
Under chronic shear stress (48h) a significant increase of membrane ENaC by 48.6±3.6% compared to controls without LSS was found. Importantly, already after 15 min. LSS αEnNaC membrane abundance was increased by 58.5±4.5%. Both (i) Brefeldin A and (ii) K^+-Canrenoate, blockers of (i) exocytosis and (ii) MR, could prevent the acute shear stress-induced EnNaC membrane insertion indicating a rapid MR-mediated effect of shear stress. EnNaC membrane abundance under NLSS in branching regions was also significantly increased compared to static controls (+24.9±4.3%). AFM measurements revealed that the shear stress-induced increase in EnNaC membrane abundance lead to stiffening of the cell cortex by 18.9±5.5% compared to static controls.
The results suggest that EnNaC, besides being a mechano-sensor, is regulated by shear stress. Since both chronic and acute shear stress increase the membrane abundance we postulate genomic and non-genomic mechanisms leading to the membrane insertion of EnNaC and subsequent endothelial stiffening. Shear stress apparently triggers a signal cascade including the MR leading to the rapid membrane insertion, changes of the endothelial nanomechanics and thus endothelial function. This might be a physiological response to changes in hemodynamics and further explain the atherogenic potential of disturbed blood flow.

OS10-8
Regulatory role of the intracellular domain of the bile acid-sensitive ion channel (BASIC)

D. Wiemuth, P. Lenzig, S. Gründer
RWTH Aachen University, Physiology, Germany

Members of the DEG/ENaC family of ion channels are characterized by a similar structural organization. A large extracellular domain links two transmembrane domains, while the N- and the C-terminal regions protrude into the cytosol. The crystal structure of cASIC1 revealed the complex structure of the extracellular domain and the transmembrane domains of DEG/ENaC channels and helped to unravel the role of these domains for gating processes. However the role of the cytosolic N- and C-termini of most members of the DEG/ENaC family is still unknown. The bile acid-sensitive ion channel (BASIC) belongs to the DEG/ENaC family. As we have shown previously, BASIC is modulated by alterations of its membrane environment. Several membrane active molecules, in particular bile acids, activate BASIC. Currently we are analyzing the influence of the cytosolic domains on channel function. Removal of the N-terminal domain strongly potentiates the current responses of BASIC induced by bile acids. However total and surface expression are not significantly affected by the removal of this domain, indicating that this region affects the function of the channel itself. Sequence analysis and structure predictions suggest the presence of an amphiphilic α-helix in the N-terminal domain, which might tether the channel to the membrane and thus stabilize its closed state. Removal of the helix or introduction of helix-breaking mutations have the same effect as the removal of the whole N-terminal domain, suggesting a crucial role of this structure for channel function. Furthermore, the fusion of the N-terminal domain to GFP induces membrane localization, supporting the hypothesis that the N-terminal domain of BASIC is interacting with the plasma membrane. Taken together our results highlight the importance of the cytosolic N-terminus of BASIC and suggest the presence of a membrane binding amphiphilic α-helical structure. These findings may contribute to understand the physiological function of the channel.

Oral Session 11
Hippocampal Network Activity

OS11-1
Altered time-frequency characteristics and aberrant cerebral excitability in the APPswe/PS1dE9 and 5XFAD model of Alzheimer's disease

M. Weiergräber[1], J. Soos[1], M. Siwek[1], V. Raj-Ginde[1], D. Ehninger[2], K. Broich[1], C. Henseler[1], A. Papazoglou[1]
[1]Federal Institute for Drugs and Medical Devices (BfArM), Neuropsychopharmacology, Bonn, Germany
[2]German Center for Neurodegenerative Diseases (DZNE), Molecular and Cellular Cognition, Bonn, Germany

Alzheimer's disease (AD) is an age-related neurodegenerative disorder characterized by cognitive and behavioral impairment. Numerous AD mouse models have been described in literature exhibiting different translational capabilities regarding homology, isomorphism and predictability. Using simultaneous video-EEG radiotelemetry, we analyzed a highly progressive AD model (5XFAD) and a slowly progressive, i.e. moderate mouse model (APPswe/PS1dE9) for aberrant cortical excitability and altered electroencephalographic time-frequency characteristics with a specific focus on hippocampal theta oscillations and gamma activity. In contrast to control mice, seizure staging revealed a complex cortical hyperexcitability pattern in both AD models. Interestingly, 5XFAD mice displayed a significant increase in hippocampal theta activity from the light to dark phase during non-motor activity. We also observed a reduction in mean theta frequency in 5XFAD mice compared to controls that was again most prominent during non-motor activity. Similar complex time-frequency alterations were observed in APPswe/PS1dE9 mice. Transcriptome analysis of hippocampal probes and subsequent qPCR validation in 5XFAD mice revealed upregulation of Plcd4 that might be indicative of enhanced muscarinic signaling. Our results suggest that both 5XFAD and APPswe/PS1dE9 mice exhibit altered cortical excitability, hippocampal dysrhythmicity, and potential changes in muscarinic signaling.

OS11-2
Porcupine controls hippocampal AMPAR levels, composition and synaptic transmission

N. Erlenhardt[1,2], H. Yu[2], K. Abiraman[3], T. Yamasaki[4], J. I. Wadiche[3], S. Tomita[4], D. S. Bredt[2]
[1]University of Düsseldorf, Medical Faculty, Institute of Neural and Sensory Physiology, Germany
[2]Janssen Pharmaceutical Companies of Johnson & Johnson, Neuroscience Discovery, San Diego, United States
[3]McKnight Brain Institute, University of Alabama at Birmingham, Department of Neurobiology, United States
[4]Yale University School of Medicine, CNNR program, Department of Cellular and Molecular Physiology, New Haven, United States

AMPA-type glutamate receptor (AMPAR) complexes contain auxiliary subunits that modulate receptor gating and trafficking. In addition to well-studied transmembrane AMPAR regulatory proteins (TARPs) and cornichons (CNIH-2/3), recent proteomic studies identified a diverse array of additional AMPAR-associated transmembrane and secreted partners.
Here, we systematically evaluated each class of protein found in AMPAR immunoprecipitates using biochemical, cell biological and electrophysiological assays. Our analysis revealed that the membrane-bound O-acyl transferase porcupine (PORCN) plays a crucial role in the regulation of AMPAR complex composition and stability. In particular, PORCN knock-down in hippocampal neurons reduces expression of all tested AMPAR complex components, decreases AMPAR currents and accelerates desensitization, and this is associated with depletion of TARP γ-8 from AMPAR complexes. These effects are independent of PORCN's enzymatic activity. Conditional knock-out of PORCN in mice leads to a proportionate reduction of mature and immature AMPARs suggesting that PORCN controls the collective AMPAR pool at the level of the endoplasmic reticulum (ER). Additionally, conditional PORCN knock-out mice exhibit changes in AMPAR gating that together with the observed changes in expression result in a reduction of basal synaptic transmission, but leave long-term potentiation intact.
In summary, this study defines a novel role for PORCN in regulating synaptic transmission by controlling AMPAR complex stability and composition at the level of the ER.

N. Erlenhardt, H. Yu and K. Abiraman contributed equally to this work.

OS11-3
Intracellular pH distribution in cultured hippocampal astrocytes between somata and processes

A. Weise[1,2]
[1]Alexander Seidinger, Cellphysiology, Bochum, Germany
[2]Sina Schuette, Düsseldorf, Germany

Our research is focused on hippocampal astrocytes of mice. The aim was, to investigate subcellular H^+ changes upon imitation of neuronal activity, by using ROI-technique not only for somata but also for processes. This separation of ROI was already done with freshly isolated purkinje neurons, where larger H^+ shifts upon depolarisation were measured in the dendrites (Willoughby&Schwiening, 2002). The method we used was hippocampal cell culture of wild type or knock-out-mice for Carbonic anhydrase II, loaded with ratiometric dye BCECF-AM. We calibrated the system with nigericin technique. Application of an acidic pulse was done to calculate buffer capacity, glutamate or D-aspartate as well as different inhibitors for acid/base regulating proteins were used to stimulate the astrocytes with or without intact pH-regulation. The results for intracellular pH distribution in steady state as well as rates of changes under transmitter application will be presented, buffer capacities will be discussed and, further, the influence of acid/base regulating membrane proteins (NBCe1/NHE1) with or without CAII (WT, KO) on the glutamate or D-aspartate induced pH-shift will be analysed. Results from immunohistochemically stained tissue shall underline the imaging data.

References

Willoughby & Schiening, J Physiol (2002)

OS11-4
Frequency-selective entrainment of lateral septum by hippocampal oscillations mediates top-down control of locomotion

F. Bender, M. Gorbati, M. Carus Cadavieco, N. Denisova, X. Gao, C. Holman, T. Korotkova, **A. Ponomarenko**
Leibniz Institute for Molecular Pharmacology / NeuroCure Cluster of Excellence, Berlin, Germany

Hippocampal theta (5–10 Hz) and concurrent gamma (30–140 Hz) oscillations support encoding of an animal's position during spatial navigation, yet longstanding questions about their behavioral functions remain unanswered. Combining optogenetic control of hippocampal theta oscillations with electrophysiological recordings in mice, we studied causal impact of hippocampal theta oscillations on locomotion. We have recently shown that the regularity of theta oscillations underlies more stable and slower running speeds during exploration (Bender et al., Nature Communications, 2015). More regular theta oscillations were accompanied by more regular theta-rhythmic output of pyramidal cells. Theta oscillations were coordinated between hippocampus and its main subcortical output, the lateral septum (LS). In contrast, hippocampal gamma oscillations were only weakly coherent with intermittent gamma oscillations (30–120 Hz) in the LS, which were accompanied by phase-locked local neuronal discharge. Inhibition of hippocampus to LS pathway, using chemo- (DREADDs) or optogenetics (eNpHR3.0), revealed its necessity for the hippocampal control of running speed. Theta-rhythmic optogenetic stimulation of ChETA-expressing LS projections to the lateral hypothalamus replicated the reduction of running speed induced by more regular hippocampal theta oscillations. These results suggest that changes of hippocampal theta but not gamma synchronization are translated via the LS into rapid adjustment of locomotion. The present study shows that movement-dependent bottom-up modulation from subcortical regions to hippocampus is complemented by the top-down feedback, signaled at theta frequencies by hippocampus to locomotor circuits.

OS11-5
Optimal synaptic integration windows in the range of highfrequency oscillations through the instantaneous time constant

A. Yanez[1], T. Hondrich[1], A. Draguhn[1,2], M. Both[1]
[1]University of Heidelberg, Institute of Physiology, Germany
[2]Bernstein Center for Computational Neuroscience (BCCN), Heidelberg/Mannheim, Germany

In the hippocampus we can find spontaneous activity, consisting of high frequency (~ 200 Hz) oscillations, denominated ripples. During these events, pyramidal CA1 cells receive highly synchronized input, mainly coming from AMPA synapses. The kinetics of AMPA synapses present a fast decaying constant (~ 2 ms). Although their kinetics have been well studied in voltage clamp studies, the effect the opening of these receptors plays on signal integration is not completely understood. When numerous AMPA receptors are synchronously activated, there is an overall increase in the conductance of the neuron. This increase changes the cell's passive properties, namely the time constant. As the time constant rules the timescale of the integration processes, its reduction yields a more efficient integration. We propose a method to study how synapse-driven conductance changes can affect integration beyond the limitations of voltage clamp recordings: We patch a cell in current clamp and inject a small (4mV amplitude) sinusoidal current and we provide the same synaptic stimulus at different phase points of the sinusoidal. With this sinusoidal perturbation, we obtain at any point of the synaptic transient triplets of (V, I, dV/dt) that can be used to fit a simplified equation for a neuron and obtain an estimation of the conductance change during integration. Computational simulations show that for synaptic AMPA-like inputs, the maximum excitatory post synaptic potential (EPSP) amplitude does not appear when inputs are simultaneousm, as expected because of the higher driving force. Instead the enhanced integration due to the reduction in the time constant makes the total EPSP amplitude maximum when inputs are synchronized in a window of .5 ms. In conclusion, our method allows to measure the conductance change in the cell during synaptic activity in the more physiological current clamp configuration. Moreover, we use it to see the existence of a window of optimal integration that, in the case of AMPA synapses, falls in the ripple frequency.

OS11-6
Hyperpolarization-activated currents facilitate high-frequency action potential firing in cerebellar mossy fibers

N. Byczkowicz, S. Hallermann
University of Leipzig, Carl-Ludwig-Institute for Physiology, Germany

Mammalian axons and presynaptic terminals express a variety of different classes of ion channels that secure the initiation, propagation and transmission of action potentials (APs). Hyperpolarization-activated currents (I_h) have been described in axons[1]. However, the axonal function of I_h remains controversial[2-4]. Mossy fibers (MFs), one of the major afferent systems of the cerebellum, can fire APs at frequencies of more than 1 kHz[5].
In this study, whole-cell patch-clamp recordings from cerebellar mossy fiber boutons (cMFBs) in acute cerebellar brain slices allowed direct analysis of the function of I_h in central axons. Presynaptic I_h was activated by hyperpolarizing voltage steps, with half-activation at -104 mV. Activation and deactivation time constants were voltage dependent, being 23.7 ms at 150 mV (activation) and 31.7 ms at -130 mV (deactivation). Inhibition of I_h by application of 30 µM of the selective blocker ZD7288 hyperpolarized cMFBs, increased the membrane time constant, and increased the input resistance. High-frequency MF stimulation with a remote pipette was used to analyze the function of I_h in AP conduction. Furthermore, application of ZD7288 reduced the maximum failure free frequency of APs and increased AP broadening and amplitude reduction during fast trains of cMFB APs.
These data reveal that I_h participates in setting the resting membrane properties of cMFBs and is functionally relevant for the propagation of high-frequency APs in these fast spiking, myelinated axons.

References

1. Eng, D. L. *et al.* Current-clamp analysis of a time-dependent rectification in rat optic nerve. *J. Physiol.* 421, 185-202 (1990).
2. Elgueta, C. *et al.* Persistent discharges in dentate gyrus perisoma-inhibiting interneurons require hyperpolarization-activated cyclic nucleotide-gated channel activation. *J. Neurosci.* 35, doi:10.1523/jneurosci.3671-14.2015 (2015).
3. Soleng, A. F. *et al.* Unmyelinated axons in the rat hippocampus hyperpolarize and activate an H current when spike frequency exceeds 1 Hz. *J. Physiol.* 552, 459-470, doi:10.1113/jphysiol.2003.048058 (2003).
4. Cuttle, M. F. *et al.* Modulation of a presynaptic hyperpolarization-activated cationic current (Ih) at an excitatory synaptic terminal in the rat auditory brainstem. *J. Physiol.* 534, 733-744, doi:Doi 10.1111/J.1469-7793.2001.00733.X (2001).
5. Ritzau-Jost, A. *et al.* Ultrafast action potentials mediate kilohertz signaling at a central synapse. *Neuron* 84, 152-163, doi:10.1016/j.neuron.2014.08.036 (2014).

OS11-7
Variable topography of pre- and postsynaptic proteins in the hippocampal mossy fibre tract

M. Pauli[1], M. M. Paul[1], S. Poppert[1], M. Heckmann[1], M. Sauer[2], A. - L. Sirén[3]
[1]Julius-Maximilians-University Würzburg, Institute of Physiology, Department of Neurophysiology, Germany
[2]Julius-Maximilians-University Würzburg, Department of Biotechnology and Biophysics, Biocenter, Germany
[3]University Hospital of Würzburg, Department of Neurosurgery, Germany

Projections from hippocampal granule cells to CA3 pyramidal neurons give rise to large mossy fibre boutons (MFBs) that exhibit a pronounced form of presynaptic plasticity (Nicoll & Schmitz, 2005). Recent work suggested that the Ca^{2+} channel-release sensor coupling at these synapses is loose (~70 nm, Vyleta & Jonas, 2014). This so far uniquely described feature for mature, glutamatergic mammalian synapses originates at presynaptic active zones (AZs), elaborated subneuronal compartments for vesicle fusion and transmitter release that show complex protein-protein interactions within a range of a few hundred nanometers.
To gain insights into the molecular arrangement of hippocampal mossy fibre to CA3 synapses we employed super-resolution light microscopy by using *direct* stochastic optical reconstruction microscopy (*d*STORM, Heilemann et al., 2008; van de Linde et al., 2011). Providing a lateral resolution of typically about 20 nm it offers the unique possibility to study subsynaptic structures in combination with protein specificity due to conventional antibody labeling. We used horizontal, semithin cryo-slices from adult, male Thy1-EGP-F(M) mice to study MFB-synapses using antibodies against the AZ-scaffold protein Bassoon and against Homer, a marker for the postsynaptic density. Performing two-colour *d*STORM imaging we were thus able to define the exact orientation of each imaged synapse, *i.e.* in top view or in plane view. We obtained quantitative estimates for the area, length and width of Homer and Bassoon clusters for synapses in both orientations, as well as for the number of localizations in one cluster. Measurements of the peak-to-peak distance between the pre- and postsynaptic markers revealed a distance of ~150±20 nm (sd). Length of the Bassoon clusters varied from 200 to 900 nm, those of Homer from 100 to 700 nm. We employed a standardized procedure to compare the molecular dimensions of MFB-synapses in the left and right hippocampus, at different positions within the mossy fibre tract and at different heights. Furthermore, comparison between Bassoon clusters at hippocampal MFBs with cerebellar parallel fibre to Purkinje cell synapses and cholinergic neuromuscular junctions revealed that AZs in hippocampal MFBs show the highest variability concerning protein amount and size.

References

Heilemann M, van de Linde S, Schüttpelz M, Kasper R, Seefeldt B, Mukherjee A, Tinnefeld P, Sauer M. 2008 Subdiffraction-Resolution Fluorescence Imaging with Conventional Fluorescent Probes. Angew Chem Int Ed 33:6172-6
van de Linde S, Löschberger A, Klein T, Heidbreder M, Wolter S, Heilemann M Sauer M. 2011 Direct stochastic optical reconstruction microscopy with standard fluorescent probes. Nat Prot 7:991-1009
Vyleta NP, Jonas P. 2014 Loose coupling between Ca^{2+} channels and release sensors at a plastic hippocampal synapse. Science 343:665-70
Nicoll RA, Schmitz D. 2005 Synaptic plasticity at hippocampal mossy fibre synapses. Nat Rev Neurosci 6:863-76

OS11-8
Lobule- and layer-specific frequency dispersion in the cerebellar cortex

I. Straub[1], M. Hoidis[1], A. Eshra[1], I. Delvendahl[1], K. Dorgans[2], S. Elise[2], I. Bechmann[3], M. Krüger[3], P. Isope[2], S. Hallermann[1]
[1]Universität Leipzig Carl-Ludwig Institut für Physiologie, Germany
[2]Université de Strasbourg, Institute des Neurosciences Cellulaires et Intégratives, CNRS, France
[3]Universität Leipzig, Institute of Anatomy, Germany

To control timing of motor function, the cerebellar cortex receives broad-bandwidth neuronal signals with up to kilohertz frequencies from mossy fibers. However, it is still unclear if the postsynaptic granule cells (GCs) are tuned to specific frequencies and whether such frequency dispersion is topographically organized. Here, we combined structural and functional analyses to investigate frequency tuning of GCs from different lobules. We found that, in lobule IV/V and lobule IX, GCs near white matter (inner-zone GCs) functionally differ from GCs near Purkinje cells (outer-zone GCs). Inner-zone GCs fired action potentials with higher current-threshold, shorter half-duration, and higher frequency during current injection. Consistent with these functional differences, we recorded larger voltage-depended potassium currents from inner-zone GCs. Furthermore, inner-zone GCs gave rise to parallel fibers located close to Purkinje cell somata (inner-zone parallel fibers). The diameter of these inner-zone parallel fibers was larger compared with outer-zone parallel fibers. In addition to the functional differentiation within the GC-layer, there were also differences between lobules: GCs from lobule IV/V fired, age independently, action potential with shorter half-with and higher frequency compared to GCs from lobule IX. These data suggest that the broad-bandwidth input signal from a single mossy fiber is distributed to hundreds of postsynaptic GCs in a frequency dependent manner. Furthermore, the diameter and location of GC axons are tuned to optimally convey a preferred frequency to Purkinje cells. Thus, we demonstrate frequency dispersion within and between different lobule of the cerebellar cortex, which provides a new concept for cerebellar information processing.

Oral Session 12
Endothelial Cell Physiology

OS12-1
Distinct stimulus dependent dilatory mechanisms in the murine coronary vascular bed: NO and Cx40-dependent coupling during reactive hyperemia, but prostaglandins upon ACh

R. Windler[1,2], C. de Wit[1,2]
[1]Universität zu Lübeck, Institut für Physiologie, Germany
[2]DZHK (German Centre for Cardiovascular Research), partner site Hamburg/Kiel/Lübeck, Germany

Endothelial dilatory mechanisms such as NO, cyclooxygenase (COX) products, or the hyperpolarizing mechanism (EDH) are crucial for active and reactive hyperemia, but also for dilations upon acetylcholine (ACh). Their contributions vary substantially between vascular beds and, importantly, also between different stimuli. In addition, direct communication between cells through gap junctions is essential for transmission of dilatory signals along endothelial cells in the vessel wall. Gap junctions are composed of connexins (Cx) and Cx40 is crucial for intact active hyperemia in murine skeletal muscle. The aim of this study was to examine endothelial dilator mechanisms in the intact and Cx40 deficient ($Cx40^{-/-}$) coronary vascular bed in mice.
We perfused wildtyp (WT) and $Cx40^{-/-}$ hearts in a Langendorff setup at constant pressure (100mmHg) measuring coronary flow. Vascular reactivity was assessed by applying increasing amounts of ACh, active hyperemia by external pacing (300-700 bpm) and reactive hyperemia by flow stoppage for up to 30s. NO synthase (NOS) was inhibited by Nitro-L-arginine (LNA, 100µM) and COX by indomethacin (indo, 3µM) to study their respective contribution in these dilatory response.
Basal flow, maximal flow change during reactive hyperemia and repayment/debt ratio was reduced in $Cx40^{-/-}$ compared to WT mice. LNA reduced basal flow only in WT, whereas LNA+indo reduced basal flow in both genotypes. Maximal flow change during reactive hyperemia was decreased after NOS blockade in both genotypes by ~20% and after combined blockade of NOS and COX by 35% in WT and by 20% in $Cx40^{-/-}$. The repayment/debt ratio was reduced in both genotypes after NOS as well as after combined NOS and COX blockade by roughly 35%. Active hyperemia remained mostly unaffected by these blockers in all mice. ACh induced dilation was attenuated by NOS blockade only in $Cx40^{-/-}$. Surprisingly, ACh responses were nearly abrogated after combined blockade of COX and NOS in both genotypes (by 79%).
We conclude that Cx40 is required to maintain basal and full reactive hyperemia. NO release supports basal flow and also contributes (independent of Cx40) to reactive hyperemia. In contrast, prostaglandins are key mediators of the dilation upon ACh in murine coronaries while NO is invoked only in the absence of Cx40. We suggest that, in contrast to common belief, coronary dilations involve distinct mechanisms depending on the stimulation. Specifically, ACh cannot be considered as a NO/EDH stimulus in this model.

OS12-2
Functional inhibition of ENaC alters the cortical cytoskeleton

L. Herrnböck, M. Maase, K. Kusche-Vihrog
University of Münster, Institute of Physiology II, Germany

Endothelial ENaC is a crucial determinant for cellular mechanics and thereby vascular function. Its membrane abundance affects the stiffness of endothelial cortex, an actin-rich region 50–200nm beneath the plasma membrane. The endothelial rigidity in turn can be seen as parameter for the physiological function of vessels as it regulates the release of the vasodilator nitric oxide (NO) Cortical actin dynamics determine cortical stiffness and directly influence the release of NO. In particular, a shift from G- to F-actin leads to increased rigidity of the endothelial cortex. ENaC, however, was shown to physically interact with F-actin.
Recently, it could be shown that amiloride, a specific blocker of ENaC function, reduces the cortical stiffness of endothelial cells which leads to immediate softening of the cell cortex. In presence of jasplakinolide, an inducer of actin polymerization, the effect of amiloride fails to appear. From this observation it is hypothesized that the functional inhibition of ENaC alters the conformation of cortical proteins and thus endothelial nanomechanics.
To study the effects of ENaC inhibition on the cortical actin web, confocal fluorescence microscopy was performed. Endothelial cells (EA.hy926) were incubated in medium containing 1 nM aldosterone and treated with amiloride (1µM), benzamil (0,1µM) or cytochalasin D (CyD, 50nM). DAPI was used for staining the cell nucleus and Alexa Fluor 546 phalloidin for staining the actin filaments of fixed cells. Z-stacks were performed with a Z-step size of 0,5µm.
In order to analyse the fluorescence originating mainly from the cell cortex we chose a focal plane right above the cell nucleus.
Analysis of the confocal fluorescence images revealed that amiloride provokes a decrease of the fluorescence intensity by 42% compared to control. Application of another specific ENaC inhibitor benzamil even diminishes the fluorescence intensity to 50% of control. Upon treatment with low concentrations of the actin-disrupting agent CyD the fluorescence intensity of F-actin, however, is lowered by 28% compared to control.
We conclude that the functional inhibition of ENaC – and thereby Na^+ influx – by amiloride or benzamil causes a depolymerisation of actin and thus a decrease of F-Actin. This indicates that ENaC-dependent endothelial stiffness involves dynamical processes of the cortical web and directly influences vascular function.

0S12-3
Supramolecular organization of junction associated intermittent lamellipodia (JAIL) *in vivo*

S. März[1], N. Lindemann[1], J. Cao[1], M. Taha[1], E. Montanez Miralles[2], H. - J. Schnittler[1]
[1]UKM, Institute of Anatomy and Vascular Biology, Muenster, Germany
[2]Ludwig-Maximilians University, Walter-Brendel-Center of Experimental Medicine, Munich, Germany

Stability of endothelial cell contacts is crucial for maintaining the barrier function of the blood vessel wall. Additionally, endothelial cell integrity needs to be loosened to enable leukocyte transcytosis to sites of inflammation. Therefore, the endothelium developed multiple mechanisms that control composition and regulation of endothelial junctions.
Besides several adhesion molecules vascular endothelial cadherin (VE-cadherin) together with catenins form the VE-cadherin-catenin complex that directly and indirectly associates with the actin cytoskeleton. The interdependent regulation of actin and VE-cadherin/catenin complex plays an important role in the maintenance and dynamic of adherence junctions.
Dynamics of VE-Cadherin was shown to depend on junction associated intermittent lamellipodia (JAIL) that are actin driven and Arp2/3-controlled plasma membrane protrusions. JAIL not only drive VE-cadherin dynamics but also control entire cell motility in sheet forming cell layers. Here we demonstrate the appearance of JAIL *in vivo* in arteries, veins and microvasculature. The supramolecular organization of JAIL including actin, VE-cadherin and catenins, parvin and the ARP2/3 complex were investigated by structured illumination microscopy.
The data demonstrate JAIL at endothelial cell junctions *in vivo*. We propose JAIL as relevant structures of endothelial cell junctions, which most probably drive VE-cadherin dynamics and cell motility *in vivo* as well.

0S12-4
Adenosine receptors regulate gap junction coupling in endothelial cells by different pathways

A. Bader[1], D. Begandt[2], A. Klett[1], W. Bintig[3], A. Ngezahayo[1,4]
[1]Leibniz University Hannover, Institute of Biophysics, Germany
[2]University of Virginia School of Medicine, Robert M. Berne Cardiovascular Research Center, Charlottesville, United States
[3]Charité Universitätsmedizin Berlin, Charité CrossOver, Germany
[4]University of Veterinary Medicine Hannover, Center for Systems Neuroscience (ZSN), Germany

The regulatory interaction between adenosine receptors and gap junction coupling in vascular endothelial cells was analysed using the bovine aortic endothelial cell line GM-7373 and the human microvascular cerebral endothelial cell line hCMEC/D3. Physiological analysis using scrape loading/dye transfer assays showed that dipyridamole, an inhibitor of adenosine transporters, and the adenosine analogue 2-phenylaminoadenosine (2-PAA) induced a dose-dependent increase in gap junction coupling of up to 140% in both cell lines. Immunocytochemical analysis showed that the increase in gap junction coupling correlated with an increase in gap junction plaques containing connexin43 (Cx43) between the cells. In contrast, induction of connexin gene transcription or protein synthesis was not found within 6 h. Pharmacological experiments showed that the dipyridamole- and 2-PAA-related enhancement of gap junction coupling was suppressed by inhibitors of the cAMP/PKA-dependent pathway in the GM-7373 cells but not in the hCMEC/D3 cells. A detailed pharmacological analysis of the human microvascular cerebral endothelial cell line hCMEC/D3 revealed that the A_{2B} adenosine receptor subtype was predominately responsible for the 2-PAA-induced enhancement of gap junction coupling. Furthermore it was found that the enhancement of the gap junction coupling in the hCMEC/D3 cells was inhibited in cells preloaded with the Ca^{2+} chelator BAPTA and was suppressed by the cyclic nucleotide-gated (CNG) channel inhibitor L-*cis*-diltiazem. PCR and Western blotting experiments showed that the hCMEC/D3 cells expressed CNG channels. Correspondingly, patch-clamp experiments showed that 2-PAA activated CNG channels. The results suggest that the activation of adenosine receptors in the microvascular cerebral endothelial cell line induces a Ca^{2+} influx via CNG channels. By activating calcium-dependent signalling cascades, Ca^{2+} induces in turn the enhancement of the gap junction coupling. The results further suggest that the gap junction coupling is differently regulated in endothelial cells originating from vessels of different vascular beds. Moreover we propose an involvement of the gap junction coupling in tissue protective effects related to adenosine receptor stimulation in the vascular system.

References
Begandt et al., J Bioenerg Biomembr. 2010 Feb;42(1):79-84. doi: 10.1007/s10863-009-9262-2
Begandt et al., J Bioenerg Biomembr. 2013 Aug;45(4):409-419. doi: 10.1007/s10863-013-9518-8

0S12-5
Long-term exposure to shear stress stimulates endothelial glycocalyx recovery

T. Gloe[1], L. Devermann[1], G. Ramos-Espinosa[1], U. Stefanie[2], K. Bieback[3]
[1]med. Faculty Mannheim, Heidelberg-University, Cardiovascular Physiology, CBTM, Germany
[2]med. Faculty Mannheim, Heidelberg-University, Flow Cytometry Core Facility, CBTM, Germany
[3]med. Faculty Mannheim, Heidelberg-University, Institute of Transfusion Medicine and Immunology, CBTM, Germany

Question: Endothelial cells (EC), lining the inner surface of the vasculature, control barrier function and cellular adhesion. Under physiological situations the EC are decorated with a glycocalyx, composed of heparansulfates and proteoglycans anchored to the cell surface via linker proteins like syndecans. It is known that under hypoxic conditions this glycocalyx is significantly reduced by shedding. Since hypoxia is often associated with low- or no-flow conditions, we tested here the hypothesis that loss of flow (low shear stress) induces shedding of glycocalyx and that long-term exposure to flow enables EC to regain their typical cell surface modification. **Methods:** Primary isolates of EC from human umbilical veins (HUVEC) were subjected to normal static cell culture conditions or exposed to laminar flow (15 dyn/cm²) for up to 5 days. The presence of the glycocalyx was traced by flow cytometry using FITC-labeled lectins. To test functional effects of glycocalyx coverage, we performed adhesion assays using endothelial precursor cells (ECFC), HUVEC, monocytes (MonoMac 6) or non-stimulated human platelets. Those “adhesive” cells were fluorescently labeled with calcein-AM and exposed to the “acceptor” HUVEC mono-layer using low flow conditions (1.5 dyn/cm² for 20 min) to minimize unspecific cell adhesion. Adhered cells of 10 optical fields of each experiment were counted. Finally, real-time RT-PCR was used to quantify gene expression of the possible glycocalyx anchor proteins (Syndecan 1, 2, 4 and Glypican 1, 4). **Results:** HUVEC cultivated under static monolayer culture conditions show only limited lectin binding. However, if those cells were exposed to long-term flow they regained a glycocalyx coverage indicated by significant stronger binding of the lectins. Importantly, a stop-flow of only 4 hours after an initially 5 day-flow significantly reduced lectin binding, indicating rapid loss of the glycocalix in static conditions. The long-term flow induced glycocalyx formation corresponded to a significant change of adapter molecules as Syndecan 1 and 2, which were up-regulated compared to their static controls (1.6 or 1.5 fold). Similarly, Glypican 1 and 4 were slightly up-regulated. In contrast, Syndecan 4 was down-regulated by approx. 30%. Those re-established glycocalyx coverage by exposure to shear stress resulted in less adhesion of all cell types tested (ECFC, HUVEC, MonoMac, as well as platelets) to flow-exposed HUVEC. **Conclusion:** Endothelial cells rapidly lose their physiological glycocalyx surface layer in static culture. However, they might regain that surface modification during long-term flow-exposure. The glycocalyx coverage prevents cells adhesion and might be important for proper barrier function of the vessel wall. Interestingly, although it takes days to re-build the glycocalyx, it is destroyed within a few hours of no-flow.

0S12-6
Reduced NO sensitivity in arterioles deficient for the soluble guanylyl cyclase alpha 1 subunit *in vivo*

K. Schmidt[1,2], Z. Aherrahrou[3,2], E. Mergia[4], D. Koesling[4], J. Erdmann[3,2], C. de Wit[1,2]
[1]Universität zu Lübeck, Institut für Physiologie, Germany
[2]Deutsches Zentrum für Herz-Kreislauf-Forschung (DZHK) e.V. (German Center for Cardiovascular Research), Partner site Hamburg/Kiel/Lübeck, Germany
[3]Universität zu Lübeck, Institut für Integrative und Experimentelle Genomik, Germany
[4]Ruhr-Universität Bochum, Institut für Pharmakologie und Toxikologie, Germany

Introduction:The vasodilator nitric oxide (NO) acts via activation of its receptor, the soluble guanylyl cyclase (sGC), thereby generating the second messenger cyclic guanosine-3’,5’-monophosphate (cGMP). cGMP activates the protein kinase G (PKG) which elicits vasorelaxation in part by reducing intracellular calcium concentration in vascular smooth muscle cells. sGC is a heterodimeric protein composed of an α- and a β-subunit. Two isoforms of the α-subunit (α1 and α2) are found in smooth muscle of which the α1 isoform is the predominant form (about 94% of total). A decreased sensitivity for NO donors was demonstrated in the aorta of mice deficient for the α1-subunit before (Mergia E. *et al.*). However, vascular signalling in the microcirculation is very different from large conductance vessels such as the aorta. Therefore, we studied the impact of α1-deficiency on vascular responses in arterioles *in vivo*. **Methods:** We performed intravital microscopy in the cremaster muscle of mice which lacked the sGC α1-subunit (*Gucy1a3*-KO) and wild type controls (WT). Arterioles with a maximal diameter between 14 and 81 µm (mean: 33 µm) were examined. Concentration response curves for acetylcholine (ACh), the NO donors sodium nitroprusside (SNP) and DEA-NONOate (DEA) were obtained by superfusing the dilator compounds onto the microcirculation. A cGMP analogue (8-pCPT-cGMP) to circumvent sGC was also studied. **Results**: Resistance vessels of *Gucy1a3*-KO mice exhibited a similar spontaneous tone as WT (50±2 vs. 49±2% of maximal diameter). The endothelium-dependent dilator ACh induced concentration-dependent dilations in both genotypes, but the EC_{50} was shifted towards higher concentrations in *Gucy1a3*-KO mice. Dilator responses to the NO donor SNP were significantly reduced in *Gucy1a3*-KO at medium concentrations (by about 50%), but not different at the highest concentration of SNP (10 µM) which led to a dilation of about 50% of maximal response. DEA induced a dilation of 43% in WT (at 10 µM) that was reduced to 23% in *Gucy1a3*-KO. 8-pCPT-cGMP (10 µM) induced a similar dilation in *Gucy1a3*-KO and WT mice (8±2 vs. 6±2%). **Conclusion**: The data demonstrate a reduced NO sensitivity *in vivo* in arterioles of mice deficient for the α1 subunit of the sGC. However, a substantial dilation is preserved in these mice indicating that sGC composed solely of α2 and β subunits acts as a significant NO receptor in these vessels.

References
Mergia E, Friebe A, Dangel O, Russwurm M, Koesling D.
Spare guanylyl cyclase NO receptors ensure high NO sensitivity in the vascular system.
J Clin Invest. 2006 Jun;116(6):1731-7.

OS12-7
Endothelial cell labeling and magnet-assisted purification using a transgenic PECAM/eGFP mouse model

F. Winkler[1], K. Herz[1], S. Rieck[1], T. Hu[1], J. Heinemann[2], B. Engelbrecht[2], M. Hesse[1], W. Röll[2], B. K. Fleischmann[1], D. Wenzel[1]
[1]University of Bonn, Institute of Physiology I, Germany
[2]University of Bonn, Department of Cardiac Surgery, Germany

Question: In order to monitor vascular development and to test potential pro- and antiangiogenic strategies, endothelial cell-specific reporter gene models are extremely valuable tools. Because platelet endothelial cell adhesion molecule (PECAM) is highly expressed in endothelial cells at all developmental stages we generated a transgenic PECAM/eGFP mouse model which was used to characterize vascularization *in vitro* and *in vivo*. **Methods:** PECAM/eGFP expression was analyzed in mouse embryos at different developmental stages and adult organs using fluorescence microscopy. The endothelial-specific expression pattern of PECAM/eGFP was assessed by immunohistochemical stainings, in an aortic ring assay *in vitro* as well as in a myocardial cryoinfarction model *in vivo*. Moreover, PECAM/eGFP+ cells were isolated from transgenic mouse hearts by magnetic cell sorting (MACS), and local positioning of the cells and the developing networks was explored using a magnetic field. **Results**: Mouse embryos at E9.5 and E15.5 showed strong eGFP expression in the developing vasculature. In adult mice eGFP expression was found in vascular networks of various organs (e.g. heart, kidney, skin, lung, uterus, skeletal muscle) and also in vessels of all calibers. Endothelial cell-specific expression was confirmed by eGFP+PECAM+ sprouts in an aortic ring assay. Even in a myocardial cryoinfarction model eGFP+ sprouts could be found in the border zone of the lesion proving the utility of the mouse model to assess and quantify re-vascularization upon injury. By MAC sorting with magnetic beads coupled to an anti-PECAM antibody we obtained a highly purified eGFP+ endothelial cell fraction. The magnetic labeling of the isolated endothelial cells could be used to locally attract the cells by a magnetic field, with this approach we could demonstrate site-specific formation of eGFP+ vascular networks *in vitro*. **Conclusion**: Transgenic PECAM/eGFP mice display strong endothelial cell-specific eGFP expression at all developmental stages and even after injury. MAC sorting enabled purification of magnetically labeled eGFP+ endothelial cells. The labeling was used for local vascular network formation by a magnetic field. This technology could be further developed and employed for therapeutic angiogenesis approaches.

OS12-8
EPLIN isoforms differentially control adherens junction dynamics in endothelial cells

M. Taha, J. Seebach, S. März, H. - J. Schnittler
UKM, Institute of Anatomy and Vascular Biology, Muenster, Germany

Adherence junction dynamics is critical for endothelial integrity, barrier function, inflammation and angiogenesis. The vascular endothelial (VE)-cadherin/catenin complex interacts with actin filaments via α-catenin either directly via a catch bound connection or indirectly via the epithelial protein lost in neoplasm (EPLIN). However, the mechanisms and regulations of actin VE-cadherin interactions are not completely understood. EPLIN is an actin binding protein that competes with the actin related protein 2/3 (ARP2/3) complex for actin binding and connects VE-cadherin to the actin filament cytoskeleton. Thus, EPLIN appears to be a suitable candidate to integrate actin and VE-cadherin dynamics. Immunofluorescence microscopy of endothelial cells *in vitro* and *in vivo* localized EPLIN at cell junctions, stress fibers, JAIL and in migrating cultured cells at free lamellipodia. Endothelial cells express two isoforms α- and β-EPLIN, but α-EPLIN is highly upregulated in subconfluent cultures. Increasing cell density down regulates α-EPLIN. Live-cell imaging of fluorescent tagged EPLIN isoforms revealed that both EPLIN isoforms localized at actin stress fibers and at mature junctions. We recently discovered an actin driven and ARP2/3 complex controlled lamellipodia like structure at the cell junctions that were termed junction associated intermittent lamellipodia (JAIL) which control VE-cadherin dynamics and monolayer integrity. We found α- but not β-EPLIN to be associated with JAIL and lamellipodia in migrating cells while β-EPLIN remained at lamella and seem to have an impact on retraction. Application of fluid shear stress on HUVEC increased the fluorescence intensity of α and β-EPLIN at the junction, a process that seems to be accompanied with a transient increase in barrier function. To better understand the impact of the isoforms we overexpressed each of them separately in HUVEC cultures. Under those conditions both isoforms decreased the barrier function but the overexpression of α-EPLIN additionally increased stress fibers formation and its dynamics. Furthermore, EPLIN depleted cells failed to recruit actin filaments to the junctions upon cAMP upregulation. Together, these data indicate that EPLIN is a critical component of endothelial cell junctions by which the two isoforms display a divers function.

Oral Session 13
Transporters

OS13-1
The ammonia transporter RhCG modulates vacuolar H⁺-ATPase function in renal collecting duct cells

S. Bourgeois[1], L. Bounoure[1], I. Mouro-Chanteloup[2,3], Y. Colin Aronovicz[2,3], D. Brown[4,5], C. A. Wagner[1]
[1]University of Zurich, Institut of Physiology, Switzerland
[2]INSERM UMR665, Paris, France
[3]University Paris Diderot, France
[4]Massachusetts General Hospital, Center for Systems Biology, Program in Membrane Biology, Department of Medicine, Boston, United States
[5]Harvard Medical School, Boston, United States

Ammonium (NH_4^+) is excreted into urine along the kidney collecting duct representing the predominant mechanism of excreting acid into urine. This process is dependent on the concomitant secretion of ammonia (NH_3) by the NH_3 transporter RhCG and protons (H^+) by the vacuolar multimeric H^+-ATPase pump. Since mice lacking Rhcg excrete more alkaline urine despite lower urinary ammonium, we studied a possible interaction between RhCG and H^+-ATPase.
In rat kidney medulla, we showed that RhCG and the B1 subunit of the H-ATPase were able to be coimmunoprecipitated. Next, we demonstrated in *ex vivo* microperfused cortical collecting ducts (CCD) that H^+-ATPase activity was reduced by 89 % in CCD from *Rhcg*$^{-/-}$ mice compared to control littermate CCDs. However, kidney expression of the B1 H-ATPase subunit was enhanced while the B2 H-ATPase subunit was reduced in kidneys from *Rhcg*$^{-/-}$ mice. Moreover, expression of the a1, a4, and E2 H^+-ATPase subunits was similar in the renal medulla of *Rhcg*$^{+/+}$ and *Rhcg*$^{-/-}$ and immuno-gold detection of the A subunit showed similar localization and density of staining between the wildtype and Rhcg$^{-/}$ mice. Conversely, overexpression of RhCG in HEK293 cells resulted in higher H^+ secretion and increased B1 subunit mRNA (Atp6v1b1) expression.
Finally, to study the functional role of H^+-ATPase on RhCG activity we assessed the effect of the H^+-ATPase inhibitor concanamycin on RhCG activity. We showed that concanamycin which inhibits H^+-ATPase activity could also inhibit RhCG activity in the mouse *ex vivo* microperfused CCD. However, *ex vivo* microperfused CCD from mice lacking the B1 subunit of H^+-ATPase had reduced H^+-ATPase activity without altering RhCG activity.
Thus, we showed for the first time that RhCG and H^+-ATPases are located within the same cellular complex. RhCG may modulate H^+-ATPase function, whereas H^+-ATPase activity does not directly affect RhCG mediated NH_3 transport.

OS13-2
Role of the organic cation transporter 2 in nephro- and neurotoxicity mediated by chronic treatment with cisplatin

A. Hucke[1], R. Schröter[1], I. Castanheira[1], C. Ceresa[2], G. Cavaletti[2], E. Schlatter[1], G. Ciarimboli[1]
[1]University Hospital Muenster, Department of Internal Medicine D, Experimental Nephrology, Germany
[2]University of Milano-Bicocca, Department of Surgery and Translational Medicine, Monza, Italy

Antineoplastic treatment with cisplatin has a high efficacy, but is burdened with important side effects such as nephro-, oto-, and peripheral neurotoxicity, which heavily reduce life quality of patients after anti-cancer treatment. Membrane transporter have been demonstrated to be important for cellular uptake of cisplatin. Specifically, the organic cation transporter 2 (OCT2), which is expressed in renal proximal tubules, cisplatin-sensitive cochlea cells, and dorsal root ganglia (DRG), is supposed to play a critical role for cisplatin transport in cells, which are not the target of chemotherapy. In this work, we have studied the role of OCT2 for the development of unwanted toxicities in mice, which were chronically treated with cisplatin, resembling the chemotherapeutic protocol used in patients. Wild type (WT) and OCT2 knockout (OCT2$^{-/-}$) mice were treated twice per week for 4 weeks with NaCl or 4 mg/kg body weight cisplatin. At the end of treatment urine, protein, and glucose excretion, audiological brainstem response, caudal nerve conduction velocity and DRG morphometries were measured. All data are given as mean ± SEM and are normalized to body weight. Statistical differences were calculated by ANOVA and N was 15 for WT and 7 for OCT2$^{-/-}$ mice, unless otherwise specified. Compared with NaCl, treatment with cisplatin caused a significant polyuria (from 33 ± 2 (NaCl) to 176 ± 14 (cisplatin) and from 30 ± 5 to 110 ± 19 µl urine/24 h) both in WT and OCT2$^{-/-}$ mice, respectively. A significant proteinuria and glucosuria was observed only in WT (from 0.13 ± 0.01 to 0.41 ± 0.05 µg protein/24 h and from 25 ± 1 to 34 ± 2 µg glucose/24 h), but not in OCT2$^{-/-}$ (from 0.10 ± 0.02 to 0.23 ± 0.06 µg protein/24 h and from 14 ± 2 to 21 ± 2 µg glucose/24 h) mice. Cisplatin did not cause any significant ototoxicity, probably because treatment-induced specific down regulation of OCT2 mRNA expression in the cochlea (-68 ± 14 % compared to untreated mice, N = 4). Caudal nerve conduction velocity and DRG somatic area were significantly higher in OCT2$^{-/-}$ than in WT mice (28.0 ± 0.2 to 25.5 ± 0.4 m/s and 552 ± 10 to 500 ± 10 µm2, respectively, N = 4, unpaired t-test). These data suggest that OCT2 plays an important role for determining chronic nephro- and peripheral neurotoxic effects of cancer chemotherapy with cisplatin. In contrast to what we previously observed with an acute toxicity model (Am J Pathol 2010, 176(3):1169-8), chronic cisplatin treatment did not induce any measurable ototoxicity, probably because of the organ-specific down regulation of OCT2 expression. Since cancer cells generally do not express OCT2, this transporter may be the target of protective co-medication aimed at avoiding cisplatin side effects, at the same time retaining its antineoplastic efficacy.
Supported by the IZKF Münster (Cia2/013/13).

OS13-3
Dynamics of melanoma cell-cell interaction depending on Na^+/H^+ exchanger 1 expression and pericellular pH

K. A. Koch[1], V. Hofschröer[1], C. Stock[2], A. Schwab[1]
[1]University of Münster, Institute of Physiology II, Germany
[2]Hannover Medical School, Dept. of Gastroenterology, Hepatology and Endocrinology, Germany

Introduction: The Na^+/H^+ exchanger isoform 1 (NHE1) is known to contribute to cancer cell motility and tumor malignancy via its impact on cellular volume and both intra- and extracellular pH homeostasis. NHE1 creates acidic extracellular nanodomains at sites of focal contact at the front of migrating cells, which strengthen cell-matrix interactions at this cell pole. The present study investigates whether NHE1 also affects cell-cell contacts and the detachment of melanoma cells from the primary tumor, which is an early step of the metastatic cascade. **Methods:** We used human melanoma (MV3) cells and compared transfected NHE1-overexpressing cells with control cells expressing the vector only. We performed wound healing assays using live cell imaging to quantify the progression of the wound closure as well as directionality and cohesion of the migrating cells. While these experiments analyzed the detachment of the cells, we further performed cell aggregation assays to study whether changes in the extracellular pH (pH_e) values affect spheroid formation. Furthermore, we measured pH_e values in the perimembranous extracellular space at the cell-cell contacts with fluorescein labeled wheat germ agglutinin bound to the glycocalyx. **Results:** NHE1-overexpressing melanoma cells close the cell free wound area faster than control cells. However, the cohesiveness between NHE1-overexpressing cells is reduced as indicated by a higher translocation in parallel to the wound fronts and a bigger distance between adjacent cells. The aggregation assays support the idea that an acidification leads to a disassembly or prevent the formation of stable cell-cell contacts. While the NHE1-overexpressing cells were not able to form stable spheroids, those of the control cells became smaller as the pH of the surrounding solution decreased. The pH measurements revealed that NHE1 is active at the cell-cell contacts. Stimulating NHE1 by acid-loading the cells led to a drop in pericellular pH, both at the cell-cell contacts and the free cell membranes. **Conclusions:** An increased activity of NHE1 seems to facilitate different steps of the metastatic cascade. We conclude that its influence on the cell-cell contacts is contrary to its impact on the cell-matrix interaction. An acidic environment enables the cells to detach more easily from the primary tumor while simultaneously increasing their invasive potential.

OS13-4
Lactate contributes to fast recovery of activity dependent ion concentration changes in rat CA3 hippocampus

E. A. Angamo[1], J. Rosner[1], A. Liotta[2], R. Kovacs[3], U. Heinemann[1]
[1]Charité Universitätsmedizin Berlin, Neuroscience Research Center, Germany
[2]Charité Universitätsmedizin Berlin, Department of Anesthesiology, Germany
[3]Charité Universitätsmedizin Berlin, Inst. Neurophysiology, Germany

Astrocyte derived lactate supports pathologically enhanced neuronal metabolism but its role under physiological conditions is still a matter of debate. Here, we sought to determine the contribution of astrocytic lactate shuttle to the maintenance of ion homeostasis and signaling dependent energy metabolism. We tested for effects of monocarboxylate-transporter (MCT) blockers, α-Cyano-4-hydroxycinnamic acid (4-CIN) and phloretin on evoked potentials, stimulus induced changes in K^+, Na^+, Ca^{2+} and oxygen concentrations as well as on changes in FAD autofluorescence in the hippocampal area CA3. MCT blockade by 4-CIN reduced synaptically evoked but not antidromic population spikes. This effect was dependent on the activation of K_{ATP} channels. By contrast, lactate receptor activation by 3,5-dihydroxybenzoic acid (3,5 DHBA) resulted in increased antidromic and orthodromic population spikes. Recovery kinetics of all ion transients were prolonged and baseline K^+ concentration became elevated by blockade of lactate uptake. Lactate contributed to oxidative metabolism as both baseline respiration and stimulus induced changes in pO_2 were decreased, while FAD became overoxidized in the presence of MCT blockade. These data suggest that lactate shuttle contributes significantly to maintenance of ion homeostasis and synaptic signalling even in the presence of ample glucose.

OS13-5
Hypoxia-induced carbonic anhydrase IX facilitates lactate transport in human breast cancer cells by non-catalytic interaction

S. Jamali[1], M. Klier[1], S. Ames[1], L. F. Barros[2], R. McKenna[3], J. W. Deitmer[1], **H. M. Becker**[1]
[1]University of Kaiserslautern, Division of General Zoology, Germany
[2]Centro de Estudios Científicos (CECS), Valdivia, Chile
[3]University of Florida, Department of Biochemistry and Molecular Biology, Gainesville, United States

The most aggressive and invasive tumor cells, which often reside in hypoxic environments, rely on extensive glycolysis to meet their large demand for energy and biosynthetic precursors. Thereby they release vast amounts of lactate and protons via monocarboxylate transporters (MCTs), which exacerbates extracellular acidification and supports the formation of a hostile environment. In the present study we investigated the mechanisms that regulate lactate transport in cancer cells under normoxic and hypoxic condition, using human breast cancer cell lines and *Xenopus* oocytes as model systems. Hypoxia led to a drastic increase in the expression of carbonic anhydrase IX (CAIX), while the expression level of MCT1 and MCT4 remained unchanged. However, we could observe a significant increase in lactate transport capacity under hypoxia. This increase remained unaltered in the presence of the CA inhibitor 6-ethoxy-2-benzothiazolesulfonamide (EZA), but was abolished by knockdown of CAIX with siRNA. These results indicate that CAIX facilitates lactate transport in cancer cells by a non-catalytic interaction. The mechanism underlying this non-catalytic augmentation in MCT transport activity was further investigated by heterologous protein expression in *Xenopus* oocytes. Coexpression of CAIX-WT with MCT1 or MCT4 induced a robust increase in MCT transport activity, which was independent of CAIX catalytic activity. However, removal of the CAIX intramolecular H^+-shuttle by mutation of histidine 200 to alanine (CAIX-H200A) abolished CAIX-mediated augmentation in MCT activity. We conclude that CAIX functions as an extracellular 'proton-antenna' for the MCT to facilitate rapid lactate flux over the cell membrane. The importance of this non-catalytic augmentation in MCT transport activity was demonstrated by a cell proliferation assay: Knockdown of CAIX (but not inhibition of CA catalytic activity) resulted in a significant reduction in cell proliferation. Overall, the results suggest that non-catalytic function of CAIX facilitates rapid efflux of lactate and H^+, which appears to be essential for cancer cell survival under hypoxic conditions (Figure 1).

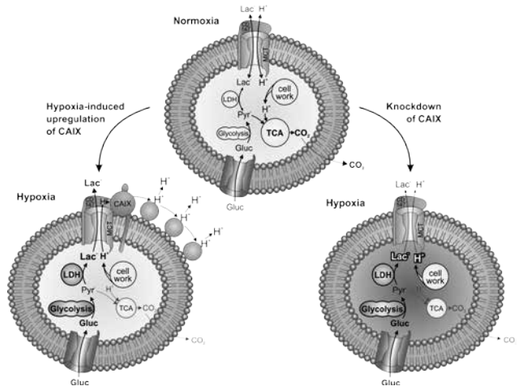

Figure 1:
Schematic model of the CAIX-mediated increase in lactate transport in cancer cells under hypoxic conditions. (Modified from Jamali et al. (2015) Sci. Rep. 5:13605)

OS13-6
Digestion physiology predicts sensitivity to CO_2-driven seawater acidification in non-calcifying marine larvae

M. Hu[1], Y. - C. Tseng[2], E. Lein[3], M. Bleich[1], M. Stumpp[3]
[1]Institute of Physiology, Christian-Albrechts-University of Kiel, Germany
[2]National Taiwan Normal University, Department of Lifesciences, Taipei, Taiwan
[3]Helmholtz Centre for Ocean Research Kiel (GEOMAR), Germany

Questions: Extensive anthropogenic combustion of fossil fuels has led to a drop in ocean surface pH and is predicted to further decrease by 0.4 pH units in the coming century; this phenomenon was termed ocean acidification. Marine larval stages were identified to be the weakest link when a species is confronted with acidified seawater. Special attention has been dedicated to marine calcifiers which were predicted to be particularly sensitive to changes in seawater carbonate chemistry due to the dissolution of $CaCO_3$ structures. Recent studies demonstrated that some non-calcifying species also respond sensitively to acidified seawater but the underlying physiological processes remain unexplored. **Methods:** We used larval cultures of a hemichordate (*Ptychodera flava)* and a sea star (*Archaster typicus*) to access the effects of near future acidification levels on these non-calcifying marine organisms. We used developmental and morphometric analysis to determine the degree of sensitivity in these species. Microelectrode measurements in combination with metabolic rate determinations were used to determine the energetic costs to regulate gastric pH in these organisms. **Results**: Larval stages of the hemichordate *P. flava* respond highly sensitive (100% mortality after 8 days) to simulated near- future acidification levels. This species has highly regulated alkaline (pH 10.13± 0.04) digestive systems and metabolic rates increase 4-fold in response to acidified sea water. In contrast, the sea star *A. typicus* is less sensitive, showing only a slight developmental delay. Larval stages of *A. typicus* do not regulate gastric pH, but are conform to the surrounding seawater. **Conclusions**: Our results demonstrate that non-calcifying marine larvae may respond very differently to simulated near-future ocean acidification. However, the present study shows for the first time that digestion physiology represents a key process that determines the degree of sensitivity. While gastric pH regulation is not challenged in the sea star *A. typicus*, the strict maintenance of an alkaline digestive pH around 10 in the hemichordate under acidified conditions is very likely linked to a substantial re-allocation of energy to gastric pH regulation. These results highlight the importance to better understand physiological processes in marine larval stages and suggest that our current knowledge underestimates the severity of ocean acidification on marine biota as many non-calcifying species were neglected.

OS13-7
Clathrin coat assembly inhibitor disassembles the nuclear pore: Implications for physiology and gene therapy

I. Liashkovich, G. Rosso, D. Pasrednik, V. Prystopiuk, **V. Shahin**
University of Münster, Institute of Physiology II, Germany

Nuclear pore complexes (NPCs) are supramolecular assemblies consisting of multiple copies of ~ 30 different proteins termed nucleoporins (Nups). They mediate all transport between the cytosol and the nucleus in a highly selective manner and are consequently referred to as a permeability barrier. The selectivity of the NPC barrier is of crucial physiological importance. However, an uptake of exogenously applied large DNA, essential for gene therapy, requires an efficient overcoming of the NPC barrier. To date, the efficiency of non-viral gene therapy in non-dividing cells, whereby the NPC barrier does not disassemble, remains marginal. A precise understanding of the NPC structure and selectivity mechanism is inevitable for the design of powerful approaches aiming at a breakdown of the NPC barrier. Very much simplified the elaborate NPC assembly can be considered to be made up of a rigid scaffold harbouring a highly flexible transport channel in its centre. Recently, we could show that NPC selectivity is attributed to the presence of phenylalanine-glycine (FG) rich Nups within the channel. Moreover, we presented an approach capable of inducing a controlled and reversible dissociation of barrier forming FG-Nups from the NPC channel. Here, we introduce another approach aiming at breaking the NPC barrier by targeting the NPC scaffold. We demonstrate that the recently discovered inhibitor of clathrin-mediated endocytosis Pitstop-2, which acts by preventing the assembly of the clathrin coat, disassembles the NPC scaffold. This effect is paralleled by a prompt, efficient and reversible breakdown of the NPC permeability barrier. In conclusion, our findings provide the first functional indication of the heatedly debated evolutionary relationship between clathrin and NPC scaffold proteins. The endocytosis-NPC-relationship remains to be explored in details and it may revisit our understanding of fundamental physiological processes. Finally, the pitstop-induced breakdown of the NPC permeability holds the promise to increase the efficiency of non-viral gene therapy.

OS13-8
OGR1 is involved in acid-induced hypercalciuria

P. H. Imenez Silva[1], C. Benabbas[1], K. Chan[1,2], M. - G. Ludwig[3], J. Gasser[3], T. Arnett[4], O. Bonny[5], K. Seuwen[3], C. A. Wagner[1]
[1]Universität Zürich, Institute of Physiology, Switzerland
[2]ETH Zurich, Inst. for Molecular Health Sciences, Zürich, Switzerland
[3]Novartis Institutes for Biomedical Research, Basel, Switzerland
[4]University College London, Department of Cell & Developmental Biology, United Kingdom
[5]University of Lausanne, Department of Pharmacology and Toxicology, Switzerland

Question: Hypercalciuria is a common feature of patients with metabolic acidosis. However, the sensing mechanisms responsible for the decreased renal calcium reabsorption during acidosis are still unknown. Here we tested if the proton-activated G protein-coupled receptor OGR1 (Ovarian cancer G-protein coupled receptor 1) is involved in this process. **Methods:** Wild type *(Ogr1$^{+/+}$)* and an *Ogr1*-deficient mouse model *(Ogr1$^{-/-}$)* were subjected to metabolic acidosis (2% NH_4Cl in food) or a non-acidotic control condition for 1 and 7 days and basic physiological parameters were collected from blood and urine. Several organs were isolated such as kidneys, intestine, brain, heart, etc. in order to extract RNA and perform RT-PCR/real time PCR. Kidneys were also used for protein extraction/western blotting and immunohistochemistry. **Results:** *Ogr1* mRNA was found in many organs such as kidney, spleen, brain and lungs. No acid-base modifications were observed in *Ogr1$^{-/-}$* mice, except for a higher plasma pH in the 1 day metabolic acidosis group (7.20±0.04 vs 7.12±0.03, $p<0.05$). As was expected, metabolic acidosis caused an increase in calcium and magnesium excretion in *Ogr1$^{+/+}$,* but this was not observed in *Ogr1$^{-/-}$*. Knockout mice presented normal plasma PTH and $1,25(OH)_2$ $VitD_3$ levels in adaptation to metabolic acidosis and normal bone morphology in all tested groups. The mRNA levels of proteins involved in Ca^{2+} and Mg^{2+} reabsorption, like Calbindin-D28k, TRPV5/6, TRPM6/7 and Claudins 16 and 19, were not altered in *Ogr1$^{-/-}$*. The expression levels of the key proteins for calcium reabsorption in the distal convoluted tubule (DCT), TRPV5 and Calbindin-D28k were increased by 96.9% and 102%, respectively, in *Ogr1$^{-/-}$* under metabolic acidosis. This may explain the lower Ca^{2+} excretion in these mice. NHE3 protein is also up-regulated in kidney apical membranes of *Ogr1$^{-/-}$* under metabolic acidosis by 74,6%. **Conclusion:** OGR1 is involved in the hypercalciuria and hypermagnesuria developed during metabolic acidosis, by a mechanism that may involve the transcellular reabsorption pathway of calcium in the DCT.